University of Southampton

The effect of coccolithophores and non-calcifying phytoplankton on the marine dissolved inorganic carbonate system

Keith Weston
Doctor of Philosophy

Department of Oceanography

Submitted May 1997

UNIVERSITY OF SOUTHAMPTON

ABSTRACT

FACULTY OF SCIENCE

OCEANOGRAPHY

Doctor of Philosophy

The effect of coccolithophores and non-calcifying phytoplankton on the marine dissolved inorganic carbonate system

by Keith Weston

Recent interest in the global climate system has focused attention on the oceanic carbon cycle due to its role in the 'Greenhouse Effect'. Calcifying pelagic micro-algae, *i.e.* coccolithophores, represent an important component of the oceanic carbon cycle due to the vast blooms which occur in many parts of the world's oceans. The dynamics of the production of both organic and inorganic carbon in coccolithophore blooms have important implications for the carbon cycle. It has been proposed that coccolithophores may decrease the flux of carbon dioxide across the air-sea interface relative to non-calcifying phytoplankton. In this study the effect of a high-calcifying strain of the coccolithophore *Emiliania huxleyi* on the dissolved inorganic carbonate system was compared to a low-calcifying strain of *E. huxleyi* and the non-calcifying chrysophyte *Isochrysis galbana*. In the high-calcifying strain of *E. huxleyi* the uptake of ^{14}C-labelled dissolved inorganic carbon showed a greater rate of calcification relative to photosynthesis in lag and exponential growth phases than in stationary phase. This caused a decreased rate of PCO_2 uptake relative to total dissolved inorganic carbon (C_T) uptake, relative to low-calcifying *E. huxleyi and I. galbana*. The dissolved inorganic carbonate system was determined from pH and one point alkalinity titrations. The relationship between PCO_2 and C_T was represented by the homogenous buffer factor (β). The buffer factor was lower in high-calcifying *E. huxleyi* cultures (β = 0.17-7.12) than for *I. galbana* and low-calcifying *E. huxleyi* cultures (β = 6.92-13.50). A net increase in PCO_2 was also noted for certain high-calcifying *E. huxleyi* cultures as C_T was declining.

Field studies, in nutrient adjusted experimental enclosures, were undertaken to measure changes in photosynthetic and calcification parameters in conjunction with measurements of the dissolved inorganic carbonate system. β measured in *E. huxleyi* dominated blooms and a mixed *E. huxleyi* and diatom bloom ranged from -0.27-4.25 and 6.80-7.59 respectively, in agreement with those calculated in culture. An increase in PCO_2 was detected during an *E. huxleyi* dominated bloom, coincident with the minimum value of β (-0.27). Rates of calcification to photosynthesis, derived from ^{14}C uptake rates, showed an average ratio of 0.4 in *E. huxleyi* dominated blooms, which increased to a maximum of 1.2 concurrent with the minimum value of β.

Rates of calcification and photosynthesis were also derived from changes in the dissolved inorganic carbonate system for both field and culture studies, and compared to those calculated from the rates of ^{14}C uptake. These showed good agreement during exponential growth phases in culture and mesocosms, but during stationary and decline phases a large discrepancy was noted, and is thought to be due to the influence of unmeasured diel respiration and dark calcification leading to an underestimation of diel C:P by ^{14}C derived measurements.

Dedicated to the memory of Nic Grochowski

ACKNOWLEDGEMENTS

I would firstly like to thank Dr. Duncan Purdie for his support and understanding throughout this Ph.D.

I would also like to thank Dr. David Crawford for his advice on, and knowledge of, the marine carbonate system, and also for the fruitful collaboration in Norway, along with Dr. Duncan Purdie.

Thanks also to David Lesley and Dr. Jorun Egge for running the mesocosm experiment, and also for supplying baseline measurements; and Bob Head for supplying the mesocosm calcite results.

Thanks also to my parents and Grandmother for their interest, Karen Meidlinger for being herself and finally Stuart and Sarah Thomson for being there.

CONTENTS

CHAPTER ONE : INTRODUCTION

Prior to 1850 the Earth's global carbon cycle was in steady state (Siegenthaler and Sarmiento, 1993) however since the Industrial Revolution emissions of fossil fuel carbon dioxide (CO_2) levels have risen almost exponentially by 25% (Keeling, 1991) reaching a level where even the U.K. government has accepted that the problem of the enhanced greenhouse effect and has legislated on fossil fuel emissions.

Figure 1.1.1 shows a schematic representation of the global carbon cycle. The ocean represents by far the largest carbon sink and source. Small changes in the fluxes of CO_2 into and out of the oceans can have a major impact on atmospheric CO_2 and hence the global climate system (Heimdal *et al.*, 1994). The largest fluxes of carbon are caused by physical processes due to water sinking at higher latitudes where air temperatures are colder, and upwells at lower latitudes where air temperature is warmer. There is a tendency towards higher partial pressures of dissolved CO_2 (PCO_2) in the surface water of areas of upwelling and lower values of PCO_2 in areas of downwelling. This apparently continuous circulation connecting the deep and surface flows throughout the world's oceans and is referred to as meridional flow (Niiler, 1993). These fluxes however do not result in sedimentation of carbon into the geological archive.

One of the major influences on surface ocean CO_2 levels are phytoplankton which influence the air-sea gradient of CO_2 through the processes of photosynthesis, respiration and calcification. This biota driven cycle is represented in figure 1.1.2 and shows the global carbon budget in the recent pelagic ocean. Two biological pumps from the surface to the deep ocean are distinguished: the carbonate pump and the organic carbon pump. In the organic carbon pump CO_2 is removed from the surface ocean and atmosphere by primary production consuming CO_2, producing particulate organic matter and dissolved organic matter which is exported to deeper water where remineralistion enriches these layers in CO_2. The export fluxes are not well quantified but it is thought they are balanced by the upward transport of dissolved inorganic matter by meridional circulation with only a minute fraction of this flux incorporated into the sedimentary archive budget (Westbroek *et al.*, 1993).

Certain members of the oceanic biota are also able to calcify and this biologically mediated calcification is the only major mechanism by which this sedimentation of PIC (particulate inorganic carbon) is initiated. This is the carbonate pump and results in total alkalinity (A_T; equivalent to the excess positive charge in seawater) and dissolved inorganic carbon (C_T) being lowered in the surface water and increased in the deep sea. The total amount of CO_2 fixed as POC (particulate organic carbon) in the euphotic ocean is far greater

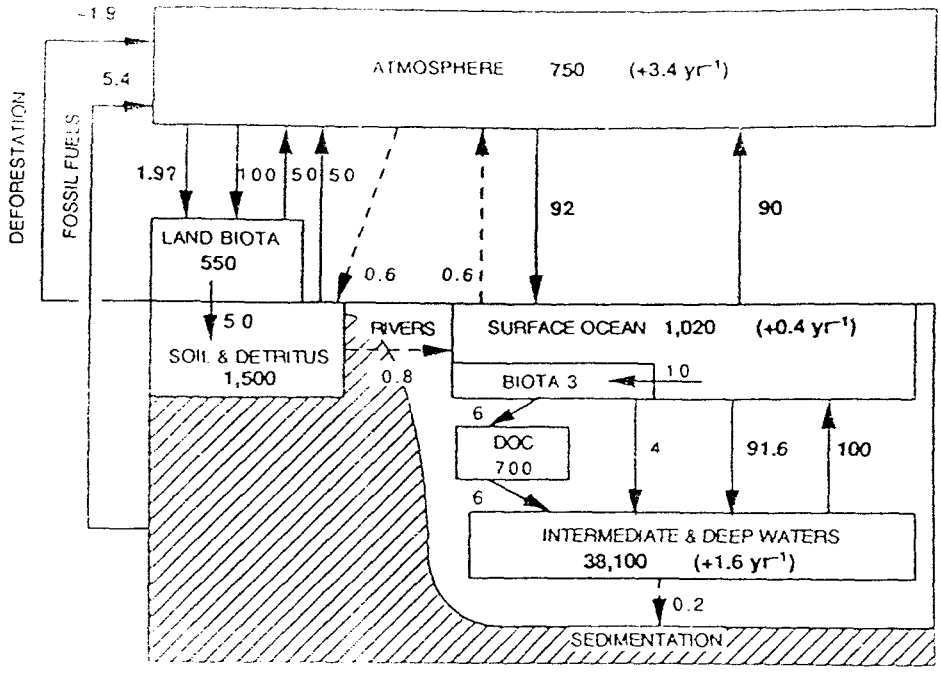

Figure 1.1.1 Global carbon cycle reservoirs and fluxes, in GtC and GtC yr^{-1} respectively (from Siegenthaler and Sarmiento, 1993)

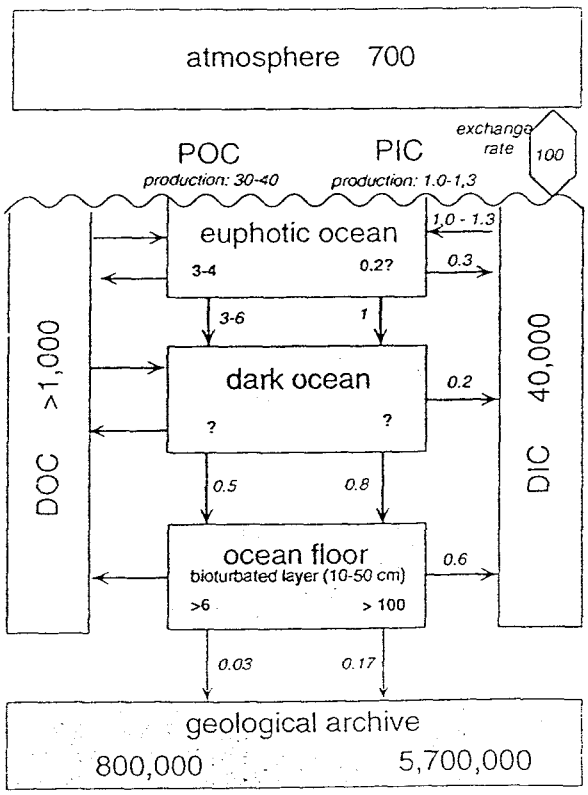

Figure 1.1.2 Carbon cycle in recent pelagic ocean. Reservoirs and fluxes, in GtC and GtC yr^{-1} respectively (from Westbroek *et al.*, 1993)

than that fixed as PIC and the probability that a biologically fixed atom of carbon, buried in the geological archive, will be in the form of calcite rather than organic carbon is about 6:1 (Westbroek *et al.*, 1993). The unicellular coccolithophorid algae are significant contributors to this sedimentation, but calcification also occurs in pteropoda, foraminifera and certain picoplankton. The relative contributions of these main calcifying taxa to total carbonate taxa at both regional and global scales remain poorly known (Holligan and Robertson, 1996).

The aim of this work is to add a piece to the jigsaw of understanding the global carbon cycle by quantifying the effect of one coccolithophorid species, *Emiliania huxleyi*, on PCO_2 levels as a part of the Global *Emiliania* Modelling (GEM) initiative (Harris, 1996), which was supported by the EC research programme MAST II. This collaboration focuses on *E. huxleyi* in order to understand the role of calcifying phytoplankton in present and past global changes. The understanding of physical, chemical, biological and geological aspects of one species may appear too reductionist but it is hoped that from this model organism general mechanisms will be revealed (Westbroek *et al.*, 1993).

A final caveat is however necessary: there are no claims that a change in marine primary productivity is already underway as a result of human activities nor is there any expectation of a direct response to additional anthropogenic emissions of CO_2 since phytoplankton are not usually considered to be carbon limited. The future stability of the Earth's carbon cycle should not, however, be based on an incomplete understanding of all its complexities.

1.1 *Emiliania huxleyi* - the organism

1.1.1 Taxonomy

E. huxleyi (Lohmann) Hay and Mohler is a globular cell with a diameter of 5-8µm. The surface may be covered by one or more layers of calcium carbonate plates, called coccoliths, with the morphology and size of the coccoliths being species specific, *e.g.* see figure 1.1.3. Coccoliths of *E. huxleyi* are constructed from crystal elements that differ in shape and size and are therefore classified as heterococcoliths, as opposed to holococcoliths which originate from crystal elements which are essentially identical in shape and size (Young, 1992). *E. huxleyi* coccoliths have a length of 2.5-4.5µm and are composed of two elliptical calcite plates or placoliths connected by an intermediate wall.

E. huxleyi belongs to the division Haptophyceae and some of the more important morphological features are summarised in table 1.1.1. Other well documented genera in this order are *Phaeocystis* spp. and *Chrysochromulina* spp.

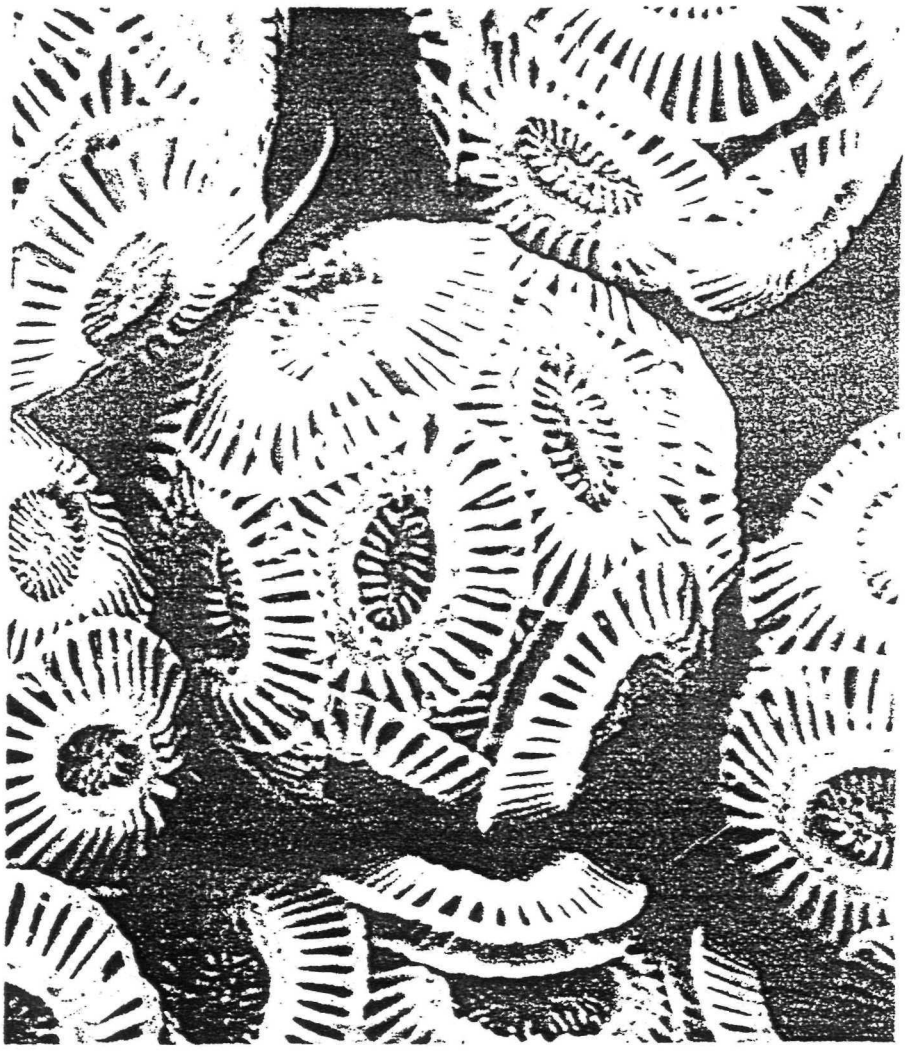

Figure 1.1.3 Electron micrograph of *E. huxleyi* cell showing coccoliths (from Young, 1994)

Chloroplasts with no girdle lamella
Non-heterokont; tubular hairs never found
Flagella usually two, equal or subequal
Haptonema or trace present
Unmineralised body scales basically a fibrillar two-layered plate
Many species with calcified coccoliths

Table 1.1.1 Principal morphological features characteristic of division Haptophyceae (Green and Jordan, 1994)

E. huxleyi was first described by Lohmann (Green and Jordan, 1994) and the current classification is shown in table 1.1.2. There are other systems of classification in current usage which show a broad measure of agreement (Green and Jordan, 1994) and none can be said to be definitive until the relationships of the haptophyte algae to each other and to other major algal groups is further elucidated.

Division	Haptophyta
Class	Prymnesiophyceae
Subclass	Prymnesiophycidae
Order	Prymnesiales
Family	Noelerhabdaceae
Genus	Emiliania
Species	*Emiliania huxleyi*

Table 1.1.2 showing classification according to Green and Jordan (1994)

1.1.2 Cell cycle

The life cycle of *E. huxleyi* is complex and has to date been only partially elucidated (Klaveness, 1972 (a)). There are four main forms of *E. huxleyi* which appear to be states of the normal life cycle, and all have the same dimensions. These types are:

1. C- cells - Calcifying non-motile cells, surrounded by a layer of coccoliths, called the coccosphere(Klaveness, 1972 (a)). Usually found in natural plankton communities.

2. N-cells - Naked non-motile cells, differing from C-cells mainly in the absence of coccoliths (Klaveness, 1972. (a)).

3. S- cells - Motile cells surrounded with a single layer of organic scales, bearing two smooth acronematic flagellae (Klaveness, 1972 (b)).

4. Ameoboid cells - Motile cells that do not bear flagella (Klaveness, 1972 (b)).

All these cell types are capable of independent vegetative propagation by simple constriction, resulting in binary division of the cell including the cover (Klaveness, 1972 (b)). It is possible, although rare, to find a mixture of the first three cell types in a culture of any one cell type. It is still not known what determines the changes between C-cells and other cell forms. The N-cells and S-cells arise spontaneously in many clones in culture, but the exact conditions causing their production are yet to be identified. Green (1994) has shown that there are two basic levels of ploidy within *E. huxleyi* with the flagellate cells being haploid relative to the C-cells. This suggests that *E. huxleyi* has a sexual life-cycle with the S-cells possibly acting as gametes.

1.1.3 Coccolithogenesis

The biogenesis of calcareous structures represents the interaction of two divergent processes of mineral organisation: crystallisation of inorganic salts and biochemical reactions controlling crystal growth (Westbroek, Young and Linschooten, 1989). Coccoliths are formed under rigorous cellular control resulting in their intricate morphology.

A tentative working hypothesis has been suggested where initially polysaccharide-containing vesicles are pinched off from the Golgi apparatus and migrate to the surface of the nuclear envelope to form the membrane-bound coccolithophore production compartment (CPC). At this stage calcite precipitation is inhibited by the presence of a polysaccharide which lines the CPC membrane and extends through the lumen. The inhibiting polysaccharide is next pulled away from the CPC interior to enable crystal formation. As more vesicles fuse with the CPC the nascent coccolith expands gradually until the final shape of the coccolith is reached. When the expansion of the coccolith is complete and crystal growth has been arrested the polysaccharide is detached from its anchor and becomes attached to the crystal surface. Finally the coccolith is extruded through the cell membrane to join the coccosphere (Westbroek *et al.*, 1984; Westbroek, Young, and Linschooten, 1989).

1.1.4 Functions of coccoliths

Coccolith production is an important part of coccolithophore biochemistry and their presence must affect the physiological ecology of the organism, however their functions are not clearly understood. Many workers have speculated on the possible significance of

coccoliths and these have been reviewed by Young (1994). These possible functions are outlined below:

1. Protection

(a) The cell membrane must be delicate since coccoliths are able to pass through it. Thus it may be vulnerable to damage, and its physical protection may be an important function of the cell covering by coccoliths (Leadbeater, 1994).

b) Coccoliths may make grazing by zooplankton more difficult and less efficient either due to an armouring effect, or by reducing grazing pressure with increased coccosphere diameter since filter feeders are size selective (Young, 1994). However cocccoliths have been demonstrated to have little effect on grazing by the marine copepod *Calanus finmarchicus* when fed on *E. huxleyi* and *Hymenomonas carterae* (Sikes and Wilbur, 1982)

2. Environmental buffering

a) The coccosphere may provide a buffer zone due to the stabilization of a 'boundary layer' by a cell covering. This will modify the movement of molecules in the microenvironment outside the plasma membrane and may act to protect the cell membrane from environmental shock. For example, Sikes and Wilbur (1982) showed that the presence of a coccosphere imparted a greater tolerance to lower salinities in both *E. huxleyi* and *H. carterae.*

b) Young (1994) suggested that the extracellular volume created by the coccosphere, if filled by macromolecules capable of absorbing nutrient ions, could increase the effective area for nutrient absorption and act as a nutrient store

2. Flotation regulation

a) The coccosphere may cause rapid sinking by increased weight of calcite of individual coccoliths, increasing the number of coccolith layers and aggregation of cells. Higher sinking rates for senescent cells than for actively growing cells have been recorded *e.g.*, Eppley, Holmes and Strickland, 1967. This may be an adaptive response since new nutrient sources are most likely to be found at depth.

b) Aspherical coccoliths and spines may reduce sinking rates. For example, the coccoliths of *Rhabdosphaera clavigera* have spines with flaring ends and therefore increase cell diameter without greatly increasing weight and so may reduce excess density and settling rate (Young, 1994).

c) Varying the number and shapes of coccoliths may allow regulation of flotation (Young, 1994).

3. Light regulation

a) Coccoliths may act as light gatherers which would increase photosynthesis and enable coccolithophores to live deeper in the water column (Gartner and Bukry, 1969). This adaptation would be of most benefit to thermocline dwelling species, which have to cope with permanently low light levels. It might also be of value for species in deep mixed layer environments, which are temporarily exposed to low lights.

b) Light scattering coccoliths surrounding the cell might provide protection from the harmful effects of high light intensities (Berge, 1962). This hypothesis has however been more recently shown to be invalid by Nanninga and Tyrell (1996) for *E. huxleyi*.

c) Light scattering coccoliths may cause an increase in the attenuation of light. This may lead to increased and more stable stratification due to a increased heating of the surface waters compared to deeper waters (Kirk, 1988).

d)The rapid attenuation of light due to coccolith light scattering may reduce light reaching the thermocline. This may prevent the establishment of high concentrations of phytoplankton in the thermocline which could intercept the upwards flow of nutrients and starve the surface phytoplankton of nutrients (Nanninga and Tyrrell, 1995).

4. Biochemical functions

a) Coccolithogenesis may be an aid to photosynthesis due to internal recycling of carbon dioxide produced by calcification for photosynthesis. This hypothesis was initially suggested by Paasche (1962) and is expanded upon in section 1.2.3.

Coccolith morphology is very diverse and so are the ecological niches occupied by coccolithophorids, thus making it difficult to discuss the functional morphology of coccoliths in general. It is however unlikely that there is a universal function or functions of coccocliths, although their role is likely to involve some of the hypotheses listed above.

1.1.5 Distribution

E. huxleyi is the most abundant coccolithophore in the world today, accounting for 20-50% of the total coccolithophore community in most ocean areas (Winter, Jordan and Roth, 1994). It is also found in the North Sea and Mediterranean Sea, and in low salinity waters close to the coast and inshore waters, such as fjords (McIntyre and Bé, 1967). *E. huxleyi* has the greatest tolerance to variations in their environment amongst coccolithophores, being found in the temperature range of 0-20^{0}C within the biogeographical limits of the subarctic and subantarctic. The poleward boundary of this distribution is the summer position of the 0^{0}C surface water isotherm (Brown and Yoder, 1994 (a)).

1.2 The role of *Emiliania huxleyi* in biogeochemical cycles

Coccolithophorids interact with the environment and climate control by their contribution to the oceanic carbon cycle and sulphur cycle, which alter the infrared radiative properties of the atmosphere due to release and uptake of CO_2, and atmospheric radiative transfer due to the albedo respectively (Charlson *et al.*, 1987). These effects are examined below with emphasis on the oceanic carbonate cycle; the area in which this work focussed.

1.2.1 *Emilania huxleyi* and the sulphur cycle

Coccolithophores, in common with most algae, have an influence on the sulphur cycle due to to their production and emmision of dimethylsulphonium propionate (DMSP). The biological function of DMSP is not fully understood but may primarily be an osmoregulatory compound (Dickson and Kirst, 1987). Laboratory studies have demonstrated that the production of DMSP is largely confined to a few classes of marine phytoplankton, primarily the Dinophyceae and the Prymnesiophyceae (Keller, 1989). When DMSP is broken down, either in seawater or by intracellular enzymes, it forms dimethylsulphide (DMS). For DMS, the two dominant removal processes are ventilation to the atmosphere and photochemical and microbial breakdown in the water column (Andreae, 1985). Atmospheric DMS may be oxidised to form a non-sea sulphate aerosol, which consists of both sulphate and methane sulphonate. This aerosol is ubiquitous in the marine atmospheric boundary layer, and acts as cloud-condensation nuclei (CCN) in the marine atmosphere (Andreae, 1990). The lack of alternative sources of sulphur-bearing gases support the hypothesis that these biologically derived gases are the probable main sources of CCN in the remote marine boundary layer (Charleson *et al*, 1987). The CCN affect cloud albedo since clouds of liquid water droplets form only in their presence. The reflective nature of the cloud albedo in turn affects the Earth's radiation budget, surface temperature and solar budget by causing a loss of solar radiation to space (Charlson *et al.*, 1987). This prompted Charleson *et al* (1987) to put forward the hypothesis that the production of DMS by marine phytoplankton might represent a climate regulating mechanism. The concept is that increased seawater temperature and,or light leads to increased DMS emmisions, followed by atmospheric oxidation, production of CCN and increased cloud albedo which would serve to counteract the initial temperature and,or light increase (Malin, Liss and Turner, 1994).

The production of DMS in algae is also an integral part of the sulphur cycle, since the clouds formed by CCN act as a sulphur carrier in the sulphur cycle and may maintain the sulphur level on land by recycling sulphur from the oceans in precipitation (Fell and Liss, 1993). The land tends to be depleted of sulphur and the supply of this nutrient element from

the ocean would increase the productivity and so lead to a return flow of nutrients to the ocean ecosystem (Charlson *et al.*, 1987).

1.2.2 *Emiliania huxleyi* and the carbonate system

Before the effects of biological activity on the marine carbonate system is examined some of the basic parameters and terminology used throughout this thesis are defined. The reactions which take place when carbon dioxide dissolves in water are represented by the following equilibria:

$$CO_{2(g)} \leftrightarrow CO_{2(aq)} \qquad 1.1$$

$$CO_{2(aq)} + H_2O \leftrightarrow H_2CO_3 \qquad 1.2$$

$$H_2CO_3 \leftrightarrow HCO_3^- + H^+ \qquad 1.3$$

$$HCO_3^- \leftrightarrow H^+ + CO_3^{2-} \qquad 1.4$$

where $CO_{2(g)}$ and $CO_{2(aq)}$ represent gaseous and aqueous phases respectively.

The following apparent constants apply to these reactions:

$$K_0 = [CO_2]/fCO_2 \qquad 1.5$$ -controls reaction 1.1

$$K_1 = [H^+][HCO_3^-]/[CO_2] \qquad 1.6$$ -controls reactions 1.2-1.3

$$K_2 = [H^+][CO_3^{2-}]/[HCO_3^-] \qquad 1.7$$ -controls reaction 1.4

where species in square brackets denote molality (mol $kg^{-1}{}_{sw}$).The molal scale gives concentrations which are independent of temperature and pressure. K_0 is the solubility coefficient of carbon dioxide in sea water in units of mol kg^{-1} atm^{-1} and fCO_2 is the fugacity of carbon dioxide gas. Fugacity is used to emphasise the possibility of a gas behaving non-ideally, but PCO_2 is generally used since the difference between PCO_2 and fCO_2 is approximately 1 µatm at 25°C and 1 atm. Dissolved PCO_2 is differentiated from atmospheric partial pressure pCO_2 by the upper case prefix 'P'. Since the bulk of H_2CO_3 and $CO_{2(aq)}$ will be present as $CO_{2(aq)}$, with less than 0.3% hydrated at 25°C and 1atm, $[CO_2]$ is assumed to equal $[CO_{2(aq)}] + [H_2CO_3]$ (Skirrow 1975).

The total alkalinity (A_T) of seawater is defined as 'the number of moles of hydrogen ion equivalent to the excess of proton acceptors (bases formed from weak acids with a dissociation constant $K \leq 10^{-4.5}$, at 25^0C and zero ionic strength) over proton donors (acids with $K > 10^{-4.5}$) in one kilogram of sample' (Dickson, 1981). The expression for total alkalinity is thus:

$$A_T = [HCO_3^-] + 2[CO_3^{2-}] + [B(OH_4)^-] + [OH^-] + [HPO_4^-] + 2[PO_4^{2-}] + [SiO(OH)_3^-] + [HS^-] + 2[S^{2-}] + [NH_3^-] - [H^+] - [HSO_4^+] - [HF^+] - [H_3PO_4^+] \quad 1.8$$

Carbonate alkalinity (A_C) is a frequently used parameter and is the portion of the total alkalinity which is due to only the carbonate system:

$$A_C = [HCO_3^-] + 2[CO_3^{2-}] \quad 1.9$$

Total dissolved inorganic carbon (C_T or TCO_2) is a commonly used parameter and is defined as:

$$C_T = [HCO_3^*] + [HCO_3^-] + [CO_3^{2-}] \quad 1.10$$

Capacity factors, such as A_T and C_T, must be given in concentrations and are independent of temperature and pressure.

The fundamental definition of pH, from Butler (1992), is:

$$pH = -\log_{10}(a_H) \quad 1.11$$

$$= -\log_{10}([H^+]_f . \gamma_H) \quad 1.12$$

$$= -\log_{10}(m^f_H . \gamma_H) \quad 1.13$$

where a_H is the relative hydrogen ion activity (Dickson, 1993) and$[H^+]_f = m^f_H$ is normally the concentration of free hydrogen ions in moles per kilogram, but other units or reference states are equally valid (Butler, 1992). pH is an intensity factor *i.e.*, the proton free energy level is independent of the quantity of solution. However the activity coefficient, γ_H, of a single ion at finite concentration cannot be directly measured (Dickson, 1993). Four alternate scales have been proposed to date but the three scales based on hydrogen ion activity are widely recognised as the most useful (Butler, 1992). These are:

1. The National Bureau of Standards (NBS) scale which consists of values such as would be read directly from a pH meter calibrated using standard NBS buffers. In high ionic strength medium, such as sea water, these measured pH values are subject to errors in relation to those determined in low ionic strength solutions *i.e.* NBS buffers. Hence such pH measurements are subject to an uncertainty of the order of ±0.01 pH units or more (Dickson, 1984).

2. The total scale of Hansson hydrogen ion concentration which includes HSO_4^- as an explicit term (Hansson, 1973).

3. The sea water scale (SWS) is a more rigorous definition of the total scale, which depends on total hydrogen ion concentration and includes protonated sulphate and fluoride (Hansson, 1973).

4. The free hydrogen ion scale which does not include HSO_4^- as an explicit term (Dickson and Whitfield, 1981).

All four scales have their advantages and disadvantages and the value of dissociation constants is also affected by which scale is used to measure them experimentally. These problems are recognised by IUPAC who are unable to recommend any one approach to scale definition (Dickson, 1984). It is important to realise that it is rarely the hydrogen ion content of the solution that is important *per se*, but rather that it is indicative of the state of the various proton-transfer equilibria occurring in solution (Dickson, 1984).

In principle, the species distribution of carbon dioxide in sea water can be calculated from any two of the following parameters: A_T, C_T, pH and PCO_2, together with the appropriate thermodynamic data.

1.2.3 Effect of *Emiliania huxleyi* in the marine carbonate system

As has been previously mentioned biological activity associated with photosynthesising marine phytoplankton alters the inorganic carbon system since the formation of organic tissue consumes carbon and hence decreases the C_T of the water. This carbon loss has no effect on the alkalinity of the water since there is no effect on any of the

ions in the expression of total alkalinity (see equation 1.8). However, the incorporation and release of nitrogen by organic matter does make small changes in alkalinity since the removal of the NO_3^- ion to form organic matter increases the alkalinity of surface water as shown in table 1.2.1. When this organically bound nitrogen is released during respiration, the NO_3^- ion produced adds to the anionic charge and reduces the alkalinity of the deep water. The pH of the seawater will increase due to the uptake of hydrogen ions during photosynthesis and since PCO_2 is inversely related to pH the effect of photosynthesis will be to decrease PCO_2. The removal of CO_2 will also act to increase the pH by driving the carbonate equilibrium (see equations 1.1-1.4) towards the carbonate ion which will further reduce the supply of CO_2 for photosynthesis and also the PCO_2 level.

The effect of calcification, shown in table 1.2.1, on the concentration of CO_2 is opposite to the organic carbon pump since CO_2 is released during calcification and absorbed by dissolution. Calcification without photosynthesis would have the net effect of generating dissolved CO_2 and increasing PCO_2. The increase in PCO_2 will also cause a decrease in pH. The removal of carbonate will result in a decrease in C_T and a drop in alkalinity, shifting the carbonate equilibrium in the direction of the dissolved gas thus further enhancing the effect on PCO_2. These changes in C_T (or DIC) and alkalinity in response to the carbonate pump (formation/dissolution of calcite), the biological pump (formation/respiration of organic matter) and the solubility pump (processes driven by the effect of temperature, pressure and salinity) are illustrated in figure 1.2.1 (Holligan and Robertson, 1996). A model of the cellular regulation of coccolithogenesis and photosynthesis has been proposed by Nimer and Merrett (1993) in which a balance is maintained between the production of H^+ during calcification and the production of OH^- during photosynthesis. Thus there is no requirement for an exogenous source of sink of OH^- or H^+ to balance intracellular production of H^+ or OH^- respectively, and therefore no evidence to suggest any influence on extracellular pH or total alkalinity other than through the carbonate system itself.

Paasche (1962) proposed that a complementary relationship between calcification and photosynthesis allows a coccolithophorid cell to take up bicarbonate for calcification, with subsequent production of CO_2 for photosynthesis. This has been called the calcification/CO_2 supply hypothesis by Balch, Fritz and Fernandez (1996). Non-calcifying algae can cause a considerable drawdown in surface PCO_2. In contrast it has been shown that production of organic carbon and calcite ($CaCO_3$) in a ratio of 1:1 may result in a reduction of the air-sea gradient of CO_2 (Robertson *et al.*, 1994). This decrease is caused by the buffering effect of seawater, since removal of the bicarbonate ion is partially compensated for by the hydration of CO_2. The concentration of CO_2 remains constant if the ratio is 1:1.2 and higher C:P ratios result in elevated CO_2 concentrations and hence PCO_2 levels (Buitenhuis *et al*, 1996). The ratio of calcification to photosynthesis (C:P) is therefore an important means of predicting the effect of biological activity on the dissolved carbonate equilibrium.

Process	Alkalinity Change for Forward Reaction
Photosynthesis and Respiration	
1) $nCO_2 + nH_2O \Leftrightarrow (CH_2O)_n + nO_2$	No change
2) $106CO_2 + 16NO_3^- + HPO_4^{2-} + 122H_2O + 18H^+ \Leftrightarrow (C_{106}H_{263}O_{110}N_{16}P) + 138O_2$	Increase
Calcification and calcite dissolution	
$Ca^{2+} + 2HCO_3^- \Leftrightarrow CaCO_3 + CO_2 + H_2O$	Decrease

Table 1.2.1 showing the effect of biological processes on alkalinity, adapted from Stumm and Morgan (1985).

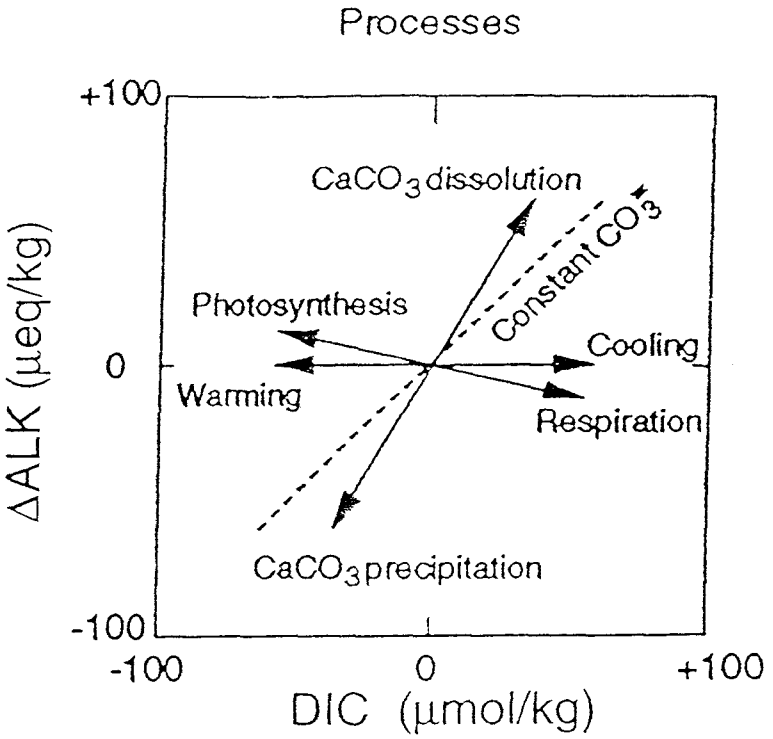

Figure 1.2.1 Vectors showing how alkalinity and C_T vary in response to three main processes; the carbonate pump, the biological pump and the solubility pump (from Holligan and Robertson, 1996).

If the intracellularly generated CO_2 was recycled internally and used in photosynthesis the free CO_2 may not be released back into the equilibrium. This suggests that calcification in the short term slows down the uptake of dissolved CO_2 for photosynthesis as carbon dioxide generated internally is preferentially used. Coccolithophores should therefore be less effective at reducing surface-water PCO_2 than other non-calcifying phytoplankton groups and would reduce the oceanic sink for atmospheric CO_2.

When CO_2 becomes potentially rate limiting phytoplankton species with alternative strategies for DIC utilisation would have a selective advantage in C_T utilisation (Riebsell, Wolf-Gladrow and Smetacek, 1993; Nimer, Iglesias-Rodriguez and Merrett, 1997). This DIC uptake may occur actively in marine microalgae due to the production of carbonic anhydrase (CA), which catalyses the interconversion of HCO_3^- to CO_2. In direct uptake of HCO_3^- bicarbonate ions are transported across the plasma membrane into the cytosol with the intracellular CA maintaining a steady flux of CO_2 to ribulose bisphosphate carboxylase-oxygenase (Rubisco); Rubisco is the only carboxylase enzyme which brings about CO_2 fixation in a compound that can be readily reduced to products at the carbohydrate level of reduction in O_2-evolving organisms (Raven and Johnston,1991). In contrast extracellular CA catalysed HCO_3^- utilisation depends upon CA external to the plasma membrane catalysing the interconversion of HCO_3^-, CO_2 and H_2O. In marine phytoplankton the presence of extracellular CA may be regulated by environmental parameters, *e.g.* in cultures of *E. huxleyi* extracellular CA has only been detected when external DIC was limiting and in the later stages of growth (Nimer, Iglesias-Rodriguez and Merrett, 1997). Due to the CO_2 supply by calcification the need for indirect HCO_3^- utilisation at low CO_2 concentrations is circumvented by CO_2 produced in calcification in coccolithophores.

The use of CA rather than passive CO_2 entry and, or the production of CO_2 due to calcification, could reduce the photon, N, Fe, Mn and Mo costs of growth, but increase with the Zn and Se costs, thereby affecting the competitive advantages of species utilising either the former or the latter strategy of DIC utilisation dependent upon environmental parameters (Raven and Johnston,1991).

Coccolith production also affects sea surface temperature through the effects of backscattering by the liths on the absorption of light energy by water. This unique ability of coccolithophorids to warm up the mixed layer would alter the carbonate equilibrium dissociation constants causing an increase in PCO_2 and thus further reducing the air-sea CO_2 gradient (Holligan *et al.*, 1993).

Any reduction in the removal of CO_2 from surface waters due to the growth of coccolithophores as opposed to non-calcifying phytoplankton could be important in reducing annual drawdown of CO_2. It is during the summer that the sea surface temperature increases with a corresponding rise in the PCO_2. The process of calcification will tend to enhance this effect reducing the seasonal oceanic sink of atmospheric CO_2, although coccolithophore blooms still represent a net sink for carbon into the sediments with respect to the atmosphere.

A few recent studies have demonstrated that the PCO_2 levels in *E. huxleyi* blooms are higher when compared to blooms of similar biomass of other phytoplankton (Purdie and Finch, 1994; Robertson *et al.*, 1994). The influence of the ratio of calcification to photosynthesis on the dissolved inorganic carbonate system, and hence the air-sea flux of CO_2, has not however been investigated under the more controlled conditions of laboratory cultures.

1.3 Objectives

Most attention in modelling the global carbon cycle has focused on the role of the organic carbon pump. This emphasis will however lead to an incomplete comprehension of the carbon cycle since, as Sundquist (1993) has stated, "Understanding the modern CO_2 budget depends intrinsically on understanding the historical and deglacial CO_2 budgets" but "A significant difficulty in understanding the origins of the deglacial increase in CO_2 levels - and in calculating the CO_2 budget properly - is the unknown contribution of changes in the cycling of marine C as $CaCO_3$". The objective of this study was to improve our understanding of the role of calcifying phytoplankton in the marine carbon cycle by demonstrating how the relative rates of calcification and photosynthetic carbon fixation affects the marine carbonate system, and how these effects will alter the natural buffering capacity of seawater. Buffer factors, which relate the change in PCO_2 to C_T, have been developed to describe the effect of CO_2 input/output into seawater, and to aid the understanding of the impact of phytoplankton on the global carbon cycle in surface waters of the oceans (Frankignoulle, 1994).

Most previous culture studies have used high concentrations of nitrate and,or phosphate, however in this study the concentration of both were reduced to more natural levels, with phosphate as the "limiting" nutrient. The effect of phosphate limitation on rates of both calcification and photosynthesis of high and low-calcifying strains of *E. huxleyi* were measured in conjunction with the dissolved inorganic carbonate system. These results were also compared to those using a non-calcifying phytoplankton (*Isochrysis galbana*). It was hypothesised that the effect of both non-calcifying phytoplankton and calcifying phytoplankton on the carbonate system, could be predicted from short term ^{14}C incubation derived rates of photosynthesis and calcification. Field work on nutrient adjusted experimental enclosures was also carried out to enable comparisons between laboratory cultures and natural blooms of calcifying and non-calcifying phytoplankton populations.

CHAPTER TWO : METHODS AND MATERIALS

2.1 Laboratory-based culture studies

Emiliania huxleyi has been isolated from a large number of marine regions and maintained in culture for extended periods. Stock cultures of these isolates are generally maintained in either Kellers (Keller *et al.*, 1987) or Guillards (f/2) (Guillard and Ryther, 1962) media at unrepresentatively high concentrations of phosphate and nitrate (see table 2.1.1). Media recipes may also include the addition of artificial buffers (*e.g.* Tris) to stabilise the pH of the media, increasing potential CO_2 availability and allowing high cell densities to develop. In more recent physiological studies media recipes have been used with more natural nitrate and phosphate levels (see table 2.1.1). Stock cultures in this study were maintained at 16μM nitrate (NO_3-N) and 1μM phosphate (PO_4-P) concentration and were subcultured every two weeks. Since the aim of this work was to investigate the impact of *E. huxleyi* on the dissolved carbonate equilibrium in seawater artificial buffers were not added to stock or experimental media.

Two strains of *E. huxleyi* were used during the laboratory-based experiments: a high-calcifying strain, 92E, isolated from the North sea was obtained from Dr. J. Green (Marine Biological Association); and a low-calcifying strain, CCAP 920/2, was obtained from the culture collection at SMBA, Dunstaffnage marine research laboratory, originally isolated from Oslo fjord. A strain of the chrysophyte *Isochrysis galbana* (CCAP 927/1; SMBA culture collection, originally isolated from the Irish Sea), was used to compare the effects of a non-calcifying phytoplankton of similar size to high- and low-calcifying *E. huxleyi* on the marine dissolved carbonate system.

2.1.1 Artificial seawater media preparation

Artificial seawater media was used for all laboratory-based culture experiments and stock cultures in preference to supplemented seawater media to allow the initial concentrations of nitrate, phosphate and bicarbonate to be defined. The composition of artificial seawater is shown in appendix table 6.1.1. The artificial seawater recipe used in this study was as described by Harrison, Waters and Taylor (1980). The two separate solutions of artificial seawater were sterilised by autoclaving at 121°C for 20 minutes. When cool these

solutions were mixed and a filter-sterilised (0.45µm cellulose nitrate filter) solution of sodium bicarbonate was added. Milli-Q water was used for all artificial seawater solutions.

2.1.2 Maintenance of stock cultures

The media recipe used for all cultures was based on that described by Keller (1987), (see appendix tables 6.1.2 and 6.1.3). All separate media solutions were filter sterilised using 0.45µm autoclaved cellulose nitrate filters. The same media was used in stock cultures as in experimental cultures minimising nutrient 'shock' when experimental cultures were inoculated. Stock cultures were maintained in a cabinet incubator at approximately 15^{0}C with a 16:8 hour light:dark cycle at an irradiance of approximately 100µEm^{-2}s^{-1} using cool white fluorescent tubes. All subculturing and inoculations were performed aseptically in a sterile hood. 200ml stock cultures were maintained in autoclaved 250ml polycarbonate conical flasks with screwtop lids. Cultures were non-axenic but regularly checked for algal contaminants.

2.1.3 Experimental incubation conditions

All experimental cultures were grown in batch conditions, with the media and artificial seawater prepared as above. The concentration of NO_3-N was 16µM in all experimental cultures. Initial PO_4-P concentrations were adjusted to: 0.5µM; 1.0µM; or 2.0µM. Following autoclaving, but prior to nutrient additions, the artificial seawater was bubbled with sterile air to equilibrate with atmospheric CO_2. The culture was pH adjusted after inoculation to control the initial PCO_2 level of the culture. This adjustment was achieved by the addition of either 0.1N HCl or 0.1N NaOH.

Two arrangements of apparatus were used in laboratory-based experiments. Initially cultures were inoculated into autoclaved 10l Pyrex flasks. These were grown in a constant temperature water bath running at 15^{0}C, with a 16:8 hour light:dark cycle. The cultures were illuminated from beneath by a bank of cool white fluorescent strip lights at 100µEm^{-2}s^{-1}. To create an even light field the sides of the flasks were covered in aluminium foil (see figure 2.1.1). Cultures were gently mixed by swirling and samples collected asceptically in a sterile hood with one subsample removed in bulk and then divided for analysis, in order to reduce the possibility of contamination of the experimental culture. Later a constant temperature controlled room was available, maintained at 15^{0}C (See table 2.1.2). Cultures were inoculated into sterile 10l Pyrex flasks stoppered with a silicon rubber bung. The flasks were gently mixed

Reference	Initial [DIN]	Initial [DIP]	Initial [DIN]:[DIP]
Keller's media (Keller *et al.*, 1987)	0.85mM	10μM	85:1
f/2 media (Guillard and Ryther, 1962)	0.8mM	40μM	20:1
Paasche (1964)	1.2mM	60μM	20:1
Paasche (1967)	1.2mM	60μM	20:1
Watabe and Wilbur (1966)	1.6mM	80μM	20:1
Eppley *et al.* (1971)	0.25mM	25μM	10:1
Brand (1982)	80μM	4μM	20:1
Fisher and Honjo (1989)	88μM	3.6μM	24:1
Linschooten *et al.* (1991)	32μM	1.6μM	20:1
Balch, Holligan and Kilpatrick (1992)	Not listed	Not listed	-
Nimer and Merrett (1992)	0.1mM	Not listed	-
Balch *et al.* (1993)	0.85mM	10μM	85:1
Nimer and Merrett (1993)	0.1mM	Not listed	-
Dong *et al.* (1993) High-calcifying strain	36.3μM	13μM	3:1
Dong *et al.* (1993) Low-calcifying strain	36.3μM	15μM	2.4:1
Merrett, Dong and Nimer (1993a)	36.3μM	20μM	2:1
Paasche and Brubak (1994)	0.125mM	0.64/1.89/ 13.14μM	195:1/66:1/ 10:1
van Bleijswijk *et al.* (1994)	35/10μM	0.3/0.1μM	117:1/100:1
Balch, Fritz and Fernandez (1996)	0.4mM	20μM	20:1
Lecourt, Muggli, and Harrison (1996)	30μM	2μM	15:1
Nimer, Merrett, and Brownlee (1996)	20μM	Not listed	-
This study	16μM	0.5/1.0/ 2.0 μM	32:1/16:1/8:1

Table 2.1.1 showing initial nutrient growth for laboratory-based culture experiments from the literature

by swirling and an initial sample run to waste via non-sterile Teflon tubing that sampled from the bottom of the flask. A tube clamp was used to prevent the residual sample from running back into the flask following sampling. The cultures were illuminated from the side by a bank of cool white fluorescent strip lights at $100\mu Em^{-2}s^{-1}$. To create an even light field in the culture vessels one side was covered with aluminium foil (see figure 2.1.2).

2.1.4 Cell counts

Culture cell density was determined using a Sedgewick-Rafter chamber. The culture sample was introduced under the chamber coverslip using a wide-mouthed pipette. The chamber was left to stand for at least 20 minutes in order to allow the cells to settle onto the bottom of the chamber. The number of cells within the area defined by at least five chamber grid squares were counted. The mean cell count was determined from three separate fillings of a Sedgewick-Rafter chamber (McAlice, 1971). A Leitz Fluovert inverted microscope was used for all microscopy. Initially cells were also viewed using epifluoresence and polarised light microscopy in order to differentiate calcified cells of *E. huxleyi* from empty coccospheres. Live samples were also counted in order to determine the number of motile cells, which increased in abundance in later experiments. When necessary samples were preserved by the addition of 20% sodium tetraborate buffered formalin solution (100µl in 15ml sample) (Steedmann, 1976; Throndsen, 1978).

The coefficient of variation for cell counts was better than 10%.

Specific growth rates (μ) were calculated using the equation:

$$\mu = \ln (n_1 / n_0) / (t_1 - t_0)$$

where n is the number of cells, t is time and μ is a quantity with the dimensions t^{-1}. Maximum specific growth rate was calculated when the culture was growing exponentially, where t_0 and t_1 were the start and end of the exponential growth phase respectively.

2.1.5 Nitrate (NO_3-N) analysis

Nitrate was determined using the copper-cadmium reduction technique described in Parsons, Maita and Lalli (1984) with samples taken in triplicate. This method involved quantitatively reducing nitrate to nitrite by passing the sample through a column containing cadmium filings coated with metallic copper. The nitrite produced was determined by diazotizing with sulphanilamide and coupling with N-(1-napthyl)-ethylenediamine to form a coloured azodye which was measured spectrophotometrically using a ChemLab flow injection

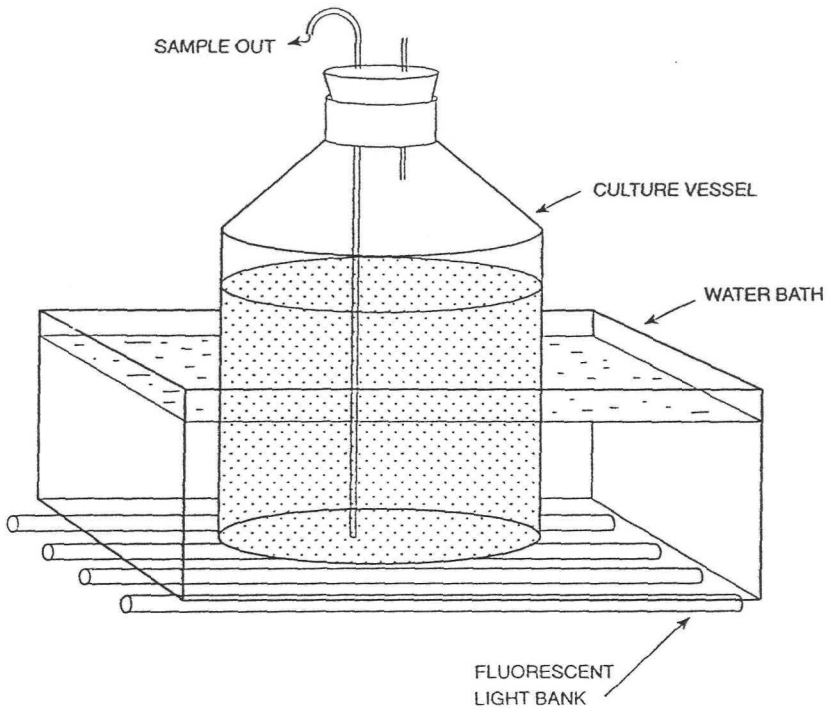

Figure 2.1.1 Water bath incubation arrangement

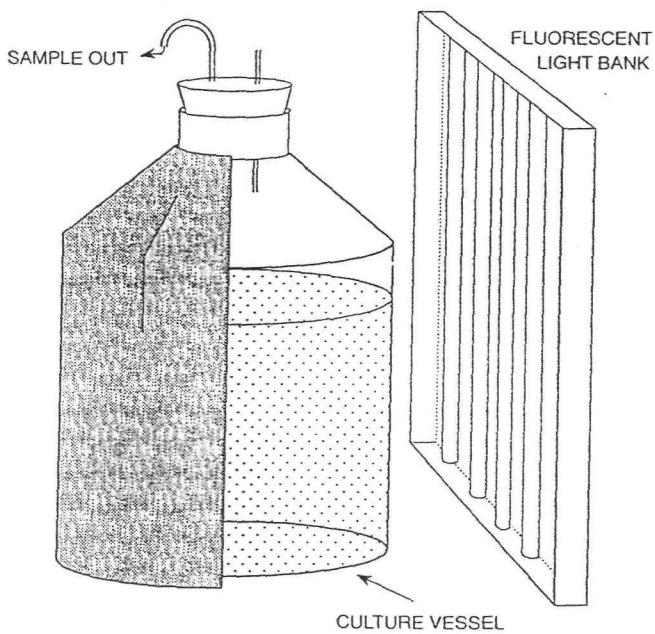

Figure 2.1.2 Constant temperature room arrangement

analyser. The nitrate:nitrite conversion efficiency of the reduction column was corrected for by running comparable standards of both nitrate and nitrite. 10ml of sample was filtered through a precombusted GF/F filter into an acid-washed sealable plastic tube and frozen prior to analysis.

The coefficient of variation for nitrate analysis was better than 5%.

2.1.6 Phosphate (PO_4-P) analysis

Phosphate was determined using the method described in Parsons, Maita and Lalli (1984) with samples taken in triplicate. The culture sample was allowed to react with a mixed reagent containing molybdic acid, ascorbic acid and trivalent antimony. The resulting complex was reduced to give a blue-coloured solution which was measured at 885nm using a Hitachi U-2000 spectrophotometer with a 4cm flow through cell. For each sample 35ml of culture was filtered through a precombusted GF/F filter into an acid-washed Milli-Q rinsed glass bottle containing 100µl 3% w/v mercuric chloride and refrigerated until analysed.

The coefficient of variation for phosphate analysis was better than 5%.

2.1.7 Bacterial number enumeration

Bacterial numbers were determined using the DNA specific stain 4,6-diaidino-2-phenylindole (DAPI) as described by Porter and Feng (1980). This method involved filtering 1ml of sample at less than 250mmHg onto a 0.2µm black polycarbonate filter with a 5.0µm membra-fil backing filter. The filter was then completely wetted with the DAPI stain, at a working concentration of 10µg ml^{-1}, and placed in the dark for 5-10 minutes. The DAPI was then drawn through the filter at a pressure of less than 250mmHg. The filter was removed from the filter tower and its underside covered in immersion oil and placed onto a slide. The upperside of the filter was then covered with immersion oil, by dripping, and a coverslip placed over the filter. These slides were stored frozen before enumeration.

2.1.8 pH measurements

pH was measured to ±0.001 units using a Mettler 350 pH meter with an Ingold 405 Automatic Temperature Compensation (ATC) probe. The meter was calibrated using Sigma standard NBS buffers at pH 4.00(± 0.01), 7.00(± 0.01) and 10.00(± 0.01) achieving a three point calibration bracketing the range of measurements made. Before the culture sample pH was measured, the probe was equilibrated in a solution of approximately the same pH, salinity and temperature. The culture pH was determined immediately after sampling (3x25 ml of culture into 3x100ml tall form beakers) to minimise the effect of temperature change.

The analytical precisions for pH were better than 0.005 units.

2.1.9 One point alkalinity titration

The alkalinity of sea water may be determined by titration using various methods:

I) Gran plots (Edmond, 1970).

ii) High precision potentiometric titrations - *i.e.* using a glass electrode (Bradshaw and Brewer,1988).

iii) High precision spectrophotometric titrations - uses pH specific dyes, *e.g.* phenol red, and measurements of the acidic and basic components of a specific indicator and the apparent dissociation constant of the indicator spectrophotometer. These indicators provide an absolute free hydrogen molality scale independent of the problems of electrode drift and liquid junction errors associated with potentiometric pH measurements (King and Kester, 1989).

iv) High precision thermometric titrations - uses the cessation of heat on completion of a reaction as an analytical endpoint (Millero, Schrager, and Hansen, 1974).

v) One/two point spectrophotometric/potentiometric titrations - past the carbonic acid endpoint. The one point potentiometric method is used throughout this study. The advantages is the time in which titration can be performed and the low sample volume but involves a corresponding loss of accuracy (Perez and Fraga, 1987);(Crawford and Harrison, 1997).

The one point acid titration method is based on that developed by Anderson and Robinson (1946), and is also described in Parsons, Maita and Lalli (1984). It should be noted that the volumes used differ from those suggested in the references. This was necessary to conserve culture volume, since many samples were needed.

Following initial pH measurement samples were filtered through a 47mm diameter GF/F under a low vacuum, (<10mmHg) to remove particulate calcite, during *E. huxleyi* culture experiments. 3x20ml samples were then pipetted into 3x100ml tall form beakers using a glass volumetric pipette. 5ml of 0.01N HCl (diluted from a 0.1N Sigma standard) was added to each beaker using an automatic Metrohm Dosimat with 10ml burette. The pH was measured immediately after addition of the acid minimising loss of $CO_{2(g)}$ from the solution. It was important when handling samples that care was taken to prevent the PCO_2 being altered, *i.e.* all pipetting and acid additions were slow and smooth, the tip of the pipette was beneath the meniscus when transferring samples and the sample was not mixed vigorously with the pH probe.

The results were then entered into a spreadsheet developed by D.W. Crawford to calculate dissolved carbonate parameters where total alkalinity (A_T) was determined according to Strickland and Parsons (1972) and Anderson and Robinson (1946). From the pH_{NBS} measurement A_T was calculated in mol l^{-1} (Strickland and Parsons, 1972) and then converted to mol kg^{-1} using the seawater density routine given by Dickson and Goyet (1994). An example of this spreadsheet is shown in appendix table 6.1.4.

For the calculations of the derived carbonate parameters all of the necessary parameters are summarised by Dickson and Goyet (1994) and converted from their original references to common units of mol kg^{-1} and for the "total hydrogen ion" pH scale. A_T was converted to carbonate alkalinity (A_C) using the salinity dependence of total boron (B_T) and the temperature and salinity dependence of the equilibrium constants for boric acid (K_B) and water (K_W). pH_{NBS} was converted to $[H^+]_{NBS}$ using $pH_{NBS} = -lg[H^+]_{NBS}$ and then $[H^+]_{NBS}$ converted to mol kg^{-1} with an estimated apparent activity coefficient $f_H = 0.85$ (Crawford and Harrison, 1997), and then to the "total hydrogen ion" scale $[H^+]_{TOT}$ with a correction for hydrogen fluoride (HF) using the salinity dependence of total fluoride (F_T) and bisulphate (K_S). Total dissolved inorganic carbon (C_T) was then calculated from A_C and $[H^+]_{TOT}$ using the standard equations summarised in Dickson and Goyet (1994) together with temperature and salinity dependence of the equilibrium constants for carbonic acid (K_1 and K_2), and the solubility coefficient for free CO_2 (K_0). The analytical precisions for the measured and derived carbonate system parameters, when measured the one point alkalinity titration in triplicate, were better than: 3µatm for PCO_2 ; 3µmol kg^{-1} for C_T; 0.87 and 0.36 µeq kg^{-1} for A_C and A_T respectively.

2.1.10 ^{14}C-labelled bicarbonate uptake rates

The $H^{14}CO_3$ method for measuring phytoplankton photosynthetic rate has been beset by methodological and interpretative difficulties (Peterson, 1980), and even more so when attempting to differentiate between inorganic carbon fixed by both calcification and photosynthesis. During this research two different procedures for differentiating between inorganic and organic ^{14}C fixation were used. Fundamentally the separation of labelled calcite and particulate organic carbon was dependent upon the acidification of a filtered sample.

2.1.11 Stock solution preparation

Stock solutions of 1mCi ml^{-1} ^{14}C labelled sodium bicarbonate (Amersham Life Sciences), were diluted using 5mM sodium hydroxide to give a final concentration of 100mCi ml^{-1} working solution *cf.* Parsons, Maita, and Lalli (1984). A stock diluted using this alkaline

solution will reduce the loss of ^{14}C from solution but was shown not to affect the pH of culture subsample when added to small incubation volumes.

2.1.12 Filter fuming technique

This method separates inorganic carbon uptake by photosynthesis from calcification by fuming a filtered sample over concentrated HCl to leave organic carbon fixed by photosynthesis. When compared to an unfumed filter the calcification rate can be estimated by difference. The method used was adapted from Nimer and Merrett (1992) and Fernandez *et al.* (1993).

In initial radiotracing experiments triplicate filters were either fumed or unfumed in order to determine calcification and photosynthesis. 40ml of sample was inoculated with 10μCi $NaH^{14}CO_3$ and a 100μl subsample taken to quantify ^{14}C added. The subsample was added to a 5ml plastic scintillation vial containing 2ml of scintillation cocktail (Optiphase 'HiSafe' 3 (Wallac Scintillation Products)) and 100μl of phenyethylamine to trap the added $NaH^{14}CO_3$ (Iverson, Bittaker, and Myers, 1976) was added to the scintillation vial. Culture subsamples were incubated for 3-4 hours in the incubator under the same conditions as the experimental cultures. On completion of the incubation 6x5ml samples were filtered through 25mm 0.40μm polycarbonate filters under a low vacuum in low light. Filters were then rinsed with 2x40ml washes of GF/F filtered seawater. The filter tower was then removed and the filter edge also rinsed with filtered seawater. All filters were dried overnight in a desiccator containing silica gel. Three of these filters were then placed in a container with concentrated hydrochloric acid for 5 minutes to remove all inorganic carbon from the filter. The filters were placed in a 10ml clear glass scintillation vial and 5ml of scintillation cocktail (Optiphase 'HiSafe' 3 (LKB Scintillation Products)) added. The samples were then counted for 60 seconds using a Wallac 1411 scintillation counter. The coefficient of variation was better than 10% and 9% for photosynthetic and calcification rates using this technique.

2.1.13 Split vial technique

This method separated inorganic carbon uptake by photosynthesis from calcification by adding the filtered sample to a weak acid solution. This drives off the carbon fixed by calcification as $^{14}CO_{2(g)}$ leaving that fixed by photosynthesis. These fumes are then trapped by a weak alkali solution. Using the split vial technique the same filter therefore gives the values

for rates of calcification and photosynthesis (*cf.* filter fuming). The split vial technique also has the advantage of using half the quantity of filters as the fuming technique, which has implications for culture volume conservation and cost. The method was adapted from Crawford and Stoecker (1996).

20ml of culture was subsampled and added to a 60ml Nalgene flask and 5μCi of $NaH^{14}CO_3$ added. From this 3x5ml samples were filtered at the end of the incubation which varied from 2-3 hours depending on culture density, time and volume constraints. Formalin killed controls were also carried out and for these a 5ml subsample of the culture was taken and 3μCi of $NaH^{14}CO_3$ added. These were then incubated under the same conditions as the live culture. Immediately after subsampling, if necessary, 100μl of sodium tetraborate buffered formalin solution was added to kill the culture control (Steedmann,1976; Throndsen, 1978). 100ml samples were taken in triplicate and added to a 5ml plastic scintillation vial containing 100ml of phenyethylamine to trap the added $NaH^{14}CO_3$ (Iverson, Bittaker, and Myers, 1976). 2ml of scintillation cocktail (Optiphase 'HiSafe' 3 (Wallac Scintillation Products)) was then added to each scintillation vial. At the end of the incubation period all samples were immediately filtered through 25mm diameter 0.40μm polycarbonate filters under a low vacuum (<10mmHg) in low light. All filters were finally rinsed with 2x20ml of recently filtered (GF/F) seawater.

For each filtered sample 2ml of 10% NaOH solution was added to a 20ml glass scintillation vial, the outer vial. Into this outer vial a 10ml glass specimen tube, the inner vial, was placed with the open end at the top. The sample filter was folded, with the algae inside, and placed into the inner vial using forceps. The outer vial was then sealed by a drilled lid lined with a plastic septum, with the inner vial also sealed from the exterior but able to exchange with the outer vial. 2ml of 0.1N HCl was then added to the inner vial via a syringe through the hole in the lid, ensuring the filter was covered with HCl. If the filter was not fully covered after the addition of acid more 0.1N HCl was added until the filter was totally covered, since the volumes of acid and alkali were not critical. The plastic septum creates a closed system so that $^{14}CO_2$ does not escape. This arrangement is shown in figure 2.1.3.

The vial was then left, supported upright, for 24 hours at room temperature. Following this period the lid of the outer vial was removed and the inner vial lifted partially out of the outer vial so that the base of the inner vial is no longer in contact with the NaOH. The inner vial outer surface was then rinsed with 2x1ml of 10% NaOH into the outer vial. The contents of the inner vial were then poured into a separate 20ml glass scintillation vial. The filter was removed, using a pair of forceps if necessary, and placed in this vial. The inside of the inner vial was then rinsed into the scintillation vial with 2x1ml 0.1N HCl. 4ml of scintillation cocktail (Optiphase 'HiSafe' 3 (Wallac Scintillation Products)) and 100μl of phenylethylamine was then added to both fractions. The vials were then counted for 60 seconds using a Wallac 1411

scintillation counter. The coefficient of variation was better than 6% and 7% for photosynthetic and calcification rates using this technique.

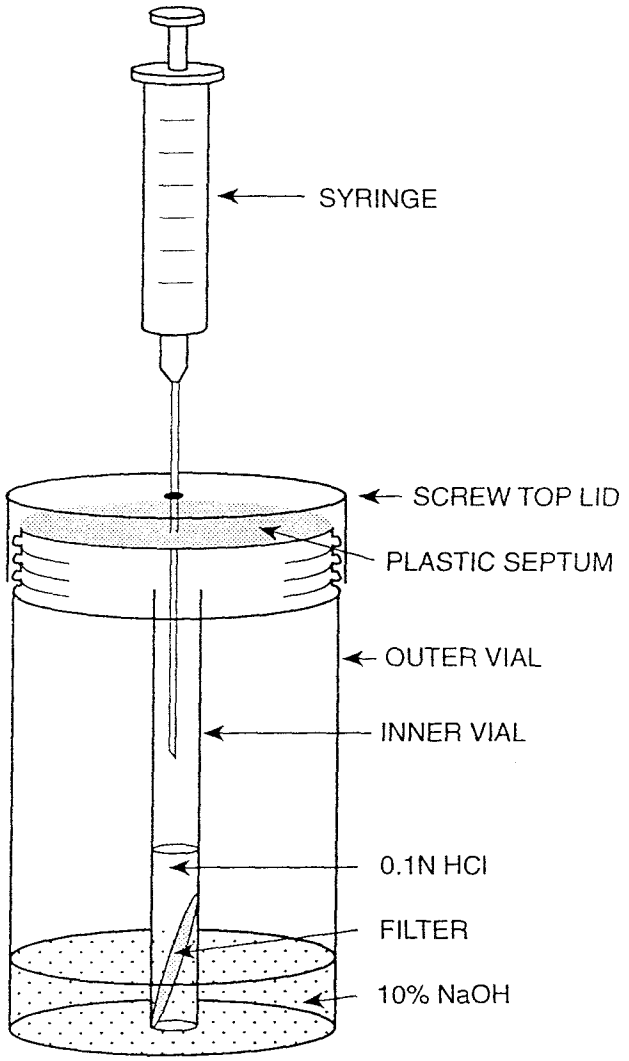

Figure 2.1.3 Split vial technique arrangement

2.1.14 Laboratory-based culture sampling regimes

Table 2.1.2 gives an outline of the parameters sampled for and the sampling frequency of the laboratory-based cultures. The frequency of sampling given is at its maximum frequency and is not correct for the whole experiment. Sampling frequency was reduced to conserve culture volume, at times when the action of the culture was already known or activity was at its lowest, *i.e.* immediately after inoculation and in stationary phase.

For all experiments samples were taken in the light period and all ^{14}C incubations were made in the light. If one sample per day of any parameter was made this was taken 8 hours into the light period, and if two samples per day were taken these were made one hour into the light period and one hour before the end of the light period. Incubations which were carried out twice per day were timed for the first to begin one hour after the start of the light period and the second to end one hour before the end of the light period.

Expt number	Expt duration /days	Species / strain	Initial nutrient concentrations / N µM: P µM	Water bath / Constant temp room	^{14}C		
						Filter fume / Split vial	Formalin-killed control
#1	22	*E. huxleyi* / 92E	16:2/16:1/16:0.5	Water Bath	1 day^{-1}	Filter fume	N
#2	16	*E. huxleyi* / 92E	16:2/16:1/16:0.5	Water Bath	2 day^{-1}	Filter fume	N
#3	21	*E. huxleyi* / CCAP 920/2 + *I. galbana* / CCAP 927/1	16:1	Constant Temp Room	2 day^{-1}	Split vial	Y

Expt	pH and alkalinity				Cell count		[DIN]	[DIP]
		Reps[a]	ATC probe[b]	Alkalinity diff[c]		Motility		
#1	1 day^{-1}	1	N	Y	1 day^{-1}	N	1 day^{-1}	1 day^{-1}
#2	2 day^{-1}	3	Y	Y	2 day^{-1}	Y	1 day^{-1}	1 day^{-1}
#3	2 day^{-1}	3	Y	Y	2 day^{-1}	N/A	1 day^{-1}	1 day^{-1}

Table 2.1.2 showing the sampling regime for laboratory-based culture experiments

Key: [a] Replications made for pH and alkalinity measurement

[b] pH probe with automatic temperature compensation was used

[c] pH of acidified unfiltered samples was taken

2.2 Norway mesocosm experiments

Between 6th June and 5th July 1995 mesocosm experiments were conducted in Espegrend field station at the University of Bergen Field station in Norway. The aim of these experiments was to investigate the growth of *E. huxleyi* in seawater enclosures (mesocosms) in the Raunefjord, 14km south of Bergen. Mesocosms have been used since the early 1960s to study the growth of marine phytoplankton populations (Anita *et al.*, 1963; McAllister, Parsons and Strickland, 1961). The water and phytoplankton community inside the mesocosms respond to the natural fluctuations of temperature and irradiance with populations of phytoplankton showing similar development to those occurring in the surrounding water (Kuiper, 1977; Takahashi *et al.*, 1975). Other studies have shown that the succession of phytoplankton in the enclosures was a miniature and typically accelerated representation of that found in the natural environment (Davies, 1982).

A raft, anchored 200m from the shore of the field station, was used to secure a series of eight transparent polyethylene bags (mesocosms), which were 4.5m long and 2m in diameter, giving a nominal volume of $11m^3$. The mesocosms were situated on the southern side of the raft in a line running east to west. Bags were filled with fjord water pumped from below the raft. When appropriate nutrient additions were made to selected bags. These were added for silicates in the form of sodium metasilicate ($NaSiO_3.5H_2O$ solution); for nitrates in the form of sodium nitrate ($NaNO_3$, Analar); and for phosphates in the form of potassium phosphate (KH_2PO_4, Analar). On the addition of nutrients air uplifts were switched on to begin the mixing process and create a homogenous water column. The water in the bags was continuously replaced by fjord water at a dilution rate of 10% per day and additional nutrients were added to compensate for this dilution. The use of the airlift was not thought to adversely affect the concentration of dissolved CO_2 in the mesocosms. The mesocosms sampled for this study were collected from; a mesocosm to which additions of 15μM nitrate, 1μM phosphate and 10μM silicate were made (Bag 3); and a mesocosm to which additions of 15μM nitrate and 1μM phosphate were made (Bag 5).

2.2.1 Chlorophyll, calcite and phytoplankton analyses and surface irradiance measurements

Water samples for chlorophyll *a* and inorganic nutrients were collected daily between 7-30 and 8-30AM from each mesocosm, and for phytoplankton species enumeration every second day, throughout the experimental period.

Samples for chlorophyll analysis (50 or 100ml) were filtered in triplicate onto 25mm GF/F filters and extracted overnight at 4°C in 10ml of 90% acetone, and chlorophyll fluorescence measured on a Turner fluorometer, before and after the addition of 2 drops of

10% HCl. The fluorometer was calibrated against a chlorophyll *a* standard (Sigma Chemical Co. Ltd.) dissolved in 90% acetone and assayed from absorbance measurements according to the method of Parsons, Maita and Lalli (1984).

Identification and enumeration of phytoplankton was carried out on water samples preserved with neutralised formalin (0.4% final concentration).

Surface irradiance was continuously measured in close proximity to the enclosures and data stored as 15 minute averages using a Li-Cor Li 1000 datalogger.

Phytoplankton and chlorophyll analyses and irradiance measurements were carried out by Dr. J. Egge and D. Lesley.

Samples for calcite were measured from material retained on Whatman GF/F filters after filtration of 0.5l of sample and subsequently frozen at -20°C. Calcite was estimated from the measured calcium content, assuming that all of the particulate calcium was present as calcium carbonate. Calcium concentration was determined by flame atomic absorption spectrometry at 422.7nm wavelength using an air-acetylene flame. Samples were made up with 1% lanthanum chloride.

Calcite analyses were carried out by B. Head at Plymouth Marine Laboratory.

2.2.2 Dark respiration measurements

Water for oxygen incubations was collected in 20l carboys from the surface of bags 3 and 5 every second morning. The carboys were immediately covered with black plastic, to prevent light shock, and kept in shade on the deck of the raft until dispensed into incubation bottles.

Using silicon rubber tubing, water was dispensed into 125ml ground glass stoppered incubation bottles. To avoid bubble formation, and thus exchange with the atmosphere, tubing was pushed as far as possible into the bottles and several bottle volumes (125ml) were allowed to flush through each bottle prior to careful stoppering: bottles with noticeable bubbles were rejected. Four replicate bottles for each mesocosm were immediately "fixed" as "zero time" bottles for initial oxygen concentration. Four replicate "dark" bottles for each mesocosm were placed in a black plastic bag within the header tank which fed the mesocosms with fresh fjord water, this ensured that the dark bottles were incubated at *in situ* temperature; "dark" bottles were incubated for 24 hours. Following incubation "dark" bottles were immediately fixed with oxygen Winkler reagents.

All bottles were titrated using an automated microprocessor-controlled titration based upon the Winkler technique of Williams and Jenkinson (1982). *In situ* temperature and salinity records from the CTD allowed corrections to be made for the thermal expansion of both the

sample and sample bottle. This allowed high precision and accuracy to be achieved in the estimation of dissolved oxygen concentration. Averaged over the whole experiment, standard deviation for 4 replicate titrations was *ca.* 1.4 mmol m^{-3}.

2.2.3 Photosynthesis (P) vs Irradiance (I) and Calcification (C) vs Irradiance (I) incubations

Samples were taken at the same time (*ca.* 9-00AM) on alternate mornings by submerging a 5l plastic container in the mesocosm. Subsamples were next immediately measured into 60ml Nalgene bottles using a cut down 50ml plastic volumetric flask. These subsamples were stored in a light proof insulated container until used in photosynthesis versus irradiance (PvI) incubations in the shoreside laboratory.

During PvI incubations 24x60ml Nalgene flasks were incubated in a light gradient caused by the arrangement of the two rows of twelve flasks in front of a halogen light source. The temperature of the incubator was daily adjusted to that within the mesocosms. Irradiance was measured with a quantum meter Model Q.101 connected to a cosine collector sensor (Macam Photometrics Ltd.). The highest light levels of these PvI incubations did not fluctuate significantly between incubations, and was minimised by allowing the equipment to warm up for at least one hour before incubations started. The light levels between incubations may not remain constant with time due to the influence of both physical and biological parameters upon the optical properties of the sample water, *e.g.* decreasing transmission due to increase in phytoplankton biomass

For PvI incubations the whole sample was filtered unless the cell density was too high resulting in clogged the filters or slow filtration rates. In these cases the filtration volumes were reduced as necessary. 10μCi of ^{14}C labelled $NaHCO_3$ was added to each sample bottle. 100μl subsamples were taken in triplicate immediately after the addition of ^{14}C radiotracer and added to a 5ml plastic scintillation vial containing 100μl of phenyethylamine to trap the added $NaH^{14}CO_3$ (Iverson, 1976). 2ml of scintillation cocktail (Optiphase 'HiSafe' 3 (Wallac Scintillation Products)) was then added to the scintillation vial.

During PvI incubations one bottle was blacked out using electrical insulation tape as a dark control and one bottle was killed immediately after subsamples had been taken by the addition of 1ml of 20% sodium tetraborate buffered formalin solution as a killed control (Steedmann, 1976; Throndsen, 1978).

After the completion of incubation all flasks awaiting filtration were stored in the dark. Filtration took place under low light conditions with the samples being filtered through 25mm diameter 0.40μm pore polycarbonate filters under a low vacuum (<10mmHg). Filters were rinsed with 2x20ml of GF/C filtered fjord water from the appropriate mesocosm. Stock solution preparation, and separation of ^{14}C fixation due to calcification and photosynthesis was using

the split vial method, was as described in the laboratory-based culture methods sections 2.1.9 and 2.1.11 respectively.

Photosynthesis (P) vs Irradiance (I) and Calcification (C) vs Irradiance (I) data were fitted to the following model of Webb, Newton and Star (1974) using a non-linear curve fitting routine in the program Sigmaplot for Windows (Jandel Scientific):

$$P = P_{max}[1-\exp(-I.\alpha/P_{max})]$$

where P is the ^{14}C photosynthesis or calcification rate ($\mu molC\ l^{-1}\ h^{-1}$) and P_{max} is the maximum photosynthetic or calcification rate. I is the irradiance ($\mu E\ m^{-2}s^{-1}$) and a is the initial slope ($\mu molC\ l^{-1}h^{-1}(\mu E\ m^{-2}s^{-1})^{-1}$). The data showed little evidence of photoinhibition of photosynthesis or calcification over the range of irradiance used.

2.2.4 Calculation of Buffer Factors and C:P from A_T vs C_T slope

Seawater has the ability to buffer changes in carbon dioxide through the equilibrium of dissolved inorganic carbon, and some analytical expressions have been developed to describe the effect of dissolved CO_2 input/output to seawater (Skirrow, 1975). The buffer factor used for these results is the homogenous buffer factor (β) which depicts the relationship between PCO_2 and C_T and can be defined as:

$$\beta = (\Delta PCO_2/PCO_2)/(\Delta C_T/C_T)$$

where ΔPCO_2 is the shift following an increase in PCO_2 and ΔC_T the consequential increase in C_T (Stumm and Morgan, 1985; Sundquist, Plummer and Wigley 1979). The homogenous buffer factor can be obtained from a data set by plotting $lnPCO_2$ versus lnC_T, and the slope of a regression line should equal b (Robertson *et al.*, 1994). This factor is called the Revelle factor when CO_2 is involved in exchange at the air-sea interface, and has a value of about 12 for average seawater conditions (Frankignoulle *et al.*, 1996). The buffer factor (β) can be significantly different from 12 if processes other than the air-sea exchange of CO_2 occur, *e.g.* through changes in alkalinity changes brought about by calcification in coccolithophores (Robertson et al. 1994). The range of b can be theoretically calculated if solely calcification or photosynthesis is occurring *e.g.* assuming a temperature of 10^0C, salinity of 35 psu, initial C_T of $2100\mu mol\ kg^{-1}$, PCO_2 of $294\mu atm$ and A_T of $2350\ \mu eq\ kg^{-1}$; β should range from 9.5 to -8.2 depending on whether just photosynthesis or calcification is taking place respectively (Robertson *et al.*, 1994). This was also calculated theoretically by Crawford and Purdie (1997) who found that under similar assumptions as Robertson *et al.* (1994), with simultaneous calcification and photosynthesis β was in the range of 10.3 to -9.4.

As noted in the introduction section 2.2.2 during organic production the change in unit A_T for a change in unit C_T is slight, being dependent on the removal of the NO_3^- ion in the formation of organic matter. During calcification there will be an effect on the A_T due to the uptake of HCO_3^- for which each double unit change of A_T there should be one unit change in C_T due to the production of CO_2 in calcification. The relationship between alkalinity (including nitrate) and C_T can therefore be summarised assuming a given ratio of x:1 units of organic to inorganic growth from Robertson *et al.* (1994):

	Organic production	Calcification
ΔC_T	$-x$	-1
ΔA_T	0	-2

In order to incorporate NO_3^- removal, without knowing NO_3^- concentration and assuming a C:N ratio of 6.7:1, this relationship will be altered to (D.W.Crawford, pers. comm.):

	Organic production	Calcification
ΔC_T	$-x$	-1
ΔA_T	$+0.15x$	-2

Therefore to calculate the ratio for the combined inorganic and organic uptake the slope (m) of ($\Delta A_T/\Delta C_T$) must equal $(2-0.15x)/(1+x)$ and hence $m = (2-0.15x)/(1+x)$. A regression line fitted to the slope of an A_T vs C_T plot can therefore give a value for the ratio of calcification to photosynthesis (C:P).

CHAPTER THREE : BATCH CULTURE EXPERIMENT RESULTS

These results are the culmination of a series of batch culture experiments studying the effect of calcifying and non-calcifying phytoplankton on the marine carbonate system. The first batch culture experiment used a high-calcifying strain of *Emiliania huxleyi* grown in defined artificial seawater media. This was superseded by the second batch culture again using the high-calcifying *E. huxleyi* strain but increasing the resolution of the parameters investigated. The final batch culture replicated the conditions of the previous experiments but used a low-calcifying strain of *E. huxleyi* and *Isochrysis galbana*, a non-calcifying phytoplankton, to compare their effects on the marine carbonate system.

3.1.1 Batch culture #1

For this experiment a high-calcifying strain of *E. huxleyi*, 92E, was used and was inoculated into three culture vessels containing 10l of artificial media. The initial nutrient concentrations in each of the three cultures were set at: 16μM nitrate and 0.5μM phosphate (0.5P); 16μM nitrate and 1μM phosphate (1.0P); and 16μM nitrate and 2μM phosphate (2.0P). Cultures were incubated in a 16 hour light to 8 hour dark diel cycle with all samples taken 8 hours into the light period. The day of inoculation was noted as day 0 and the experiment continued for 23 days.

3.1.2 Cell counts and nutrients

Figure 3.1.1 shows maximum specific growth rate was similar in all three cultures ranging from 1.03 - 1.17 d^{-1} with the maximum cell numbers in proportion with the initial concentration of phosphate, however the maximum specific growth rate (μ_{max}) showed little variation with initial phosphate supply. All cultures were in stationary phase by day 10 although some variation in cell count was seen especially in the highest phosphate culture.

Nitrate concentration in all cultures (Fig. 3.1.2) remained at approximately 16μM until initiation of exponential growth phase during which nitrate was rapidly depleted with the uptake rates of 0.5P and 2.0P lower than 1.0P. The data for this figure is incomplete as a number of samples taken were lost during analysis.

Phosphate concentration (Fig. 3.1.3) similarly showed an initial plateau during lag phase but was rapidly depleted at the end of exponential growth phase or early stationary phase in all cultures. The rate of phosphate depletion in each of the cultures was shown to be

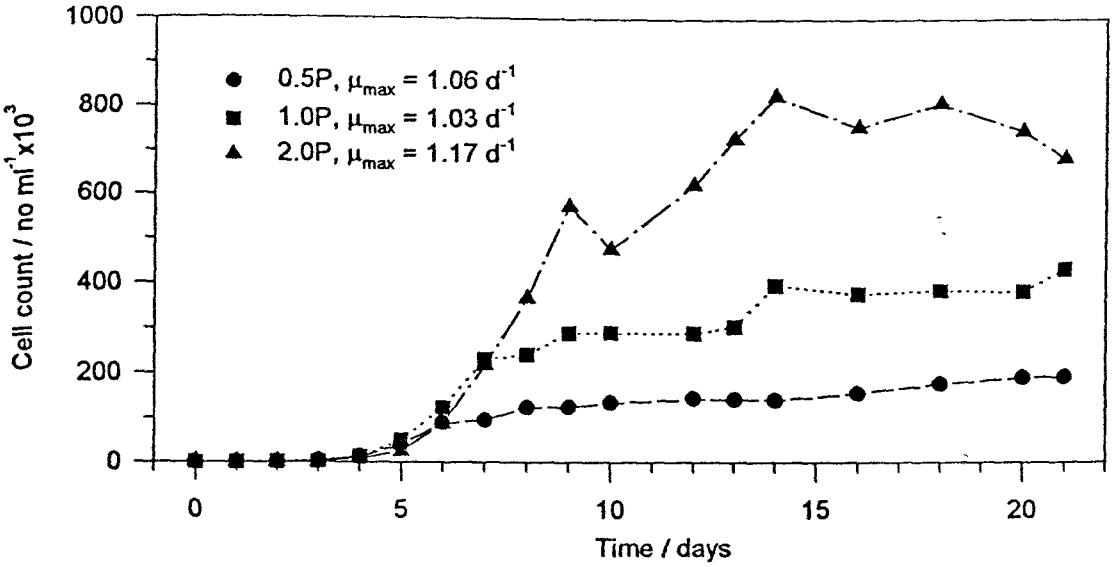

Figure 3.1.1Cell counts determined for high-calcifying *E. huxleyi* batch cultures

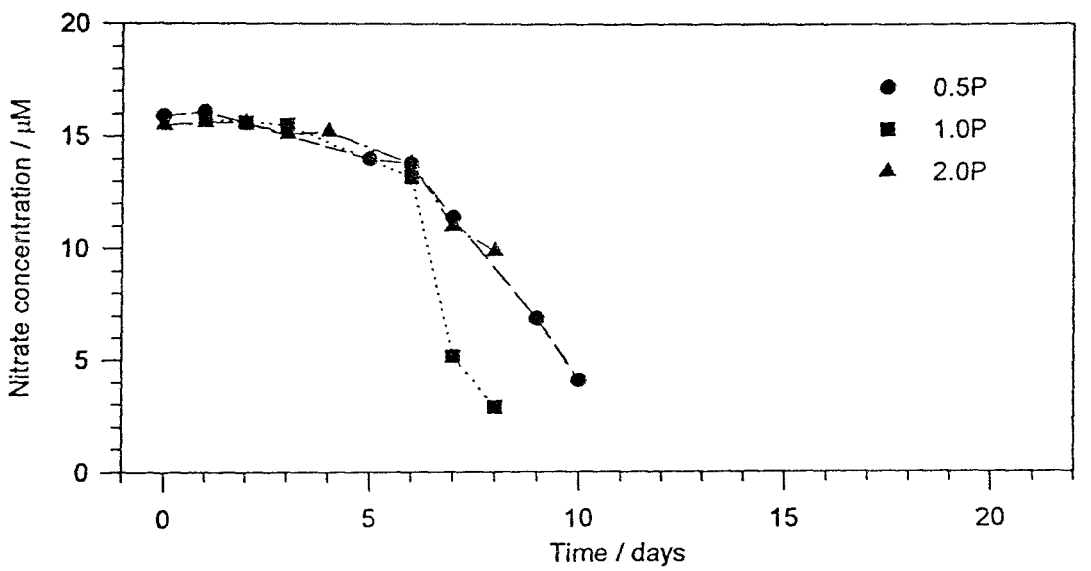

Figure 3.1.2 Temporal variation of nitrate concentration for high-calcifying *E. huxleyi* batch cultures

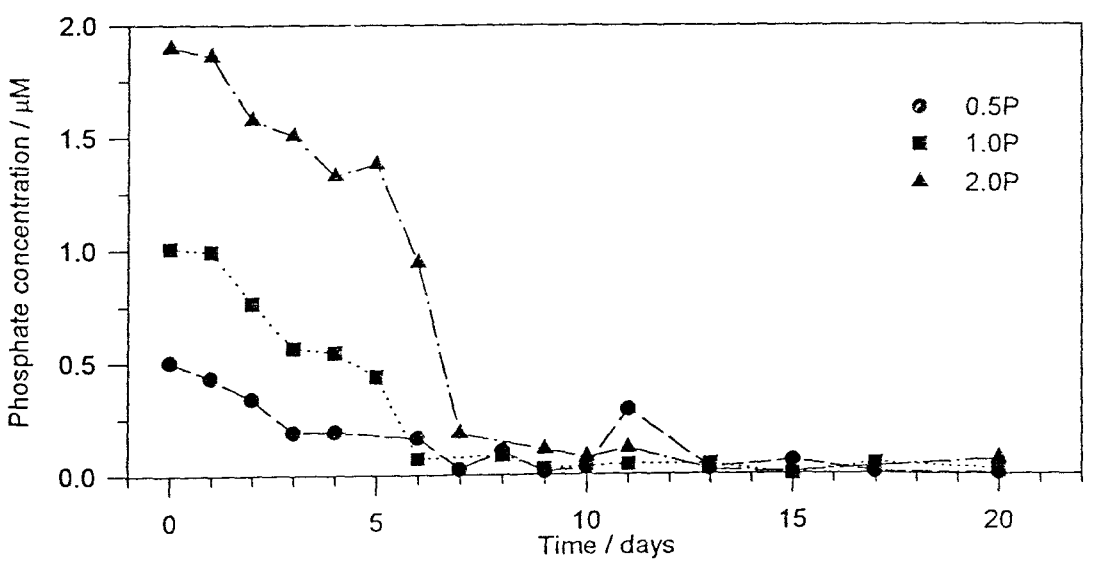

Figure 3.1.3 Temporal variation of phosphate concentration for high-calcifying *E. huxleyi* batch cultures

influenced by the initial phosphate concentration. The phosphate concentration then remained close to the detection limit (±0.02μM) for the remainder of the experiment.

3.1.3 Dissolved carbonate system

pH was initially adjusted to 8.0 in all three cultures to define the same initial PCO_2 (Fig. 3.1.4). The pH initially declined over the first three days in all cultures during the lag phase to between 7.9 and 8.0 and then increased to a maximum on day 8 for 0.5P and 1.0P, and on day 10 for 2.0P, at maximum cell numbers. The pH then showed some variation as the three cultures entered stationary phase with 0.5P maintaining the lowest pH and 2.0P the highest.

The total alkalinity (A_T) and carbonate alkalinity (A_C) (Figs. 3.1.5 - 3.1.6) show similar changes throughout the experiments as expected, with the difference being mainly due to the addition of the borate ion to total alkalinity. Alkalinity showed a slight decrease towards the end of exponential phase in all cultures with 1.0P and 2.0P declining at a similar rate and levelling off on day 14. Alkalinity in 0.5P culture decreased at a lower rate throughout the stationary phase.

PCO_2 and $CO_{2(aq)}$ increased during lag phase in all cultures (Fig. 3.1.7) and then declined at a similar rate during exponential and early stationary growth phases. PCO_2 in 1.0P and 2.0P levelled on days 10 and 12 respectively and remained stable until day 20 when a small increase was detected. PCO_2 in 0.5P culture levelled out earlier on day 8 and then increased reaching a maximum on day 15 followed by a further decline. The initial increase in PCO_2 during lag phase was caused in earlier studies by a concommitant increase in bacterial numbers during lag phase. Bacterial numbers then rapidly declined as the cultures entered exponential growth phase (pers. observation).

The total dissolved inorganic carbon (C_T) concentration (Fig. 3.1.8) showed similar changes to alkalinity in all cultures. C_T showed a slight decrease towards the end of exponential phase in all cultures with 1.0P and 2.0P declining at a similar rate and levelling off on day 14. C_T in 0.5P culture decreased at a lower rate throughout the stationary phase.

3.1.4 ^{14}C uptake measurements

^{14}C uptake (Figs. 3.1.9-3.1.11) showed that for all cultures the maximum rate of both photosynthesis and calcification occurred as cells entered stationary phase. The maximum rates of photosynthesis and calcification reflected the maximum cell numbers for each treatment with the highest rates in the 2.0P culture. During exponential growth phase the rates of calcification and photosynthesis were comparable but as the cultures entered stationary

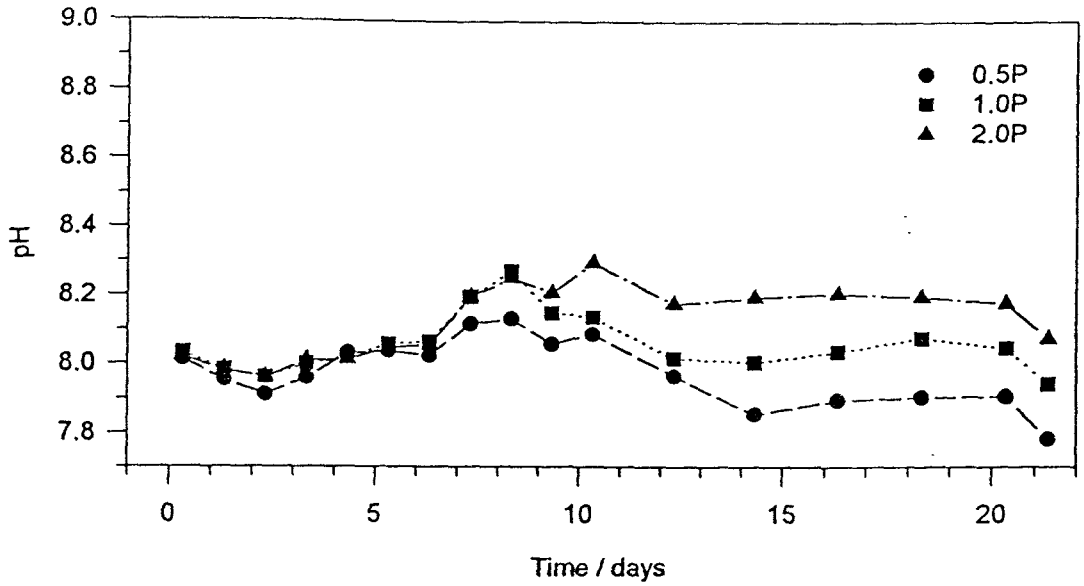

Figure 3.1.4 Temporal variation of pH for high-calcifying *E. huxleyi* batch cultures

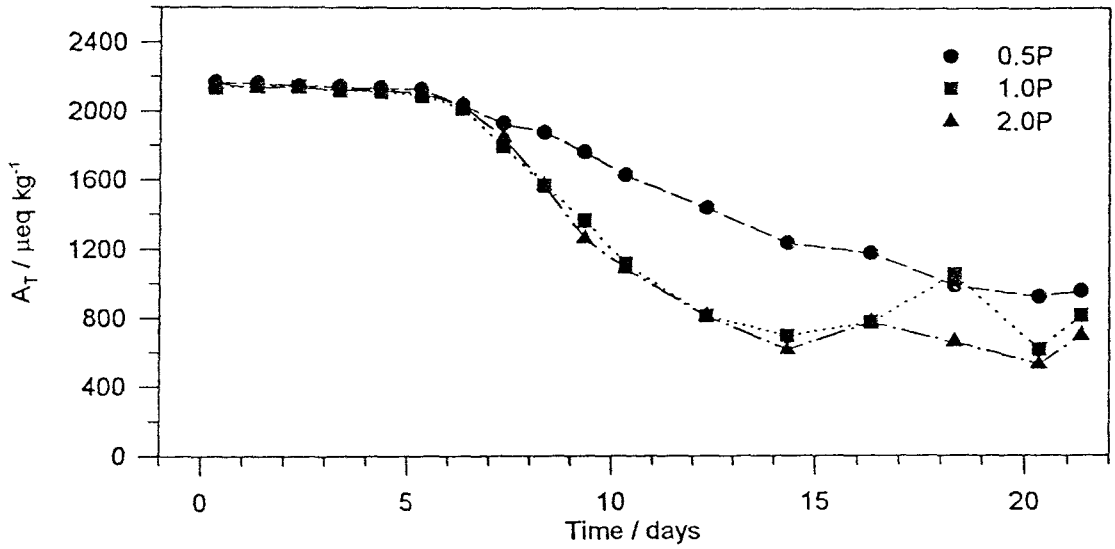

Figure 3.1.5 Temporal variation of total alkalinity for high-calcifying *E. huxleyi* batch cultures

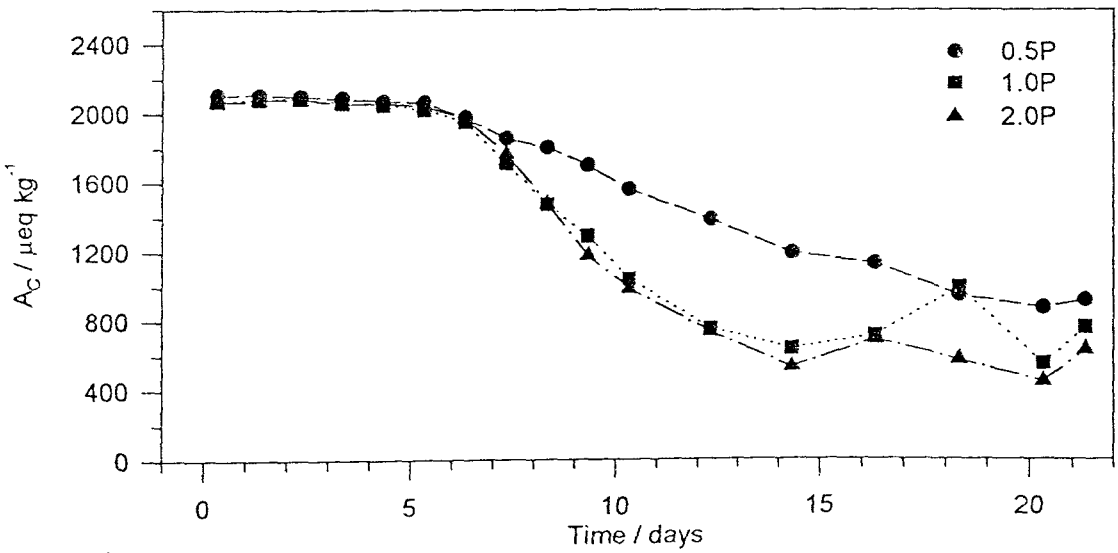

Figure 3.1.6 Temporal variation of carbonate alkalinity for high-calcifying *E. huxleyi* batch cultures

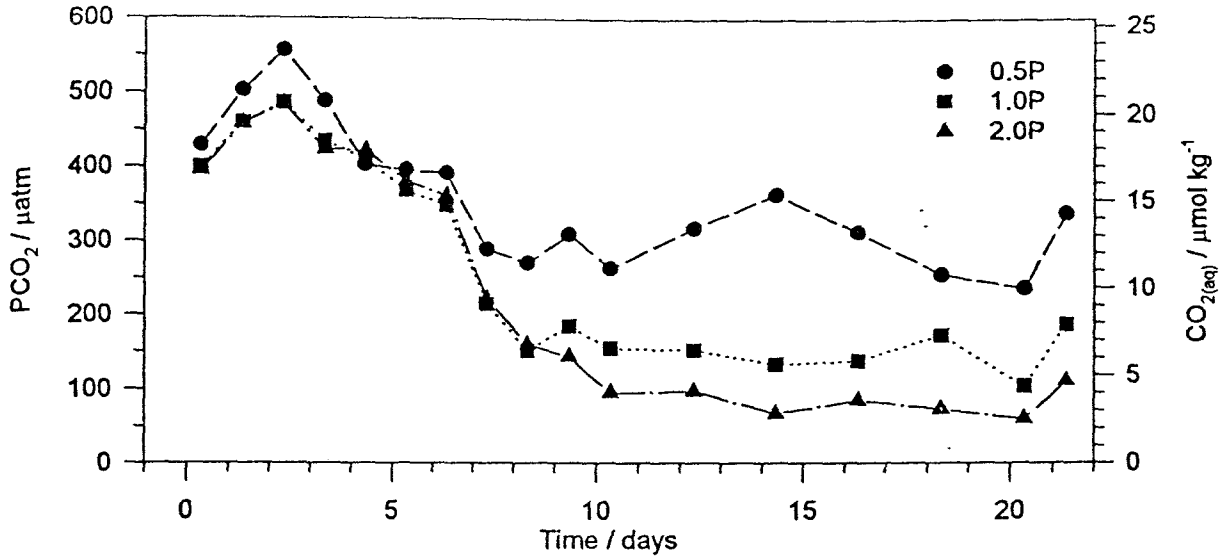

Figure 3.1.7 Temporal variation of PCO_2 and dissolved carbon dioxide for high-calcifying *E. huxleyi* batch cultures

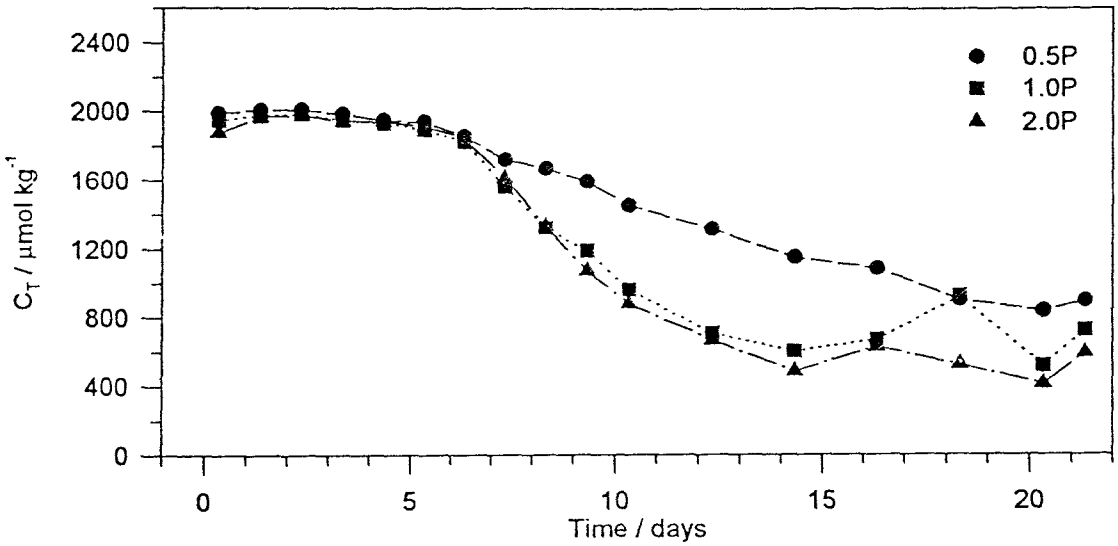

Figure 3.1.8 Temporal variation of total dissolved inorganic carbon for high-calcifying *E. huxleyi* batch cultures

phase the rates of calcification declined relative to photosynthetic rates. Calcification rates then plateaued in the 0.5P and 1.0P cultures at the end of exponential growth phase. The calcification rate in the 2.0P culture reached a distinct maximum on day 8 followed by a decline to undetectable levels on day 14.

The photosynthetic and calcification rates per cell have a slightly reduced data set because errors in the initial cell counts were too large to produce comparable data for the first ^{14}C incubation. In figures 3.1.12-3.1.14 the maximum photosynthetic rate per cell in all cultures showed a general downward trend from a peak in early exponential growth phase. Calcification per cell data follows the same trend apart from the first point on day 4 which was significantly lower. The relative rate for photosynthesis per cell was approximately equal between cultures but the maximum rate of calcification per cell increased with higher initial phosphate concentration.

Figures 3.1.15-3.1.17 show the ratio of calcification to photosynthesis (C:P). In cultures 0.5P and 2.0P the maximum C:P occurred in late exponential growth phase followed by a lesser secondary peak at the start of stationary growth phase. C:P then declined to zero as calcification became minimal. A peak in C:P during exponential growth phase was also noted for 1.0P but was followed by a second peak showing the maximum C:P. There was a correlation between initial phosphate concentration and maximum C:P with the highest C:P in the 2.0P culture. The maximum C:P was not directly proportional to the initial phosphate concentration. A C:P ratio of close to 1 was only measured in the high phosphate culture during mid-exponential growth phase.

3.1.5 Alkalinity derived calcite standing stock

Figure 3.1.18 shows the changes in standing stock of calcite derived from alkalinity measurements made on filtered and unfiltered culture samples. There was an indication of increase in net calcite standing stock with increased initial phosphate concentration. Particulate inorganic carbon (PIC) showed a slight increase towards the end of exponential phase in all cultures with 1.0P and 2.0P declining at a similar rate and levelling off on day 14. PIC standing stock in 0.5P culture continued to increase, at a lower rate, throughout the stationary phase. The total net calcification rate, calculated from the alkalinity derived PIC (Fig. 3.1.19), showed a maximum for all cultures between on day 9 for 2.0P and day 8 for both 0.5P and 1.0P (if the anomalous result on day 19 is not taken into account). After day 11 a decline towards and below zero occurred for all cultures, *i.e.* due to dissolution of calcite. There was a relationship between initial phosphate concentration and maximum total calcification rate with the highest rate in the 2.0P culture but its significance is equivocal.

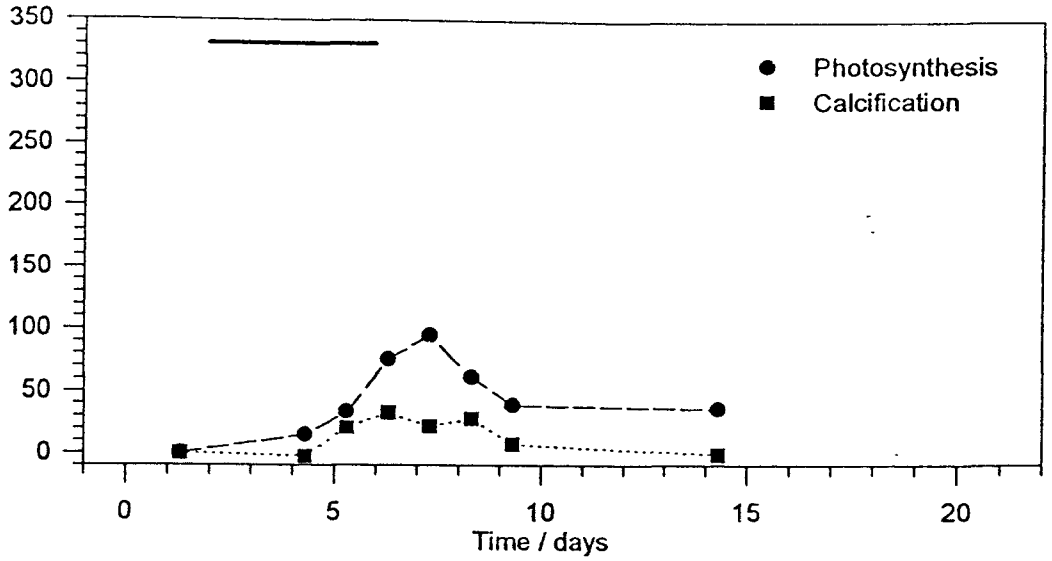

Figure 3.1.9 Total rates of ^{14}C uptake for 0.5P batch culture for high-calcifying *E. huxleyi* (Bar indicates exponential growth phase)

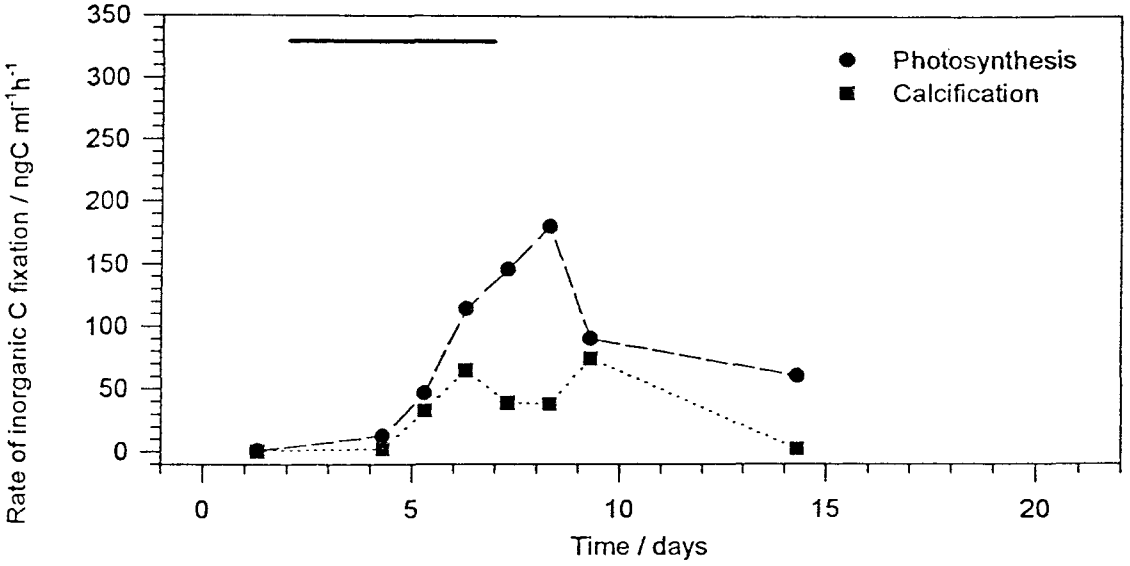

Figure 3.1.10 Total rates of ^{14}C uptake for 1.0P batch culture for high-calcifying *E. huxleyi*

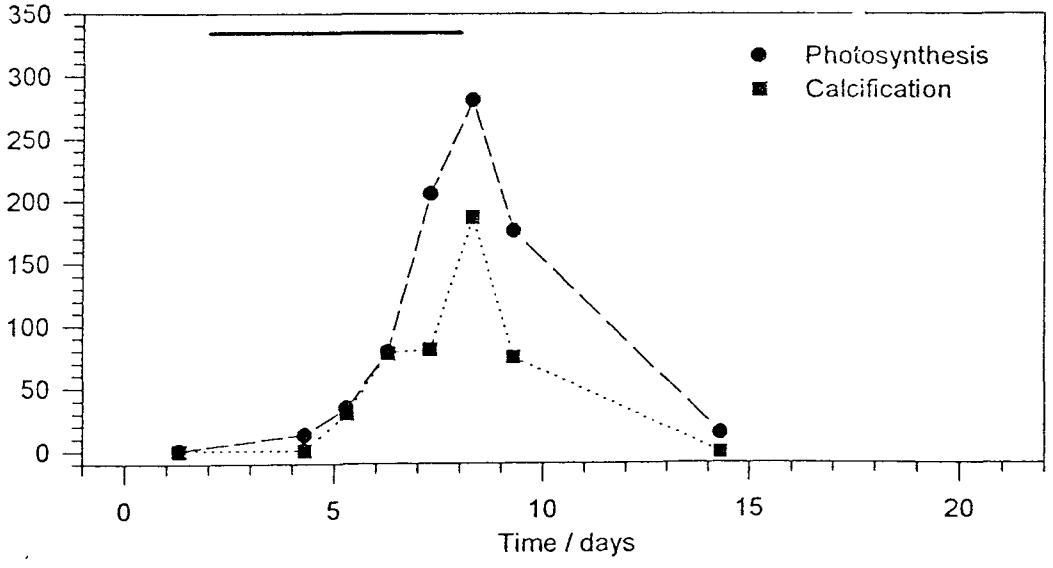

Figure 3.1.11 Total rates of ^{14}C uptake for 2.0P batch culture for high-calcifying *E. huxleyi*

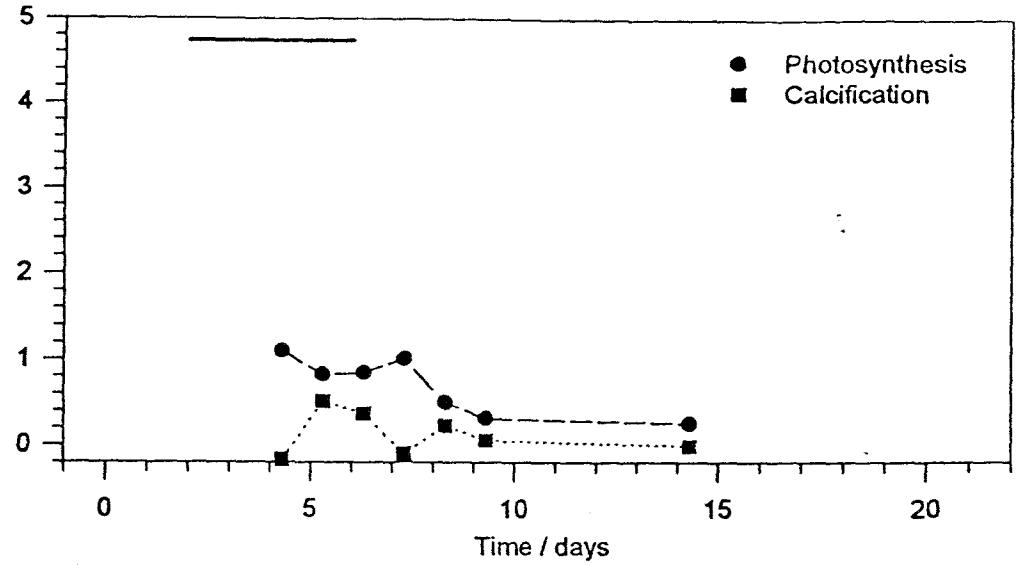

Figure 3.1.12 Rates of ^{14}C uptake per cell for 0.5P batch culture for high-calcifying *E. huxleyi*

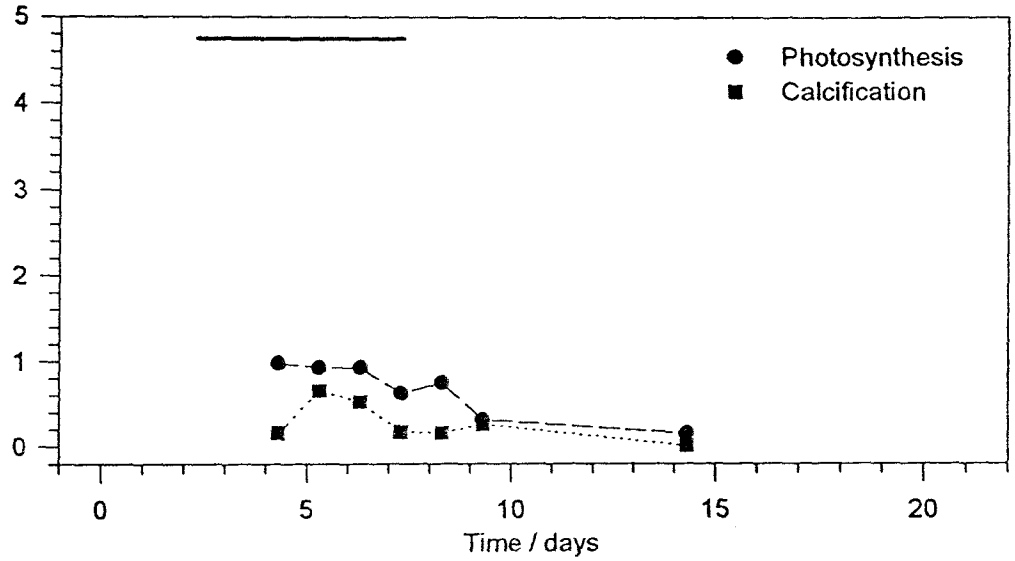

Rate of inorganic C fixation / pgC cell^{-1} h^{-1}

Figure 3.1.13 Rates of ^{14}C uptake per cell for 1.0P batch culture for high-calcifying *E. huxleyi*

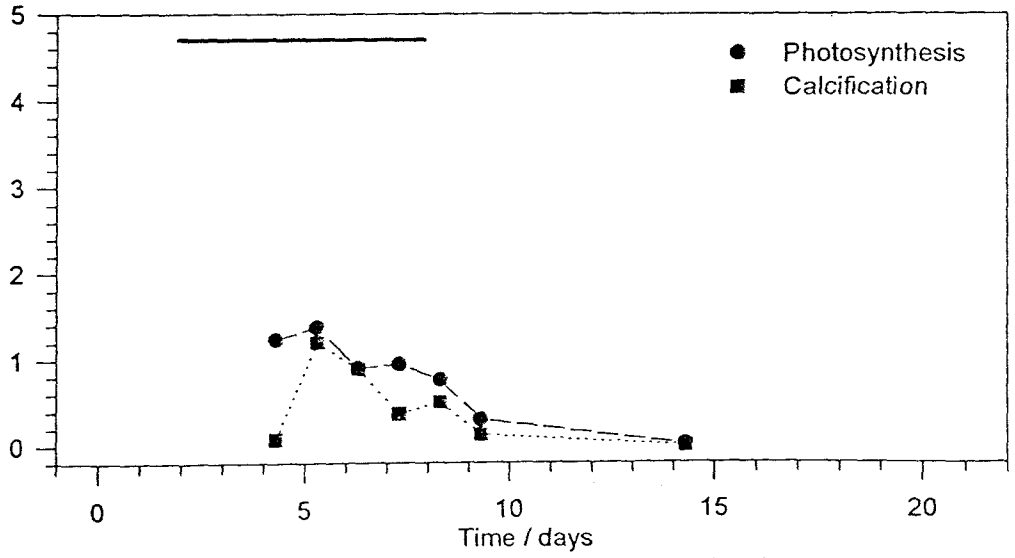

Figure 3.1.14 Rates of ^{14}C uptake per cell for 2.0P batch culture for high-calcifying *E. huxleyi*

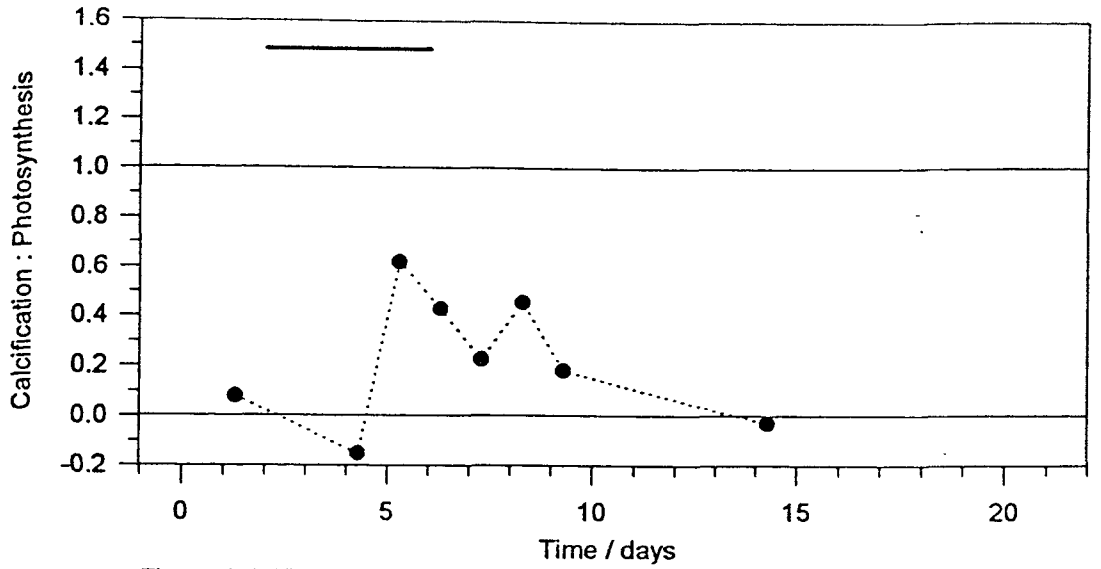

Figure 3.1.15 Temporal variation in ratio of calcification to photosynthesis for 0.5P batch culture for high-calcifying *E. huxleyi*

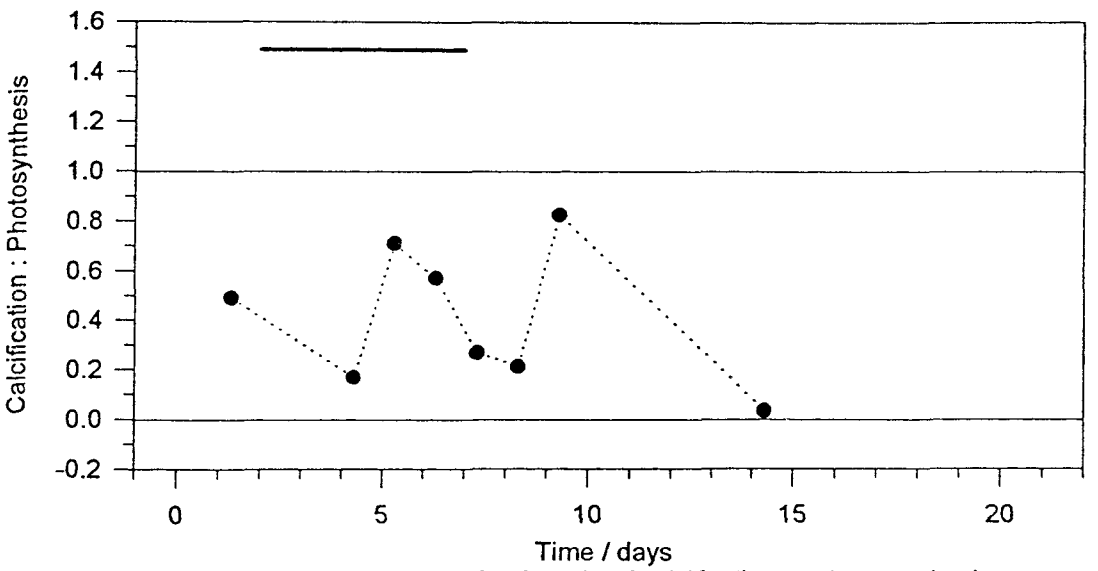

Figure 3.1.16 Temporal variation in ratio of calcification to photosynthesis for 1.0P batch culture for high-calcifiying *E. huxleyi*

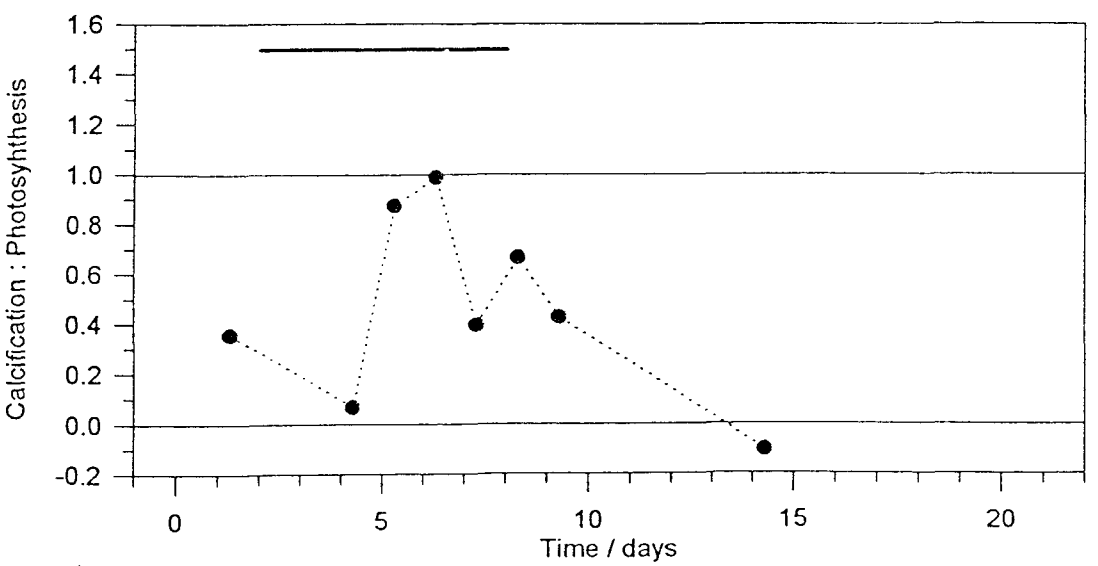

Figure 3.1.17 Temporal variation in ratio of calcification to photosynthesis for 2.0P batch culture for high-calcifying *E. huxleyi*

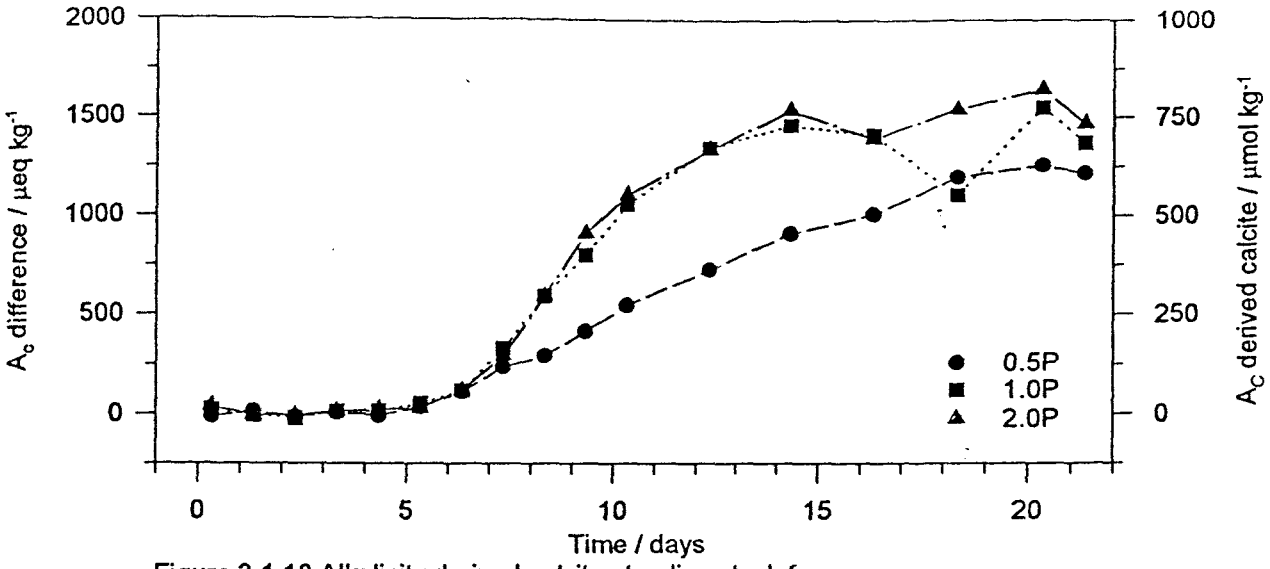

Figure 3.1.18 Alkalinity derived calcite standing stock for high-calcifying *E. huxleyi* batch cultures

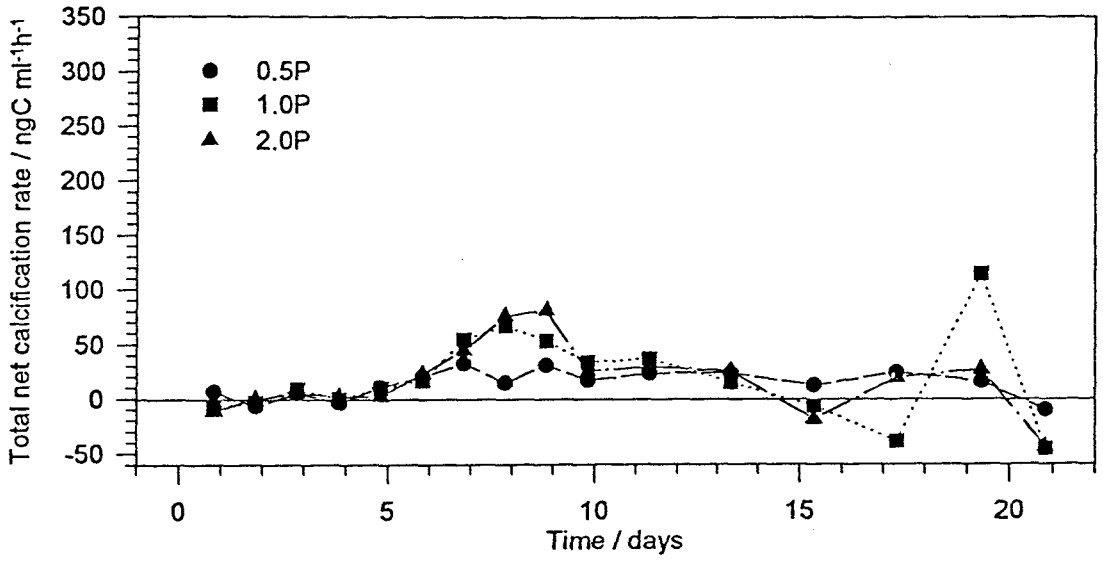

Figure 3.1.19 Carbonate alkalinity derived total net calcification rates for high-calcifying *E. huxleyi* batch cultures

3.1.6 Total dissolved inorganic carbon (C_T) vs total alkalinity (A_T) plots and buffer factor plots

During the initial growth phases the buffer factor (β) was higher than in stationary phase for all cultures (Figs. 3.1.20-3.1.22). The buffer factor showed no relationship with the initial phosphate concentration during the initial growth phases, but showed an increase relative to initial phosphate in the stationary growth phase with 2.0P buffer factor reaching the highest value of 0.76.

The C:P, calculated from C_T vs A_T slope, (Figs. 3.1.23-3.1.25) was lower during the lag and exponential growth phases than the stationary phase in all cultures. C:P reached a maximum in the stationary phase of all cultures with 0.5P and 2.0P showing similar values of *ca.* 1.5 and 1.0P showing the maximum C:P of 1.57.

3.1.7 Summary of results from batch culture #1

Results from this experiment showed initial phosphate concentration controlled the final yield of cells, but had little influence on maximum specific growth rate. The initial phosphate concentration did however appear to influence the phosphate uptake rate derived from phosphate depletion in the media.

In all cultures a decline in alkalinity occurred as expected for calcifying phytoplankton. In cultures 1.0P and 2.0P the growth of *E. huxleyi* had similar effects on the dissolved carbonate system. In the lowest phosphate culture (0.5P) the alkalinity and C_T were not drawn down to the same level and only in this culture an increase in PCO_2 was seen during the stationary phase.

The ^{14}C uptake rates of photosynthesis per cell were comparable in all cultures throughout the course of the experiment but the ^{14}C uptake rates of calcification per cell increased with initial phosphate concentration resulting in the 2.0P culture attaining the highest C:P ratios approaching a value of 1 during mid-exponential growth phase.

Comparison of the results from ^{14}C uptake derived C:P with A_T vs C_T derived C:P showed similar values during the initial growth phases but A_T vs C_T C:P was always significantly greater during stationary phase, with C:P being consistently around 1.5. The A_C derived total net calcification results were all similar to the rates of calcification seen in the ^{14}C incubations, and both also showed maxima on approximately the same day.

Table 3.1.1 shows a summary of these results.

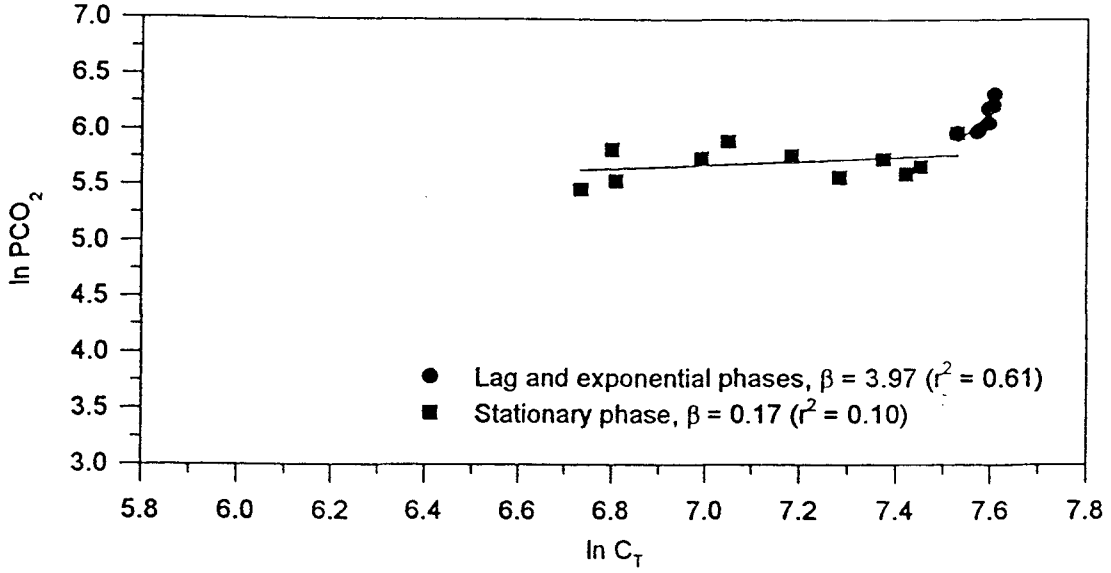

Figure 3.1.20 Plot of lnC_T against $lnPCO_2$ for 0.5P batch culture for high-calcifying *E. huxleyi* (Slope of regression line represents β)

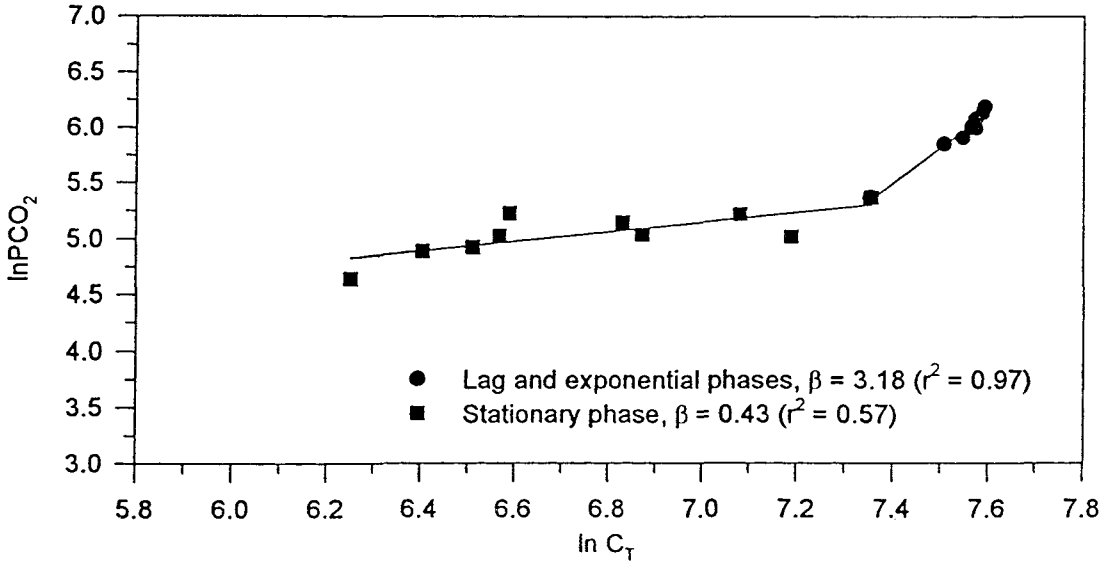

Figure 3.1.21 Plot of lnC_T against $lnPCO_2$ for 1.0P batch culture for high-calcifying *E. huxleyi*

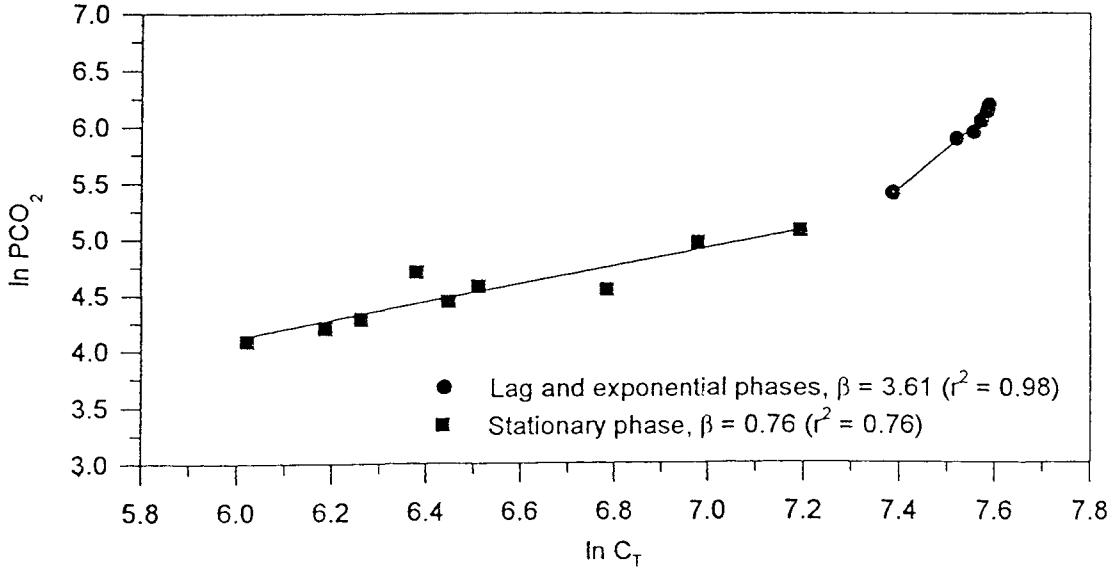

Figure 3.1.22 Plot of lnC_T against $lnPCO_2$ for 2.0P batch culture for high-calcifying *E. huxleyi*

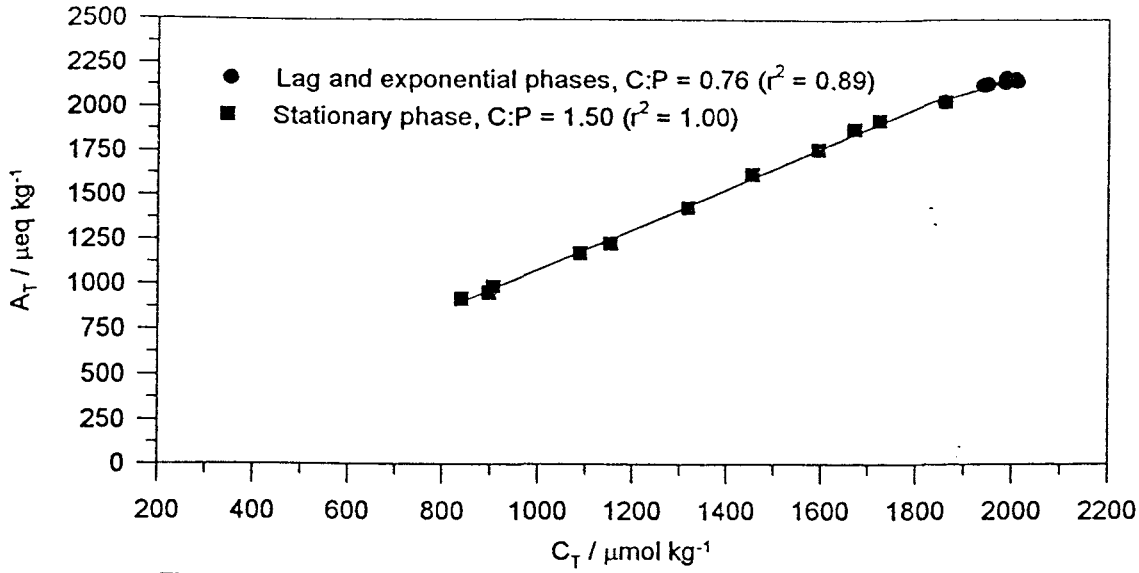

Figure 3.1.23 Plot of C_T against A_T for 0.5P batch culture for high-calcifying *E. huxleyi* (C:P derived from slope of regression)

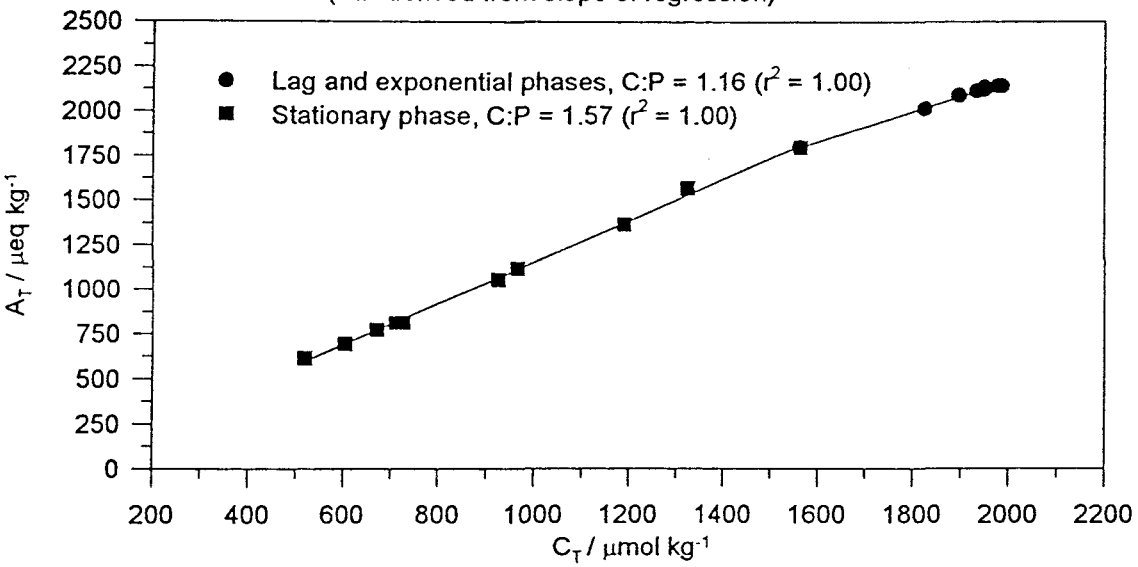

Figure 3.1.24 Plot of C_T against A_T for 1.0P batch culture for high-calcifying *E. huxleyi*

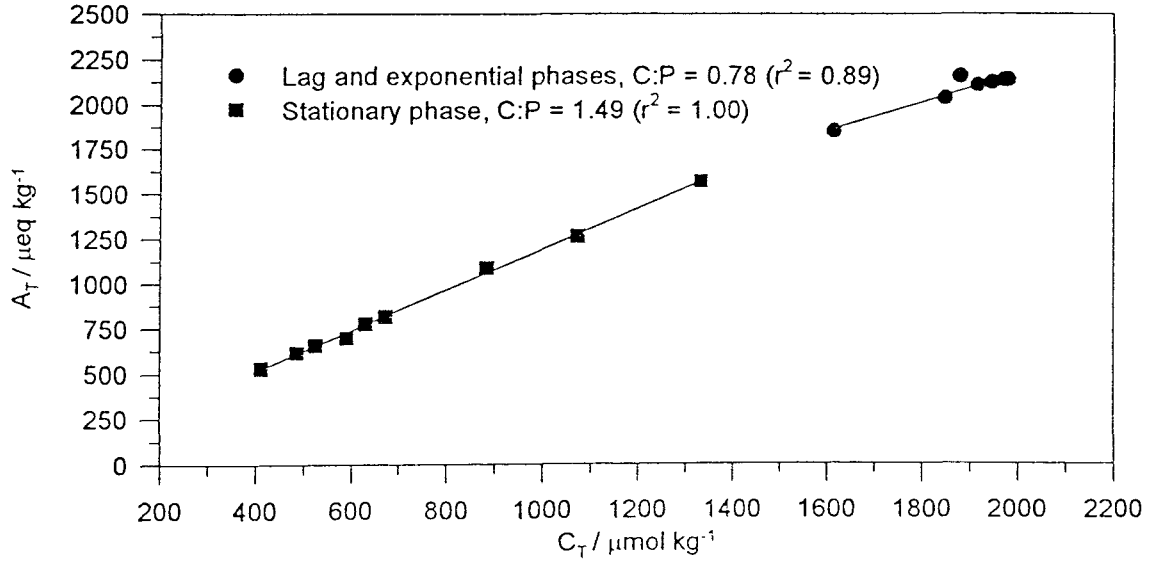

Figure 3.1.25 Plot of C_T against A_T for 2.0P batch culture for high-calcifying *E. huxleyi*

3.2.1 Batch culture #2

The same high-calcifying strain of *E. huxleyi*, 92E, was used in this experiment as in batch culture experiment #1, however the experiment was completed 5 months after the initial experiment. The cultures were grown under the same conditions as in batch culture #1 with the exception of reduced initial PCO_2 levels. The initial nutrient concentrations were again set at: 16μM nitrate and 0.5μM phosphate (0.5P); 16μM nitrate and 1μM phosphate (1.0P); and 16μM nitrate and 2μM phosphate (2.0P). The sampling frequency for all parameters was increased (except for nutrient determinations) to a maximum of twice per day until day 9 then once per day until the end of the experiment (day 15). During the first 9 days the first ^{14}C incubation was started one hour into the light period and the second 12 hours into the light period. All ^{14}C incubation experiments were run for three hours. Samples were taken for alkalinity and pH measurements 2.5 hours and 14.5 hours into the light period from the main culture vessel. Cultures were sampled once daily from day 9, at the mid-point of the light period, as in batch culture #1. The day of inoculation was noted as day 0. The increased sampling frequency in this experiment resulted in a reduction in the length of experimental period to 15 days compared to the 23 day batch culture #1, due to the constraints of total culture volume.

A significant improvement in the methods used to determine alkalinity and pH in this, and latter experiments, was the use of a pH probe and meter which was capable automatically compensating pH measurements for temperature thus improving the accuracy and precision of the derived carbonate system parameters.

3.2.2 Cell counts and nutrients

Figure 3.2.1 shows all cultures had similar maximum specific growth rates ranging from 0.86 - 0.97d^{-1}, being slightly lower than found in batch culture #1. The maximum cell numbers were again directly in proportion with initial phosphorus concentrations but are approximately half the maximum level found in the first batch culture experiment. The maximum specific growth rate (μmax) showed little variation with the initial phoshate concentration, as also noted in experiment #1.

Nitrate concentration (Fig. 3.2.2) in 0.5P and 1.0P cultures declined steadily to below the detection limit on day 8 and 7 respectively as cultures reached maximum cell numbers. After an initial delay during lag phase for 2.0P the nitrate was also depleted to below the detection limit on day 7. This pattern matched that found in the first batch culture experiment.

For all cultures phosphate (Fig. 3.2.3) was depleted as cultures entered stationary phase. The rate of depletion of phosphate in all cultures was again shown to be influenced by the initial phosphate concentration.

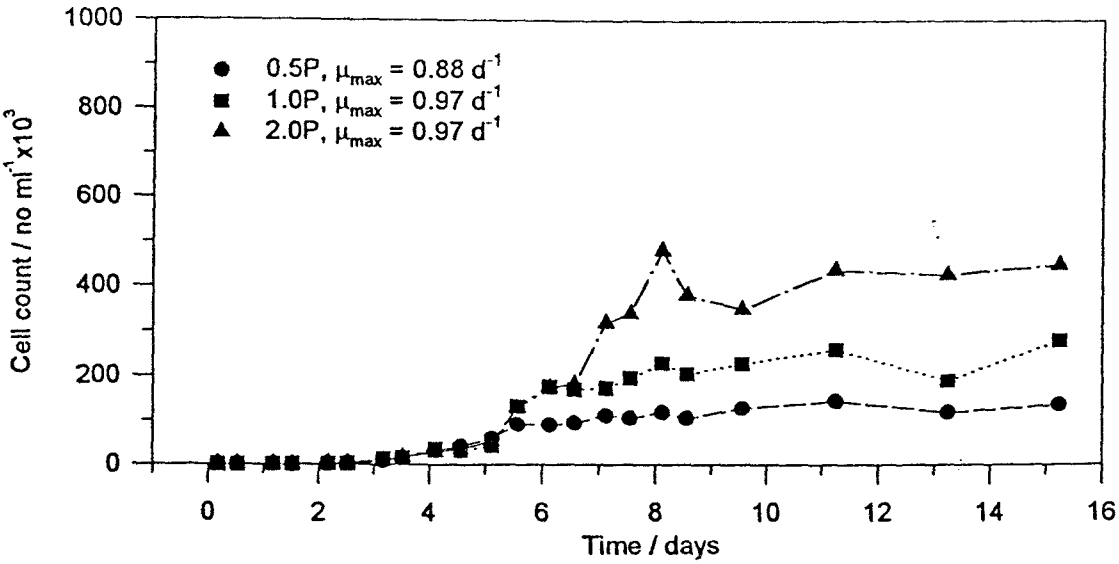

Figure 3.2.1 Cell counts determined for high-calcifying *E. huxleyi* batch cultures

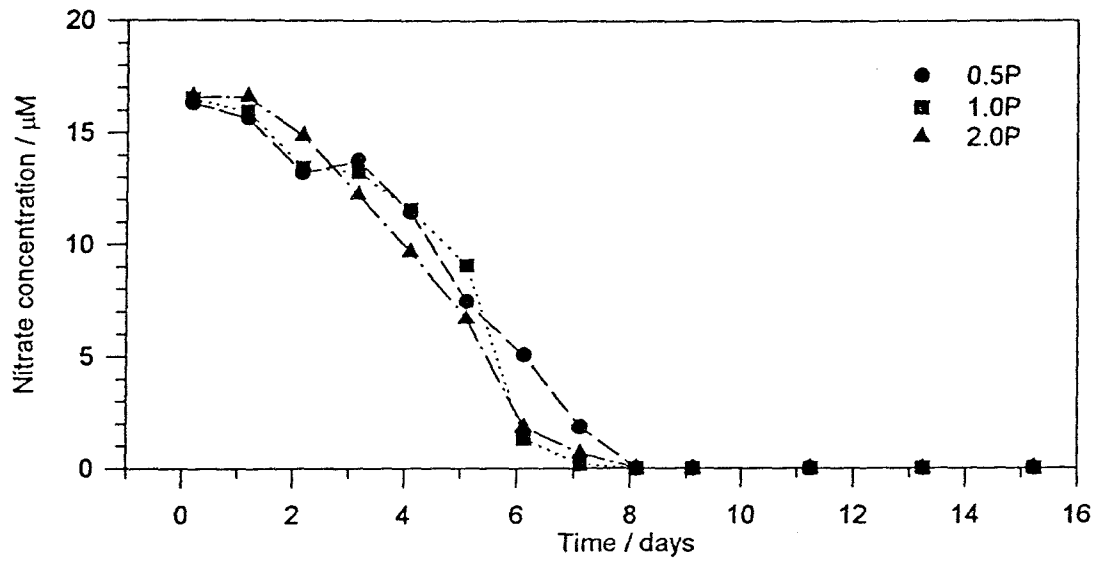

Figure 3.2.2 Temporal variations in nitrate concentrations for high-calcifying *E. huxleyi* batch cultures

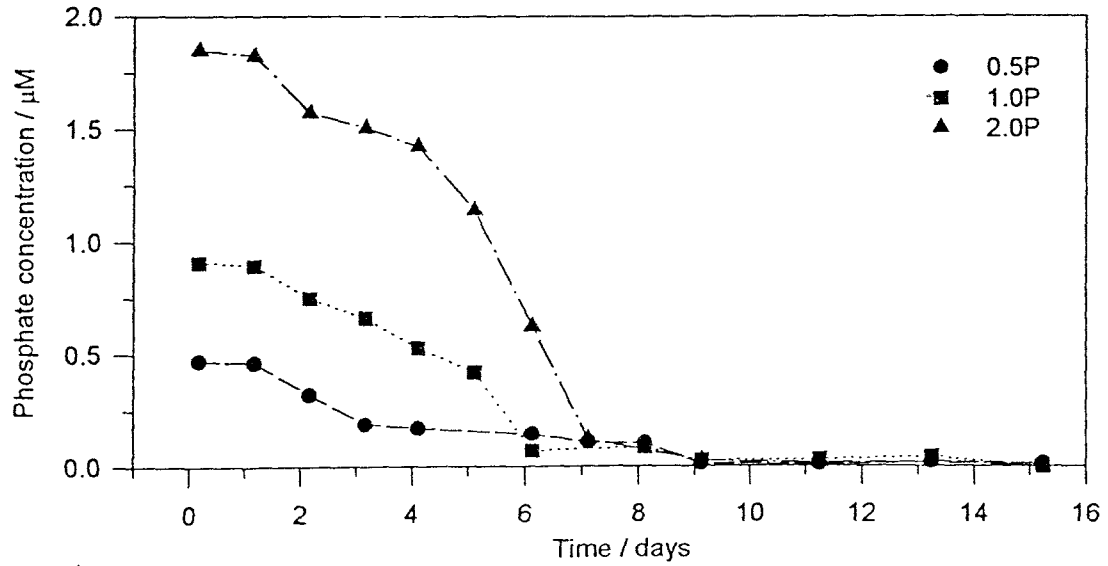

Figure 3.2.3 Temporal variation in phosphate concentrations for high-calcifying *E. huxleyi* batch cultures

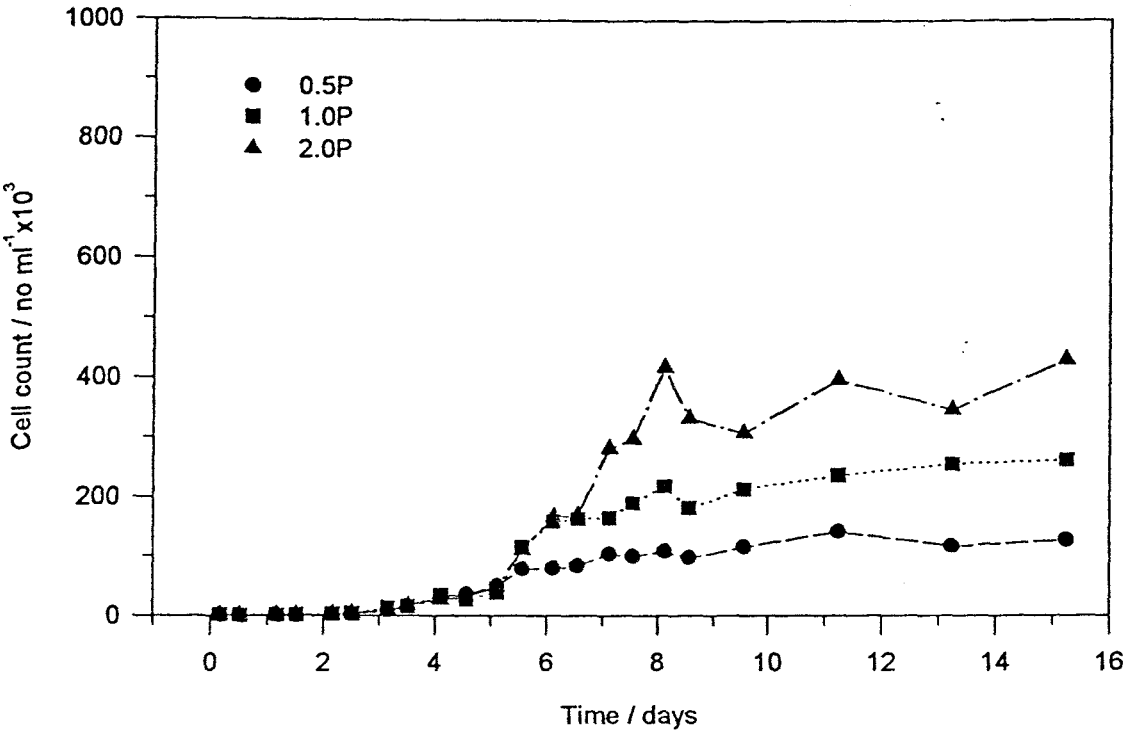

Figure 3.2.4 Non-motile cell counts determined for high-calcifying *E. huxleyi* batch cultures

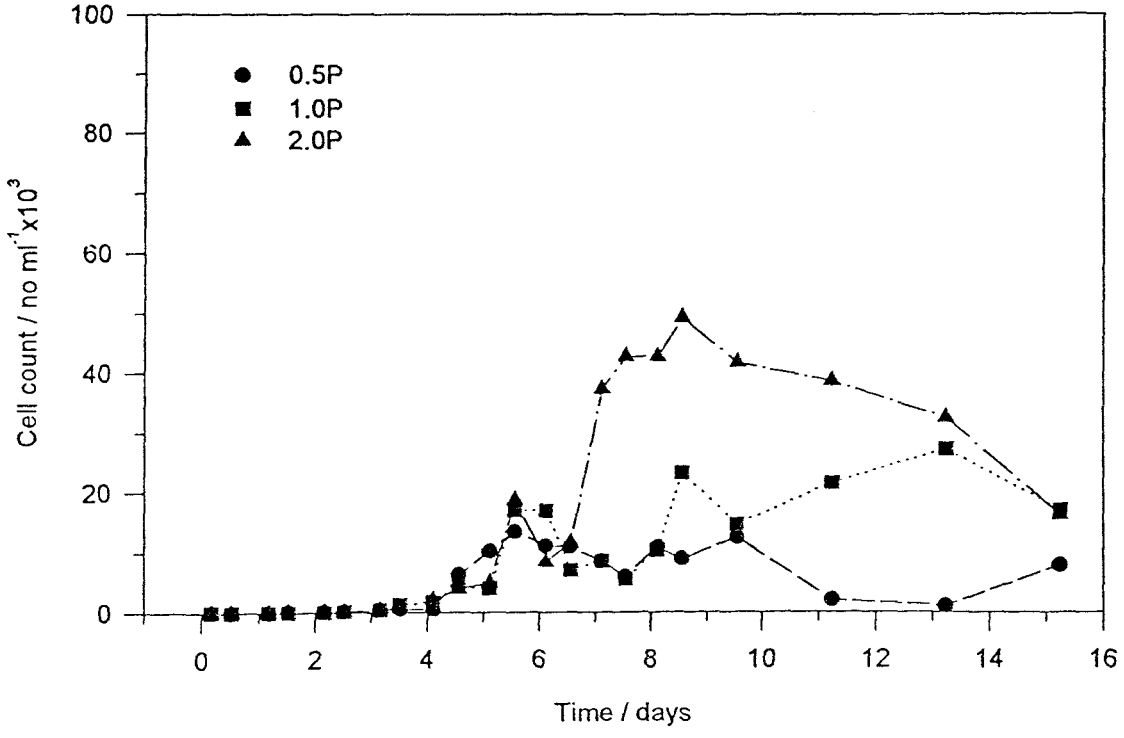

Figure 3.2.5 Motile cell counts determined for high-calcifying *E. huxleyi* batch cultures

The rate of nitrate uptake to phosphate uptake, calculated from daily changes in the ambient concentrations (*i.e.* $\Delta N/\Delta P$), was directly proportional with the rate of supply during exponential growth phase for all three cultures. In 0.5P $\Delta N/\Delta P$ was greater than 20 indicating phosphate limitation towards the end of exponential growth phase, whereas in 2.0P $\Delta N/\Delta P$ was less than 10, indicating nitrate limitation towards the end of exponential growth phase. The daily $\Delta N/\Delta P$ values for 1.0P were within the range of 12-17, and therefore approximately equal to the Redfield ratio of 16:1.

Figures 3.2.4-3.2.5 show a significant proportion of the *E. huxleyi* cells became motile for all three cultures, although the motile cell numbers relative to initial phosphate concentration is not as well defined as that for the total cell concentration. The maximum proportion of motile cells to non-motile cells can be seen to be approximately 10% of the total population during the stationary phase of all treatments.

3.2.3 Dissolved carbonate system

The initial pH in each of the three cultures (Fig. 3.2.6) was adjusted to be slightly higher than in the first batch culture experiment to reduce the initial PCO_2 to a typical seawater value (320 µatm). pH began to increase during mid-exponential growth phase in all cultures reaching a maximum as cultures attained maximum cell numbers with the highest pH determined in 2.0P. The net increase in pH in all cultures was approximately twice that found in batch culture #1. pH reached a maximum on day 10 for all cultures followed by a steady decline the rate of which was greatest in the 0.5P culture

The total alkalinity and carbonate alkalinity (Figs. 3.2.7-3.2.8) again show similar changes throughout the experiments as expected, with the difference being mainly due to the addition of the borate ion to total alkalinity. Alkalinity values showed minimal change during the lag phase until the start of day 5 after which alkalinity decreased at the same rate until day 7 when 1.0P and 2.0P cultures continued to decline and 0.5P declined at a lower rate. These trends were similar to those in the first batch culture experiment with a greater net change in alkalinity seen in the first experiment over the same time period.

PCO_2 and $CO_{2(aq)}$ started to decline at the end of exponential growth phase (Fig. 3.2.9) and reached a minimum at maximum cell numbers for all cultures, and then remained at this level for 1.0P and 2.0P. From day 10-15 only the 0.5P culture PCO_2 showed an increase similar to that observed in batch culture #1. The minimum PCO_2 reached was lower in this experiment compared to batch culture #1.

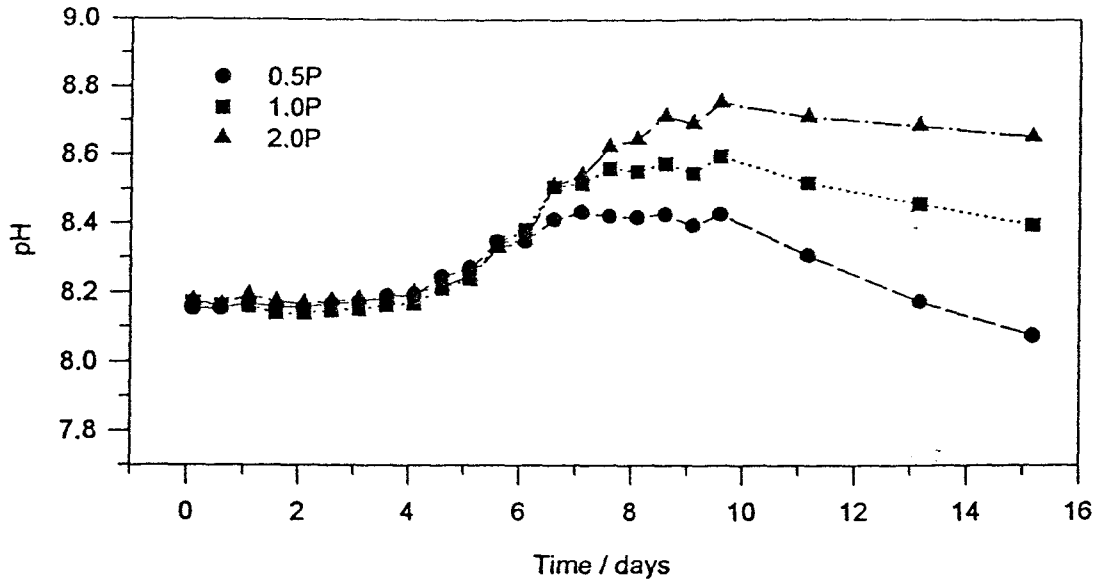

Figure 3.2.6 Temporal variation of pH for high-calcifying *E. huxleyi* batch cultures

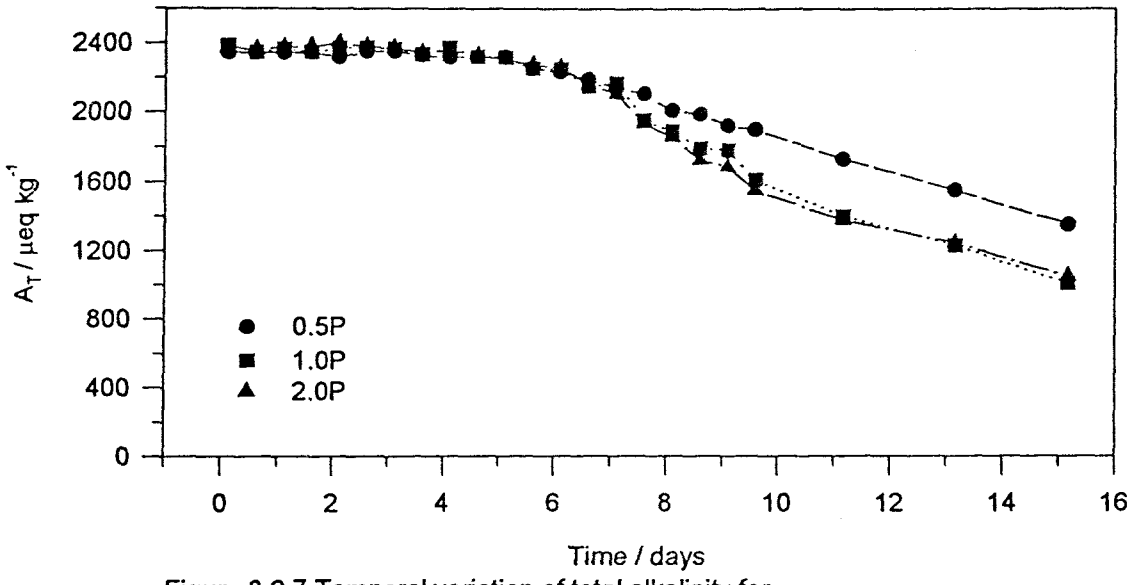

Figure 3.2.7 Temporal variation of total alkalinity for high-calcifying *E. huxleyi* batch cultures

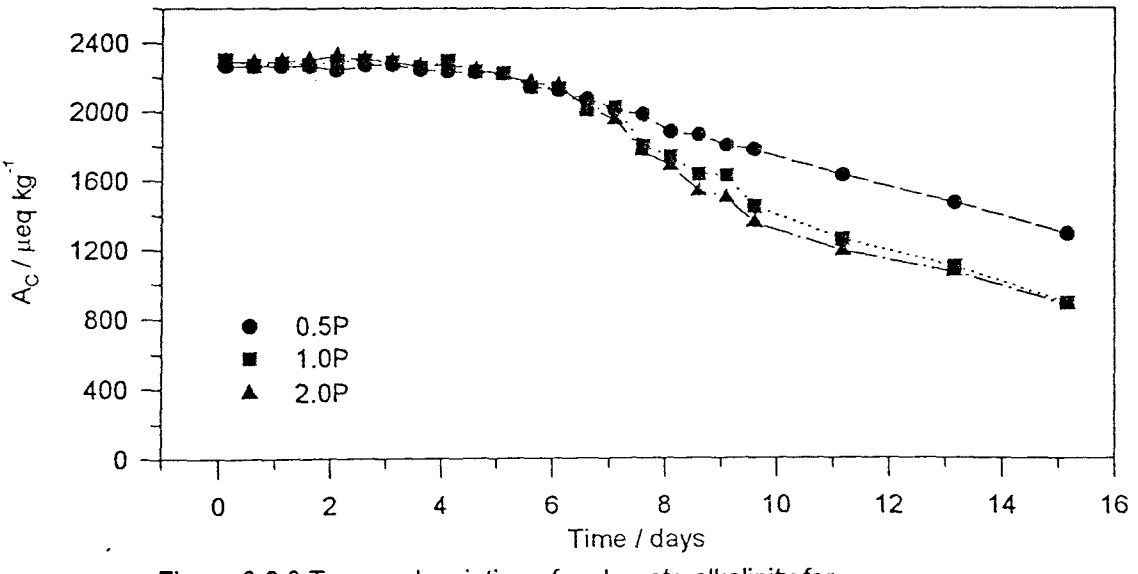

Figure 3.2.8 Temporal variation of carbonate alkalinity for high-calcifying *E. huxleyi* batch cultures

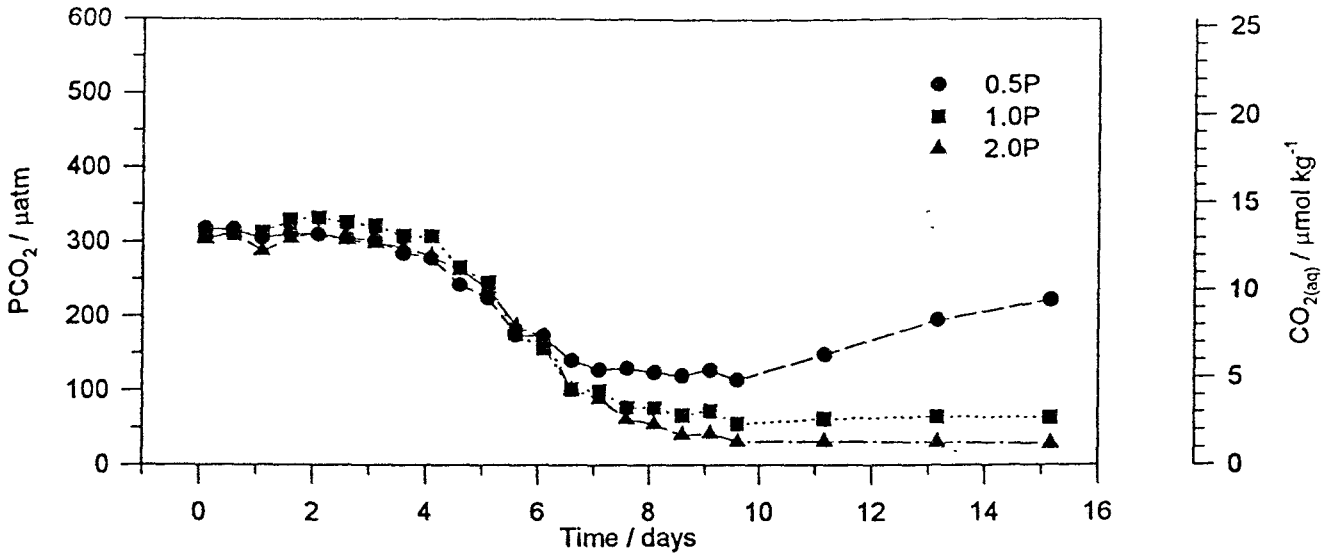

Figure 3.2.9 Temporal variation of PCO_2 and dissolved carbon dioxide for high-calcifying *E. huxleyi* batch cultures

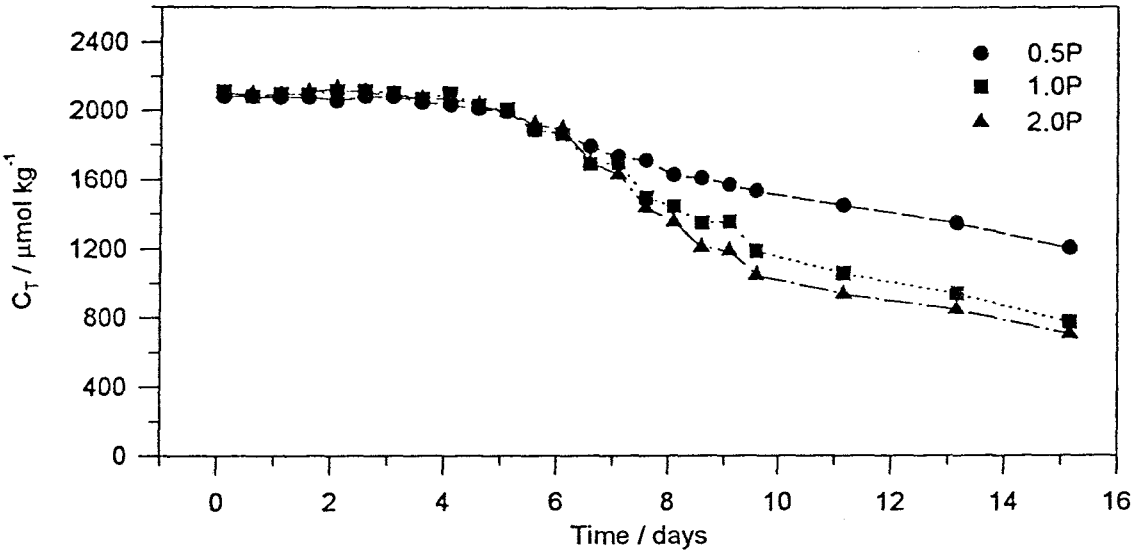

Figure 3.2.10 Temporal variation of total dissolved inorganic carbon for high-calcifying *E. huxleyi* batch cultures

The C_T concentration (Fig. 3.2.10) showed similar changes to alkalinity. C_T started to decline towards the end of the exponential phase for all cultures. This rate remained constant for 0.5P but decreased in 1.0P and 2.0P as maximum cell density was reached. Although the pattern of change was the same as that seen in the first batch culture experiment the net reduction in C_T was greater in this experiment over the same time period.

3.2.4 ^{14}C uptake measurements

Figures 3.2.11-3.2.13 show the maximum total rate of ^{14}C uptake of both calcification and photosynthesis occurred at the end of exponential growth phase as found in the first batch culture experiment. Maximum rates of photosynthesis between treatments again correlate with the initial phosphate concentration. The maximum rates of calcification were similar between 1.0P and 2.0P, with 0.5P having a lower rate. Calcification did not show a well defined maximum rate, unlike photosynthesis, but increased slowly at the end of exponential growth phase and declined as the cultures reached maximum cell numbers. During early exponential growth phase the rates of calcification relative to photosynthesis for all treatments were comparable but with increasing cell numbers calcification declined.

Maximum rates of calcification in this experiment were considerably lower (30-50%) than those found in batch culture #1. The maximum rates of photosynthesis were also lower but not to the same extent, with 0.5P being approximately the same, 1.0P *ca.* 20% lower and 2.0P *ca.* 40% lower.

The photosynthetic and calcification rates per cell (Figs. 3.2.14-3.2.16) have a slightly reduced data set because errors in the initial cell counts were too large to produce comparable data for the first ^{14}C incubation. For all cultures the rates of photosynthesis and calcification reached their maximum in the early exponential growth phase in the second incubation on day 2. The rates of calcification and photosynthesis varied within each light period from day 2 to day 4 resulting in a sawtooth pattern with calcification and photosynthetic rates being highest in the second half of each photoperiod. The exception to this was the first calcification measurement for 1.0P. This pattern can also be seen between day 6 and 8 for 0.5P. The rates of calcification and photosynthesis then decline towards zero at the end of the exponential phase for all cultures. The rates of photosynthesis and calcification do not correspond to the initial nutrient concentrations with the rates for 0.5P and 1.0P being similar and 2.0P having the lowest calcification and approximately 50% of the photosynthetic rate per cell of 0.5P and 1.0P cultures. The general trends of calcification and photosynthetic rate are similar between the first and second batch culture experiments with comparisons limited by the reduced number of results in batch culture #1.

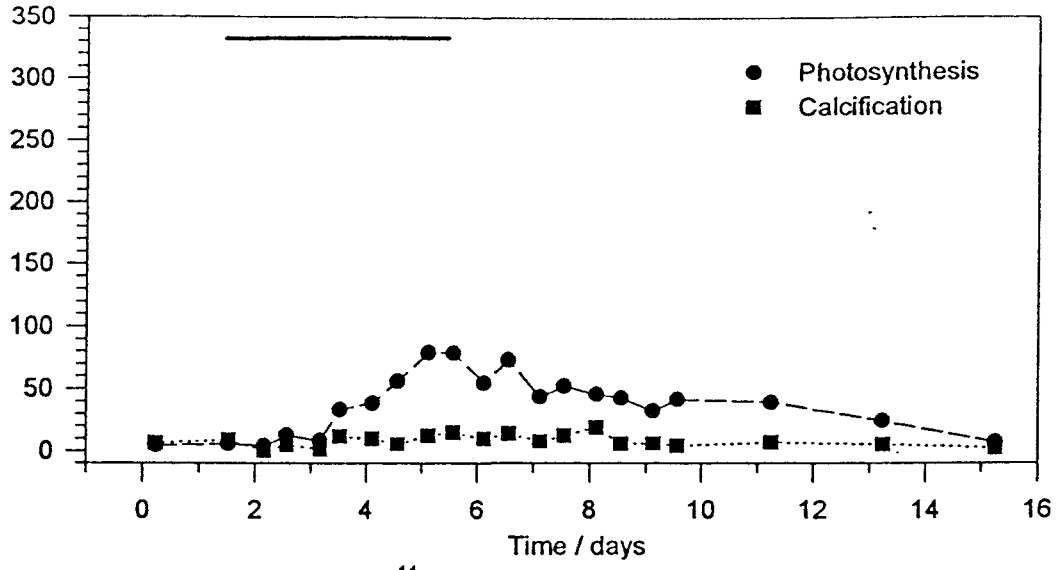

Figure 3.2.11 Total rates of ^{14}C uptake for 0.5P batch culture for high-calcifying *E. huxleyi* (Bar indicates exponential growth phase)

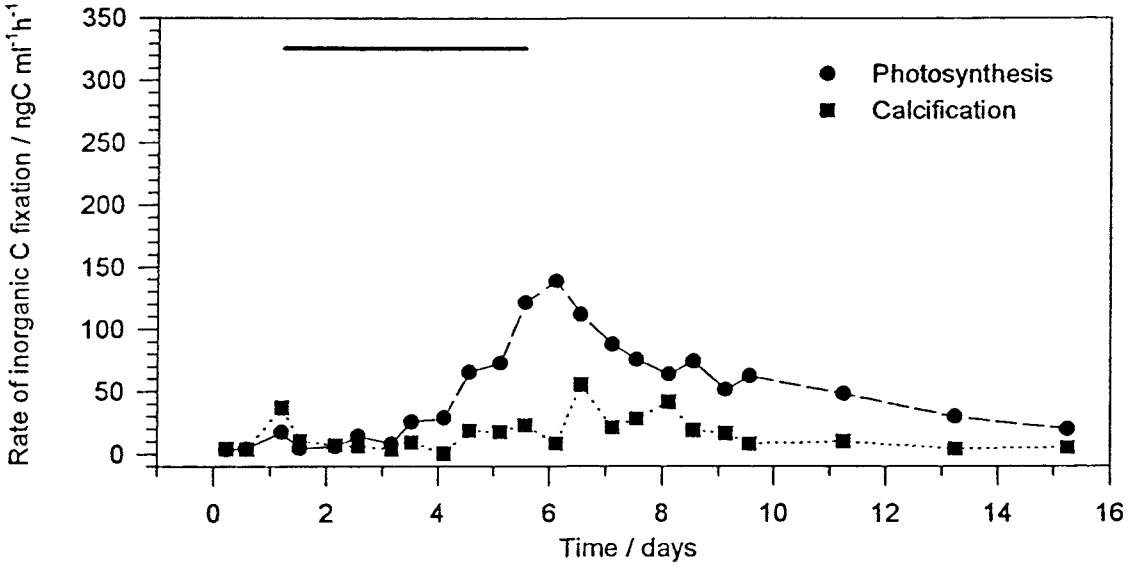

Figure 3.2.12 Total rates of ^{14}C uptake for 1.0P batch culture for high-calcifying *E. huxleyi*

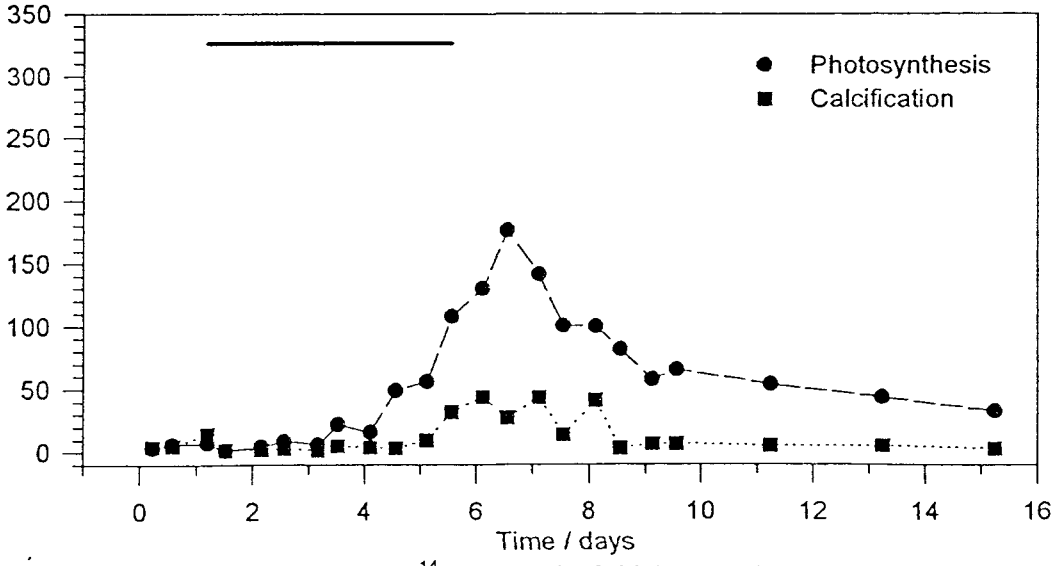

Figure 3.2.13 Total rates of ^{14}C uptake for 2.0P batch culture for high-calcifying *E. huxleyi*

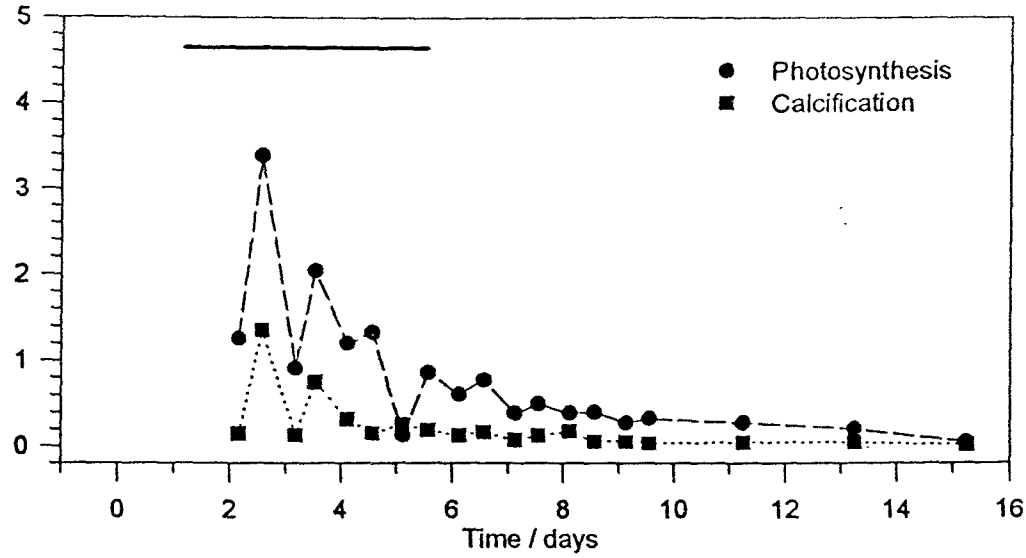

Figure 3.2.14 Rates of ^{14}C uptake per cell for 0.5P batch culture for high-calcifying *E. huxleyi*

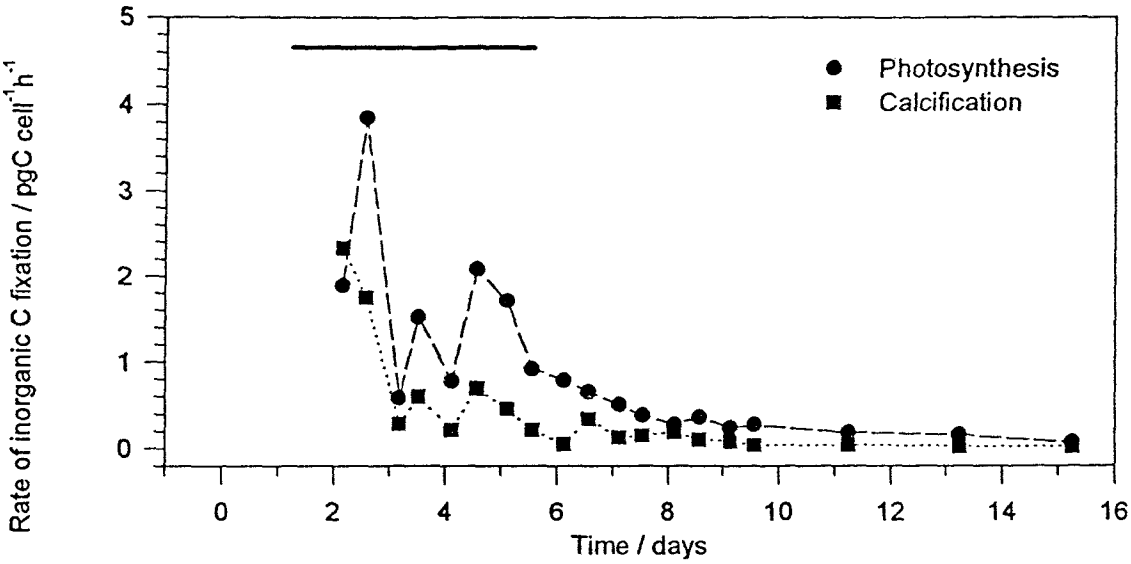

Figure 3.2.15 Rates of ^{14}C uptake per cell for 1.0P batch culture for high-calcifying E. *huxleyi*

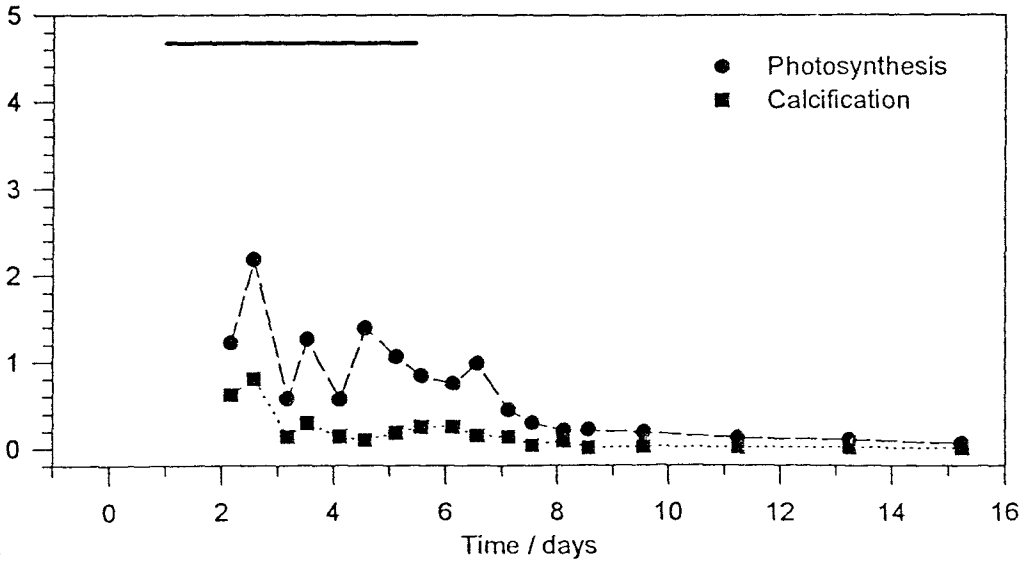

Figure 3.2.16 Rates of ^{14}C uptake per cell for 2.0P batch culture for high-calcifying *E. huxleyi*

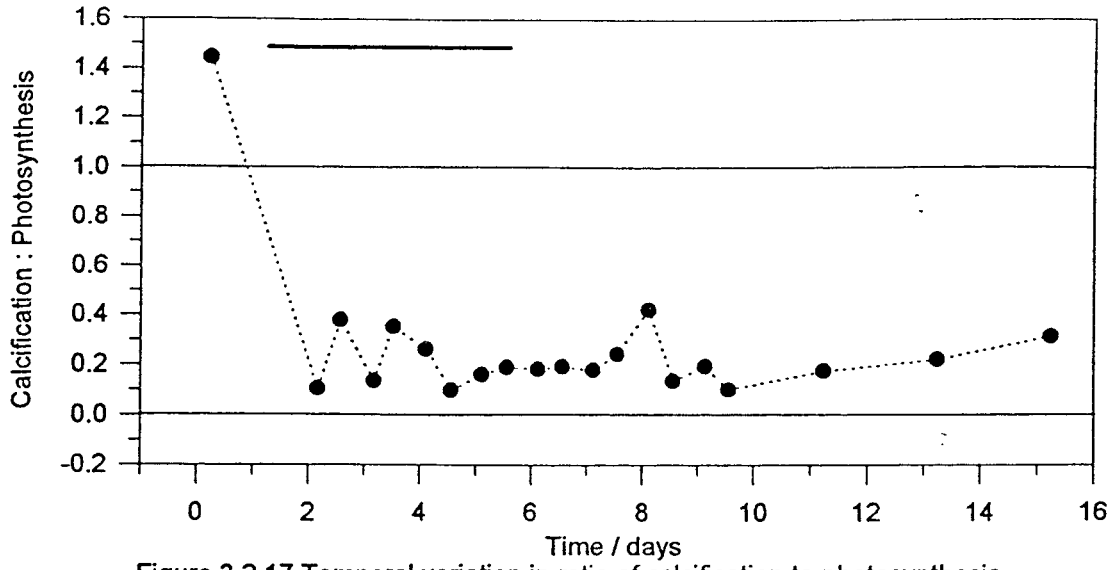

Figure 3.2.17 Temporal variation in ratio of calcification to photosynthesis for 0.5P batch culture for high-calcifying *E. huxleyi*

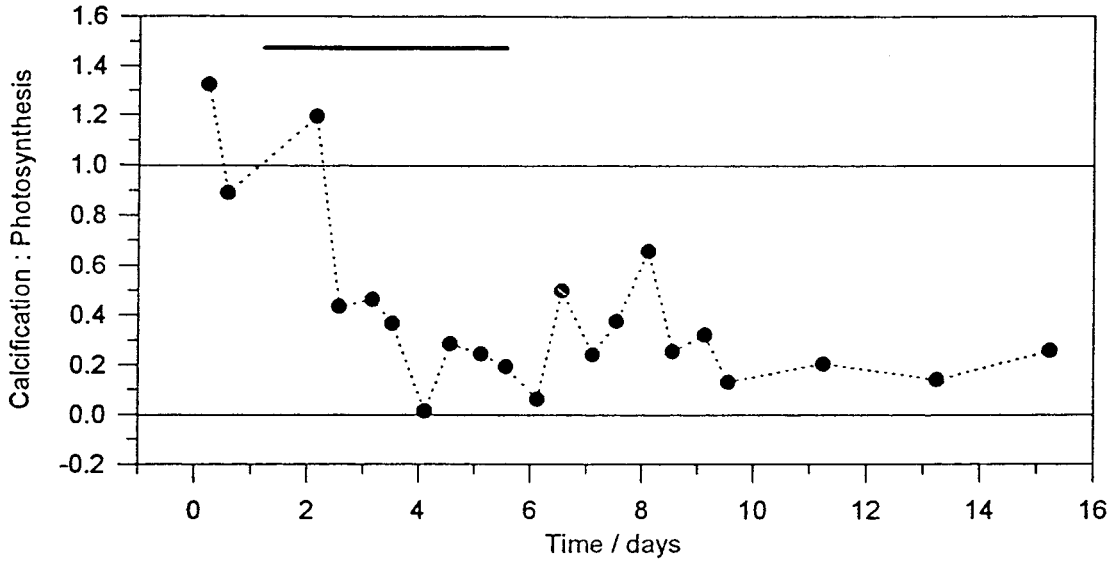

Figure 3.2.18 Temporal variation in ratio of calcification to photosynthesis for 1.0P batch culture for high-calcifying *E. huxleyi*

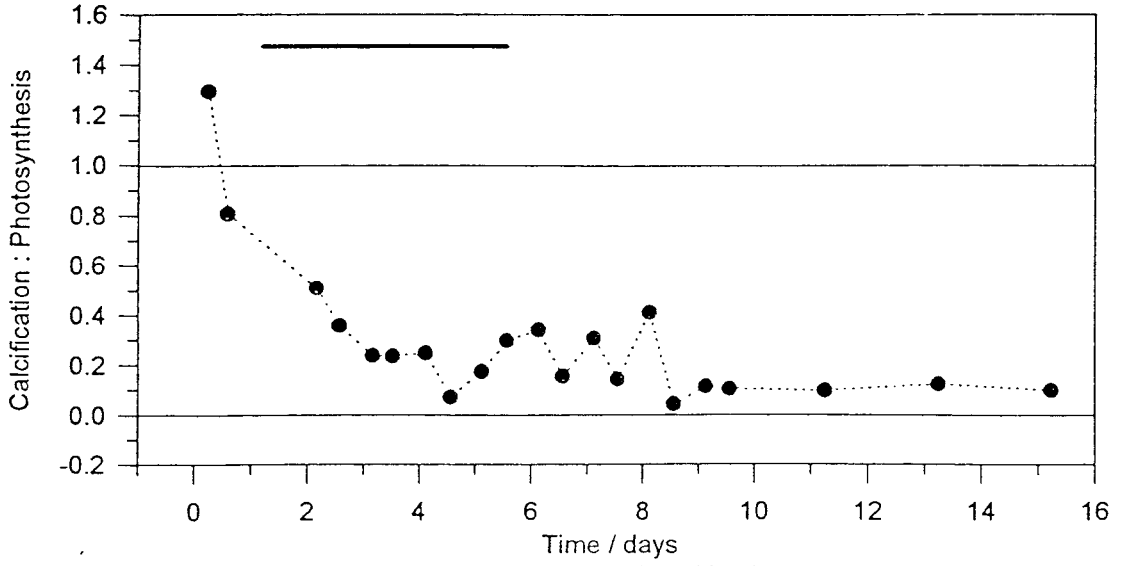

Figure 3.2.19 Temporal variation in ratio of calcification to photosynthesis for 2.0P batch culture for high-calcifying *E. huxleyi*

Figures 3.2.17-3.2.19 show the C:P ratio was greater than 1 for all cultures during the lag phase declining to 0 - 0.5 during exponential growth phase. Only 1.0P showed a C:P greater than 1 on day 2 during exponential growth phase. C:P then increased to a lower secondary peak on day 8 for all cultures at maximum cell density. C:P results were generally lower to those in the first batch culture experiment although the smaller data set for the initial experiment again makes comparison difficult.

3.2.5 Alkalinity derived calcite standing stock

PIC standing stock showed a slight increase towards the end of the exponential growth phase in all cultures (Fig. 3.2.20) with 1.0P and 2.0P increasing at a similar rate and 0.5P at a lower rate. These results were similar to experiment #1, with the levels of derived PIC on day 15 of both experiments reaching *ca.* 750 μmol kg^{-1} for 1.0P and 2.0P, and 500 μmol kg^{-1} for 0.5P. The total net calcification rate calculated from the alkalinity derived PIC (Fig. 3.2.21) showed a maximum rate for all cultures on day 9 followed by a decline. The maximum total calcification rate was highest for both 1.0P and 2.0P cultures and lower by *ca.* 30% for all cultures than noted in experiment #1.

3.2.6 Total dissolved inorganic carbon (C_T) vs total alkalinity (A_T) plots and buffer factor plots

During the initial growth phases the buffer factor (β) was higher than in stationary phase for all cultures (Figs. 3.2.22-3.2.24), as also noted in experiment #1, with the initial buffer factor being highest in the lowest phosphate culture, 0.5P (β = 7.12). The stationary phase buffer factors increased with the initial phosphate concentration, with the highest value in the 2.0P culture (β = 2.41). Comparison of buffer factors from cultures of the same initial phosphate showed higher values in this experiment than in experiment #1.

The C:P, calculated from the C_T vs A_T slope, (Figs. 3.2.25-3.2.27) was lower during the initial growth phases than the stationary phase in all cultures. The initial growth phase C:P increased with the initial phosphate concentration with the highest in the 2.0P culture (C:P = 0.66). The C:P therefore reached a maximum in the stationary growth phase decreasing with initial phosphate concentration, *i.e.* 0.5P culture showed the maximum C:P of 1.24. In comparison to experiment #1 all C:P were lower in all cultures in this experiment.

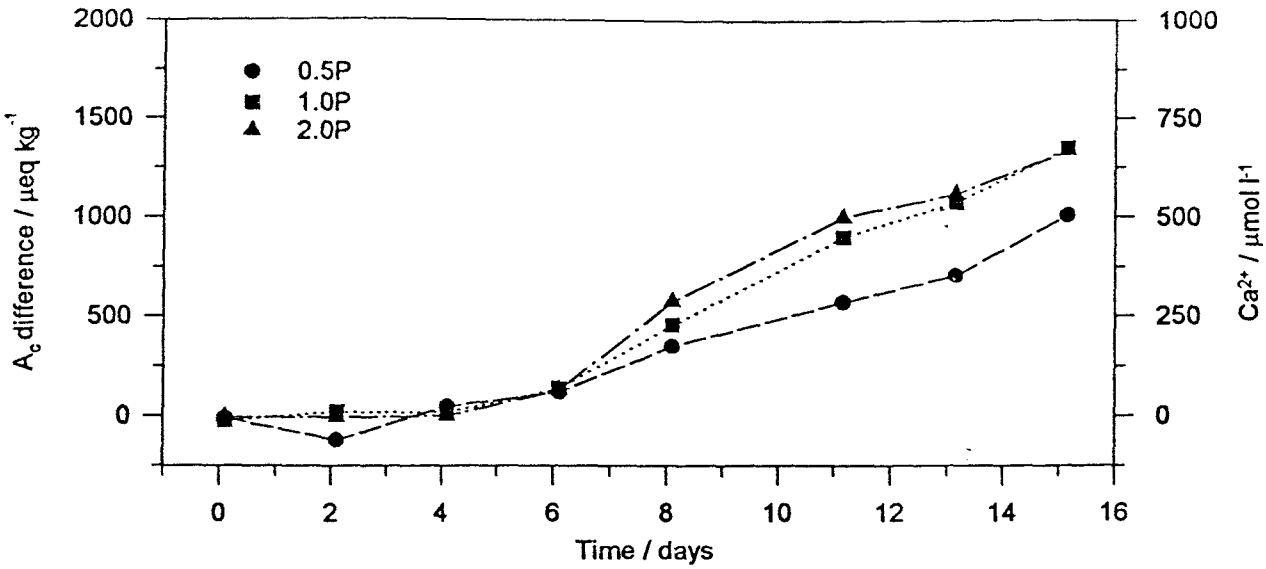

Figure 3.2.20 Carbonate alkalinity derived calcite standing stock for high-calcifying *E. huxleyi* batch cultures

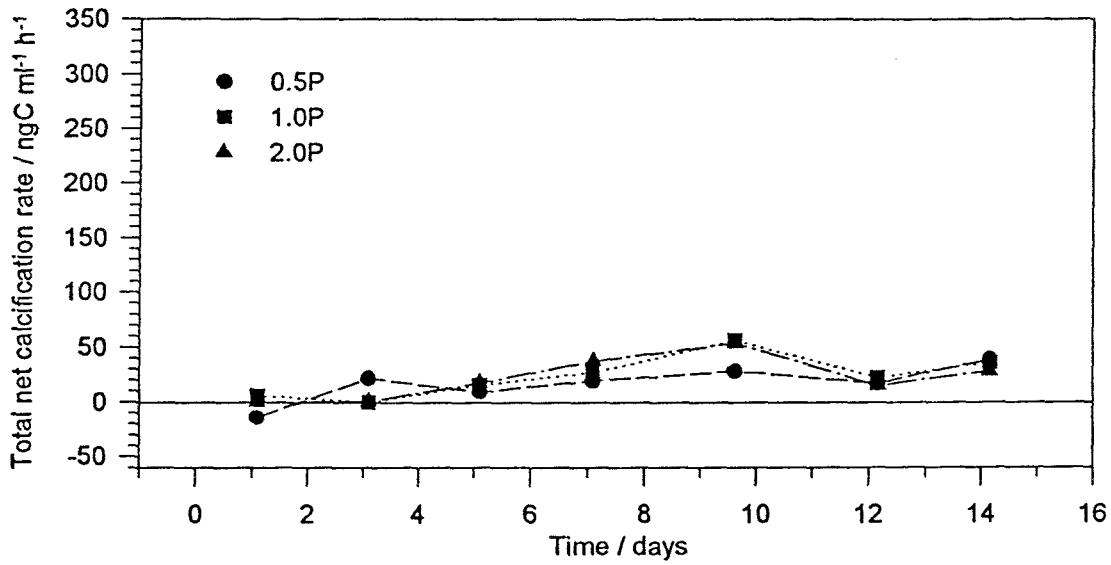

Figure 3.2.21 Carbonate alkalinity derived total net calcification rates for high-calcifying *E. huxleyi* batch cultures

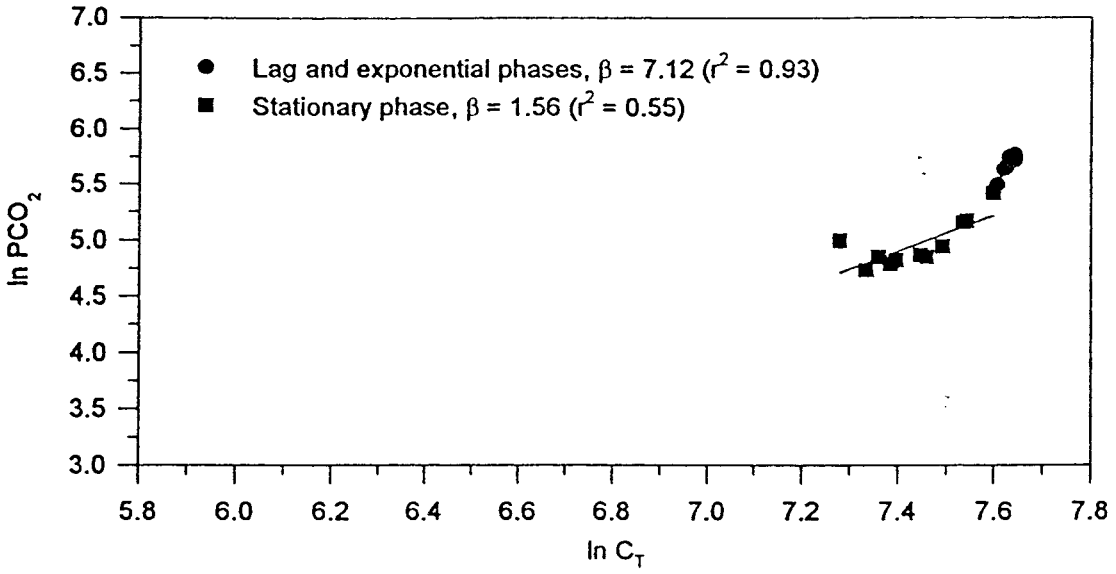

Figure 3.2.22 Plot of lnC_T against $lnPCO_2$ for 0.5P batch culture for high-calcifying *E. huxleyi* (Slope of regression line represents β)

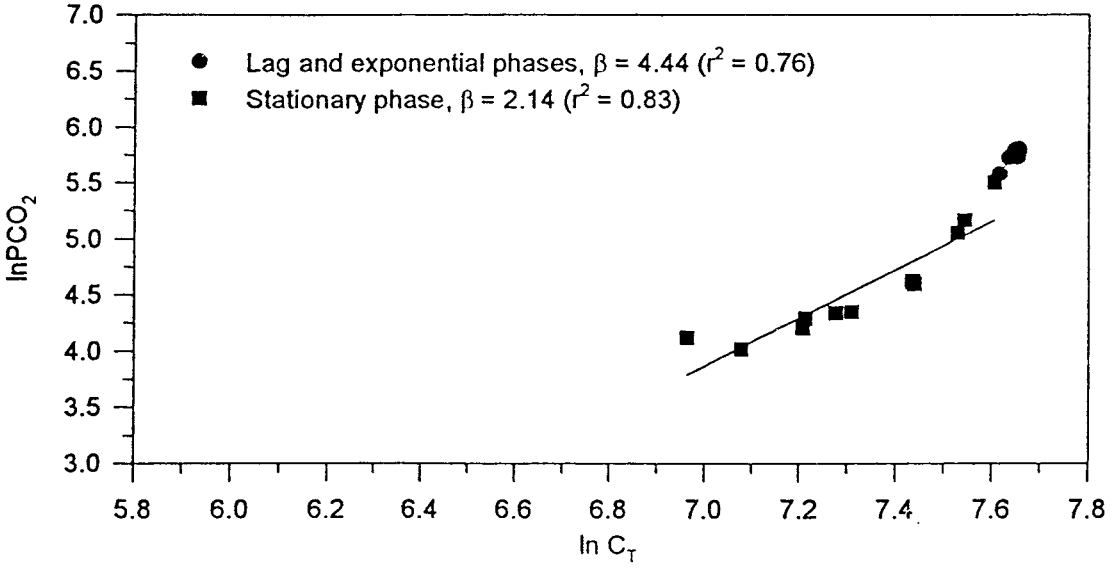

Figure 3.2.23 Plot of lnC_T against $lnPCO_2$ for 1.0P batch culture for high-calcifying *E. huxleyi*

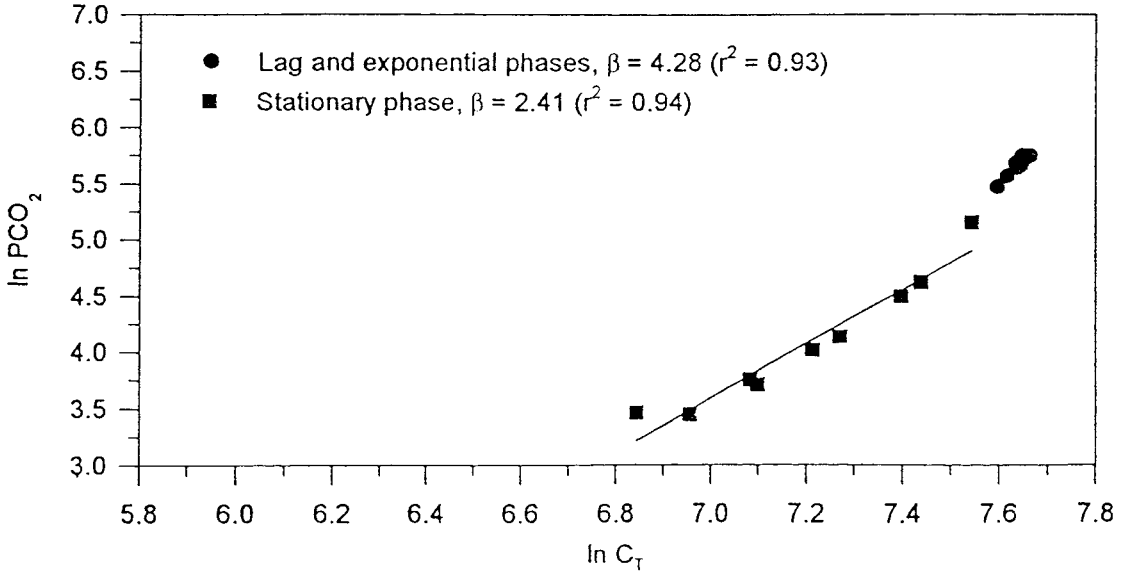

Figure 3.2.24 Plot of lnC_T against $lnPCO_2$ for 2.0P batch culture for high-calcifying *E. huxleyi*

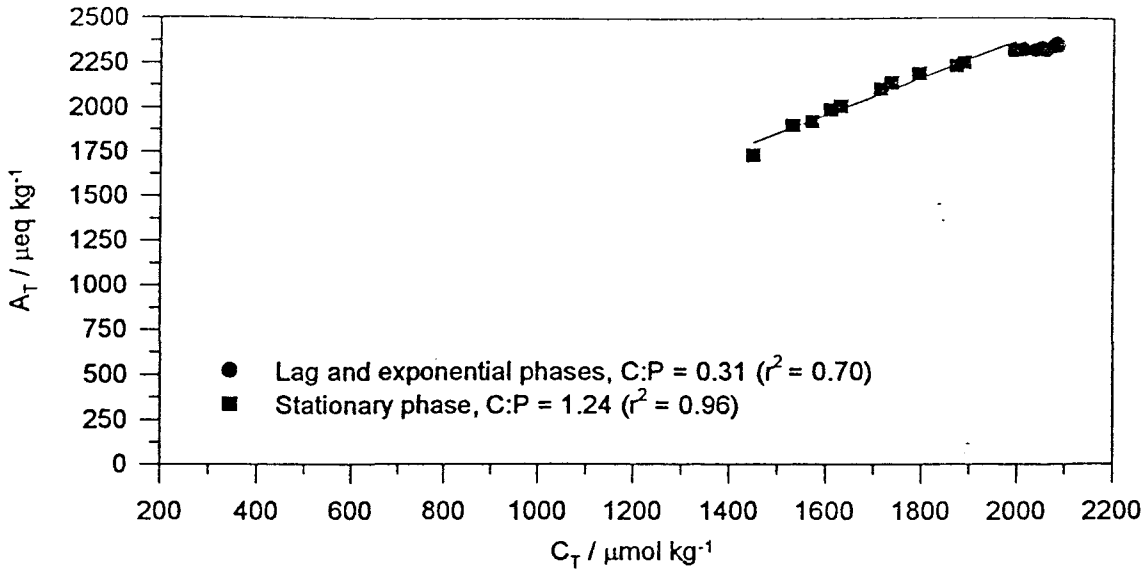

Figure 3.2.25 Plot of C_T against A_T for 0.5P batch culture for high-calcifying *E. huxleyi* (C:P derived from slope of regression)

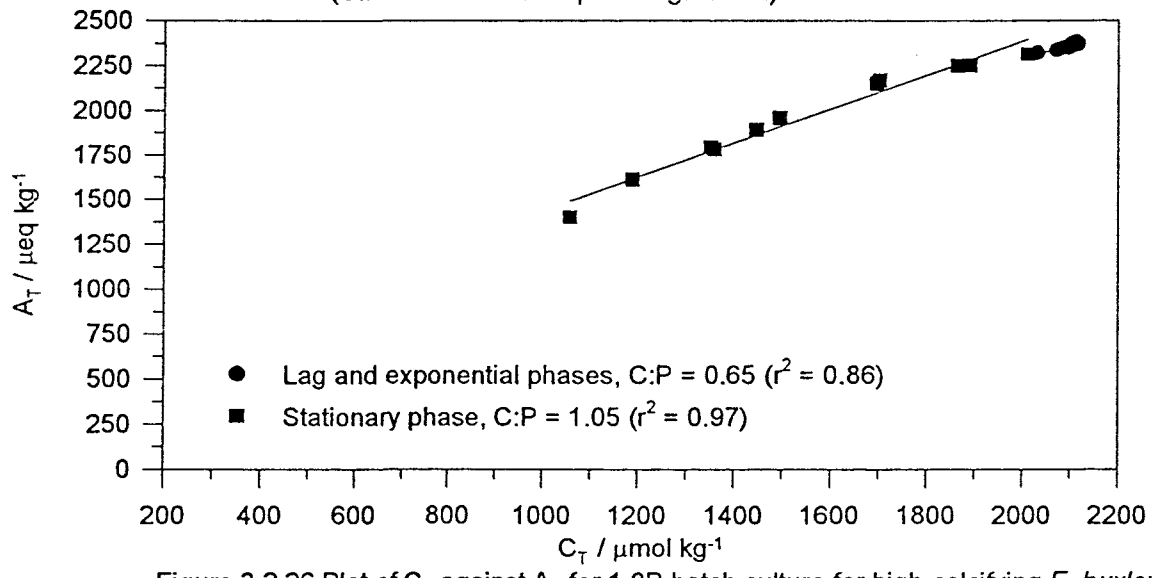

Figure 3.2.26 Plot of C_T against A_T for 1.0P batch culture for high-calcifying *E. huxleyi*

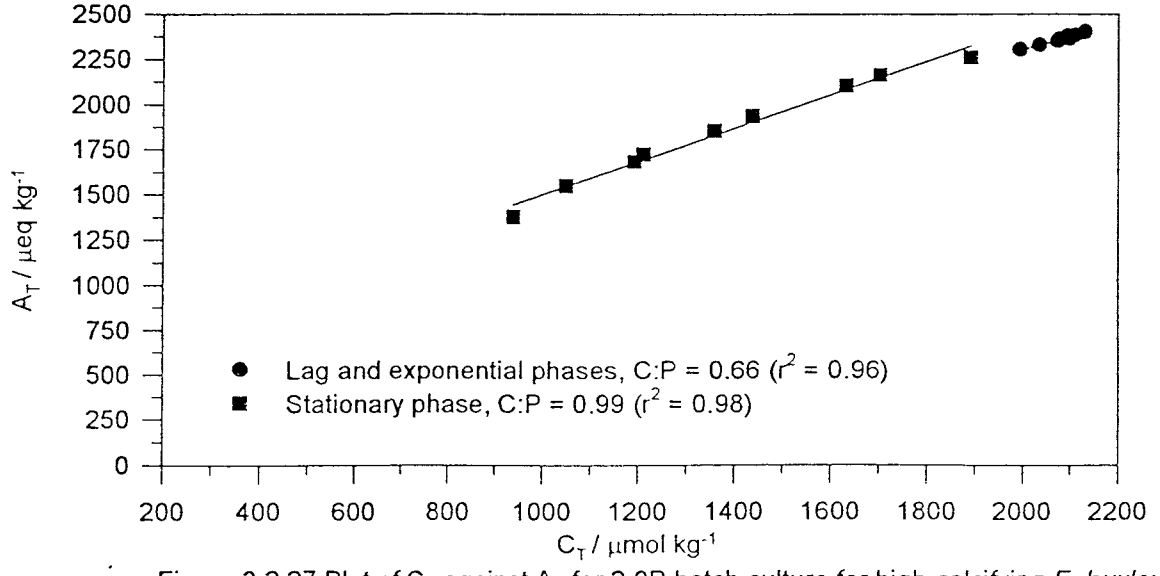

Figure 3.2.27 Plot of C_T against A_T for 2.0P batch culture for high-calcifying *E. huxleyi*

3.2.7 Summary of results from batch culture #2

Results from this experiment again showed initial phosphate concentration controlled the final yield of cells but had little influence on maximum specific growth rate. As in batch culture #1 the initial phosphate concentration appeared to influence the phosphate uptake rate derived from phosphate depletion in the media. Maximum total cell numbers were however approximately half those seen in batch culture #1. A significant number of motile cells (*ca.* 10% total cell count) were also seen in this experiment.

In all cultures there was a decline in total alkalinity as expected for a calcifying phytoplankton. In this respect cultures 1.0P and 2.0P affected the dissolved carbonate system almost identically but in the lowest phosphate culture (0.5P) the alkalinity and C_T was drawn down to a lesser extent. An increase in PCO_2 occurred during the stationary phase only in 0.5P, as also seen in the 0.5P culture in batch culture #1.

For the radiotracing incubations the rates of photosynthesis per cell were highest in the lower phosphate cultures, 0.5P and 1.0P, but all cultures showed maximum rates in early exponential growth phase and a periodicity related to the diel cycle was also seen. Maximum rates for calcification occurred in early exponential growth phase for all cultures with a periodicity related to the diel cycle. Calcification rates were comparable between all three cultures. The smaller data set for batch culture #1 makes short term comparison between experiments unreliable. Maximum C:P was greater than 1 for all treatments during the lag phase and for 1.0P during the early exponential growth phase.

Comparison of the results from ^{14}C uptake derived C:P with A_T vs C_T derived C:P showed similar values during the initial growth phases but A_T vs C_T derived C:P was always significantly greater during stationary phase, being consistently around 1.0. The A_C derived total net calcification results were all similar to the rates of calcification seen in the ^{14}C uptake incubations, but the ^{14}C calcification rates reached maxima 2-3 days earlier than that seen for the A_C derived calcification rates. This comparison between ^{14}C uptake derived figures and pH derived figures was similar to that seen in experiment #1.

Table 3.1.1 shows a summary of these results.

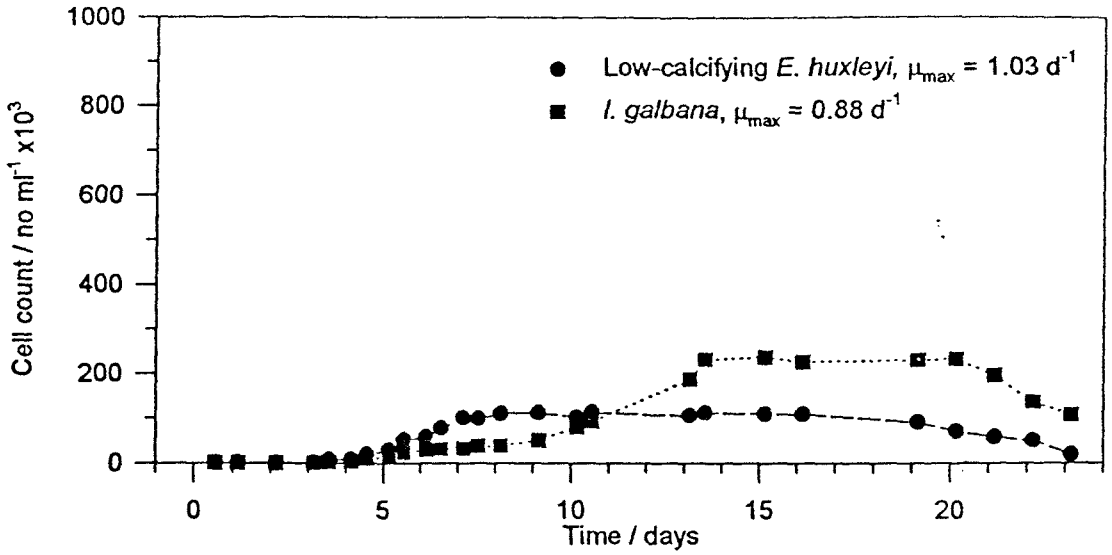

Figure 3.3.1 Cell counts determined for low-calcifying *E. huxleyi* and *I. galbana* batch cultures

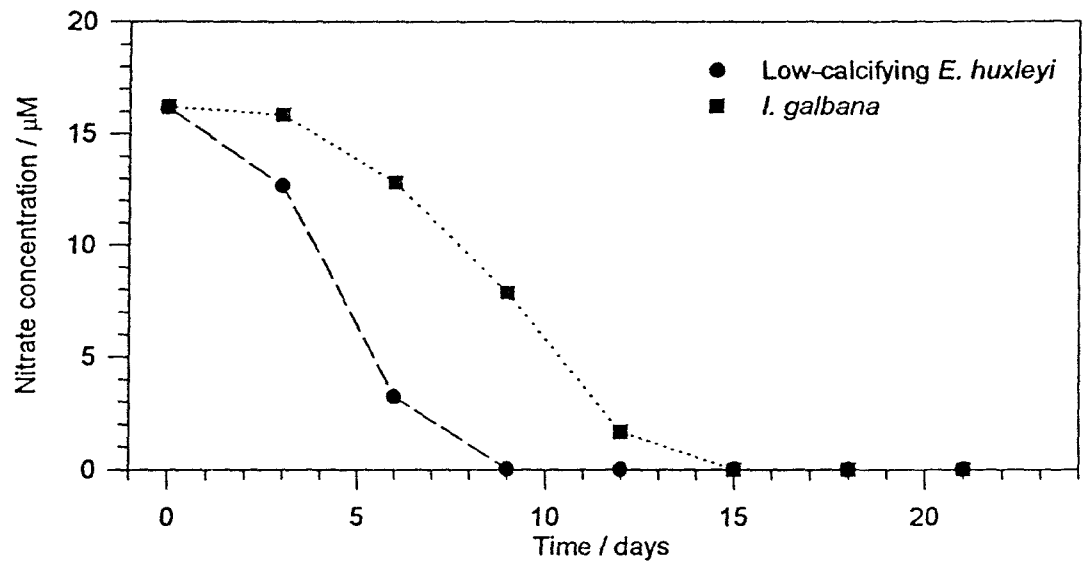

Figure 3.3.2 Temporal variation of nitrate concentrations for low-calcifying *E. huxleyi* and *I. galbana* batch cultures

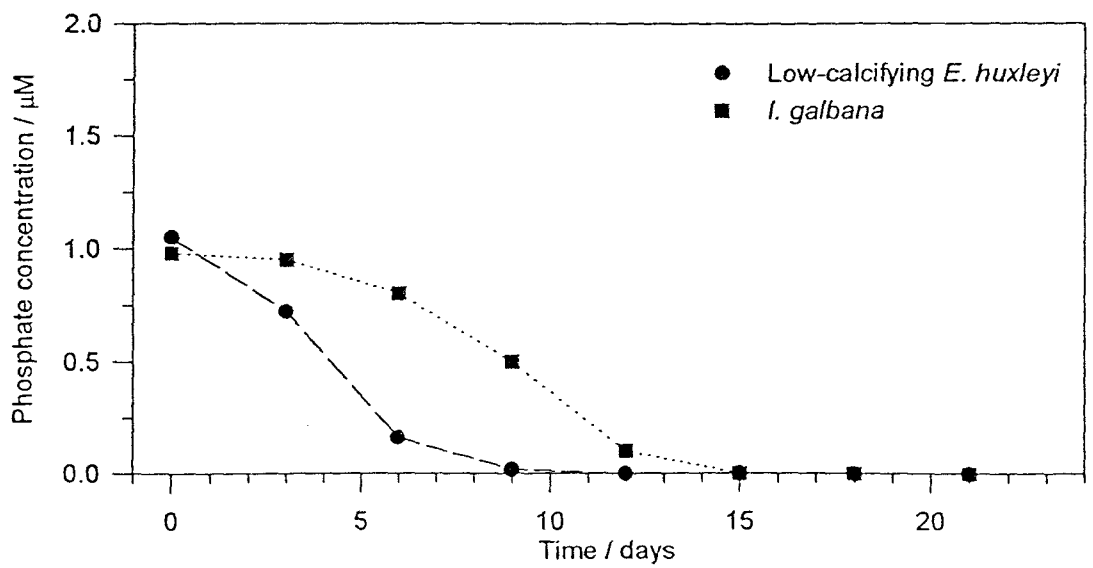

Figure 3.3.3 Temporal variation of phosphate concentrations for low-calcifying *E. huxleyi* and *I. galbana* batch cultures

3.3.1 Batch culture #3

A low-calcifying strain of *E. huxleyi*, CCAP 920/2, and a non-calcifying chrysophyte, *Isochrysis galbana* (Strain CCAP 927/1), were grown in this experiment. The timing of sampling was the same as in the batch culture #2 with sampling twice daily until day 13. The initial nutrient concentration for both cultures was 16μM nitrate and 1μM phosphate. The cultures were grown in the same culture vessels with the same light source as used in the previous experiments, but improved facilities enabled these experiments to be conducted in a constant temperature room allowing improved temperature control of the media. The day of inoculation was noted as day 0 and the experiment continued for 23 days.

3.3.2 Cell counts and nutrients

Figure 3.3.1 shows that low-calcifying *E. huxleyi* and *I. galbana* had similar maximum specific growth rates and an exponential growth phase of the same duration after which low-calcifying *E. huxleyi* attained maximum cell numbers. *I. galbana* continued to increase in cell numbers at a lower rate and reached maximum cell numbers 5 days after low-calcifying *E. huxleyi*. When the growth of the low-calcifying *E. huxleyi* was compared to that of the high-calcifying *E. huxleyi* the maximum specific growth rates were similar but maximum cell numbers were *ca.* 50 % of that observed in batch culture #2.

Nitrate concentrations (Fig. 3.3.2) declined steadily for low-calcifying *E. huxleyi* until below the limit of detection when the culture reached maximum cell numbers. *I. galbana* also followed this pattern after an initial delay due to a longer lag phase. Phosphate uptake (Fig. 3.3.3) matched nitrate uptake for both low-calcifying *E. huxleyi* and *I. galbana*. Phosphate concentrations reached the detection limit as maximum cell numbers were attained in both cultures. The rate of nitrate uptake to phosphate uptake, calculated from daily changes in the ambient concentrations (*i.e.* $\Delta N/\Delta P$) was approximately equal to the Redfield ratio (16:1) for both cultures during the exponential growth phase.

3.3.3 Dissolved carbonate system

Initial pH (Fig. 3.3.4) was adjusted to give similar PCO_2 (350 μatm) to batch culture experiment #2. Both low-calcifying *E. huxleyi* and *I. galbana* reached a maximum pH as the cultures reached maximum cell numbers. The pH in both cultures then remained constant throughout stationary phase, in contrast to the decline in pH during stationary phase for high-calcifying *E. huxleyi* cultures. The maximum pH of the media was higher than that noted for high-calcifying *E. huxleyi*. The analytical precision of pH was better than 0.003 units.

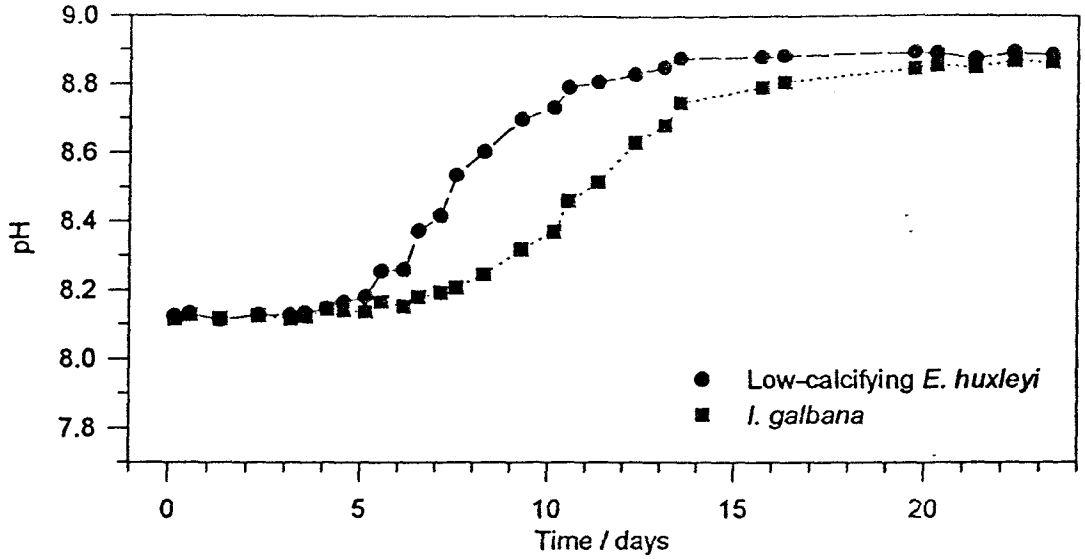

Figure 3.3.4 Temporal variation of pH for low-calcifying *E. huxleyi* and *I. galbana* batch cultures

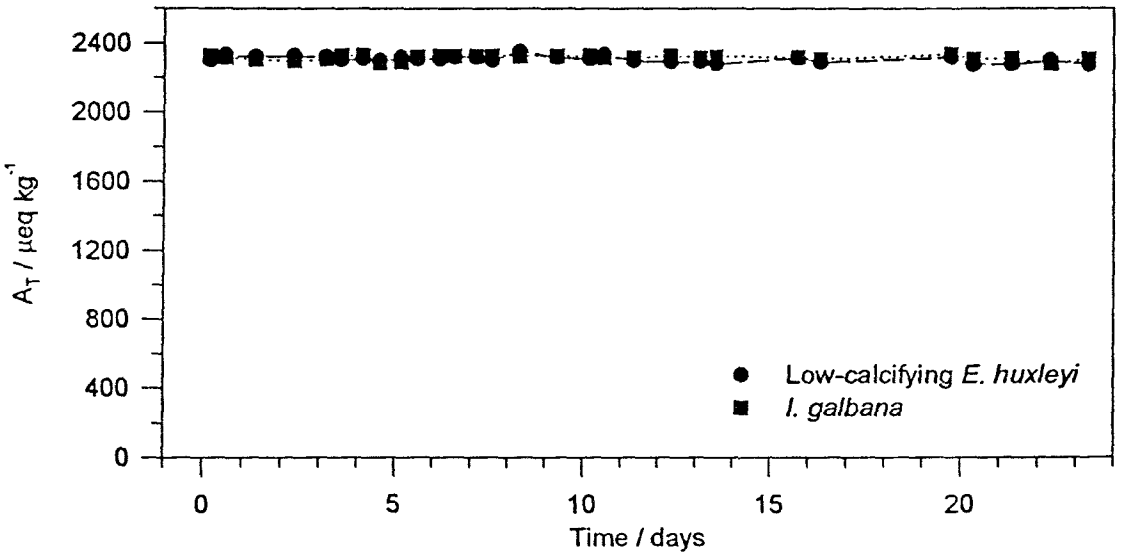

Figure 3.3.5 Temporal variation of total alkalinity for low-calcifying *E. huxleyi* and *I. galbana* batch cultures

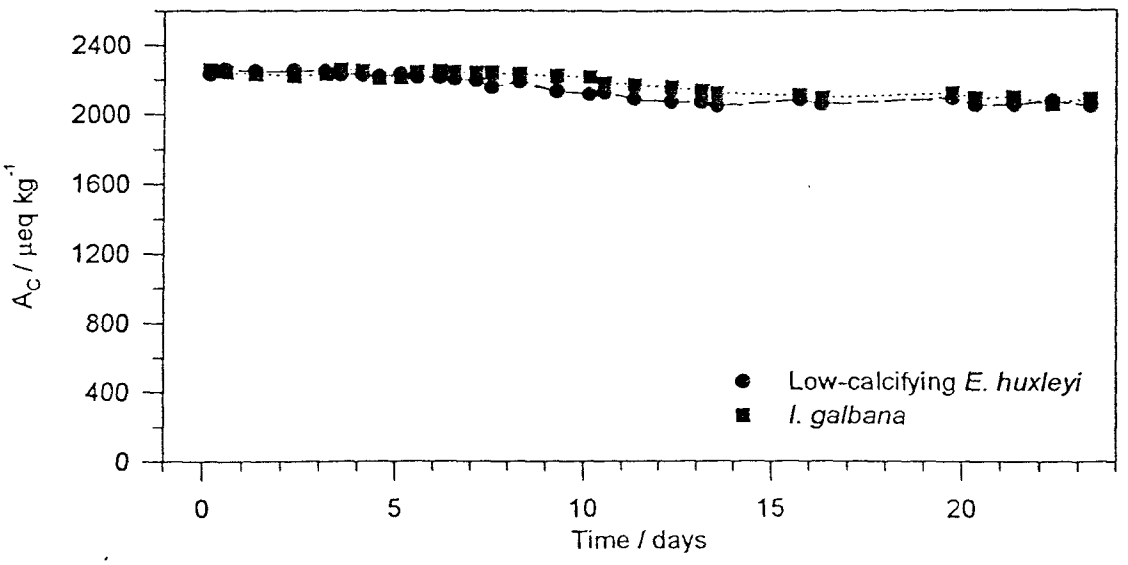

Figure 3.3.6 Temporal variation of carbonate alkalinity for low-calcifying *E. huxleyi* and *I. galbana* batch cultures

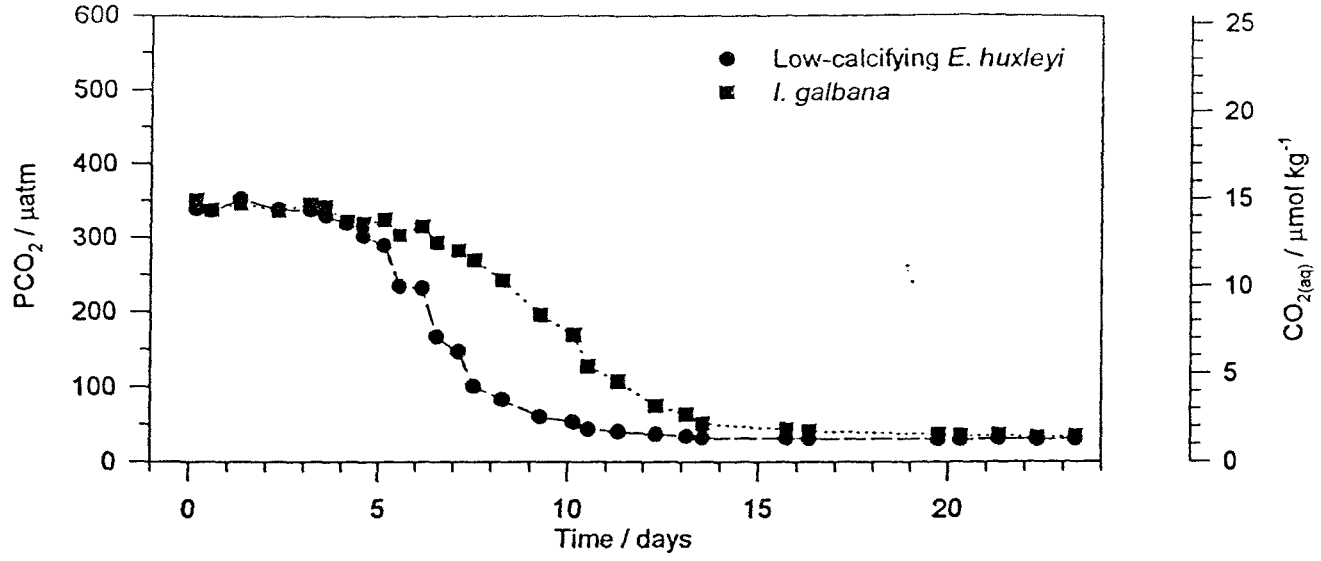

Figure 3.3.7 Temporal variation of PCO_2 and dissolved carbon dioxide for low-calcifying *E. huxleyi* and *I. galbana* batch cultures

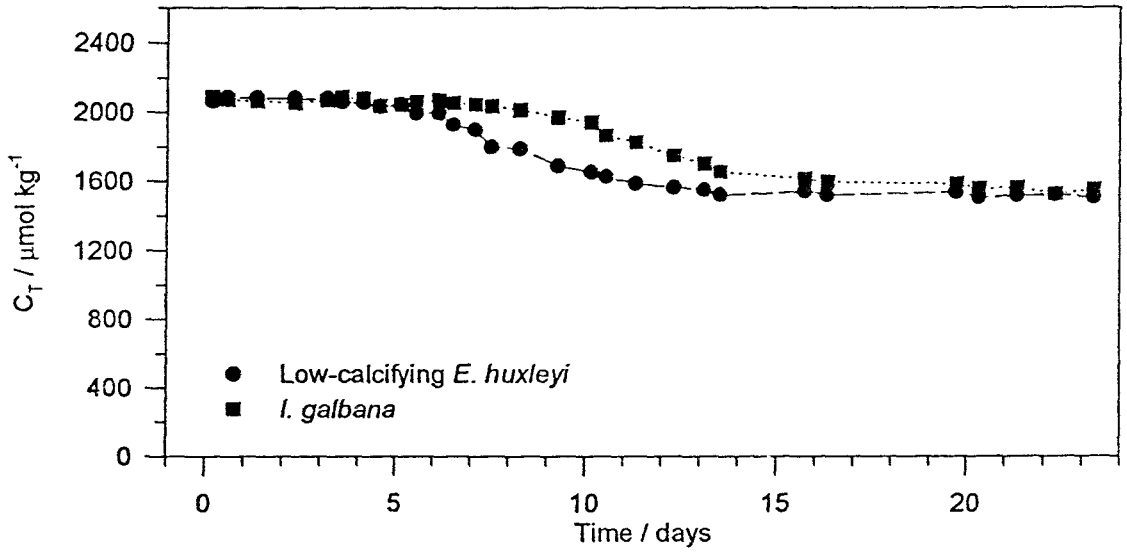

Figure 3.3.8 Temporal variation in total dissolved inorganic carbon for low-calcifying *E. huxleyi* and *I. galbana* batch cultures

The total alkalinity (Fig. 3.3.5) for both low-calcifying *E. huxleyi* and *I. galbana* did not change within the resolution of the measurement for the duration of the experiment. The carbonate alkalinity (Fig. 3.3.6) however declined by *ca.* 200 μeq kg^{-1} for both cultures. This was in obvious contrast to the large changes detected in total and carbonate alkalinity for all high-calcifying *E. huxleyi* cultures.

PCO_2 and $CO_{2(aq)}$ (Fig. 3.3.7) showed minimal change for both cultures until the end of exponential growth phase when the levels declined steadily to a minimum at maximum cell numbers. The effect of low-calcifying and high-calcifying *E. huxleyi* was similar in reducing PCO_2 to *ca.* 50μatm.

C_T for both cultures (Fig. 3.3.8) started to decline after exponential growth phase by *ca.* 400μmol kg^{-1} to a stable minimum after cultures reached maximum cell numbers. The net change for low-calcifying *E. huxleyi* was much lower than the 1400μmol kg^{-1} net change in high-calcifying *E. huxleyi* batch cultures.

3.3.4 ^{14}C uptake measurements

The results for the total rate of ^{14}C uptake incubations (Figs. 3.3.9-3.3.10) showed for both cultures the maximum rate of photosynthesis occurred at maximum cell numbers. The maximum rate of photosynthesis for low-calcifying *E. huxleyi* was *ca.* 70% lower than for high-calcifying *E. huxleyi.* For low-calcifying *E. huxleyi* no peak in calcification rate was observed although initial low rates corresponded to low photosynthetic rates.

The C:P (Fig. 3.3.11) showed high initial values for low-calcifying *E. huxleyi* during lag phase, as seen in the high-calcifying strain, which declined towards zero as calcification became undetectable.

The photosynthetic and calcification rates per cell (Figs. 3.3.12-3.3.13) have a reduced data set because the error in the initial cell counts was too large to produce comparable data for the first ^{14}C incubation. Low-calcifying *E. huxleyi* and *I. galbana* showed maximum levels of photosynthesis per cell in early exponential growth phase followed by a lesser secondary peak in stationary phase. The rate of photosynthesis per cell was far greater for high-calcifying *E. huxleyi* than low-calcifying *E. huxleyi.* The calcification rate per cell remained negligible for low-calcifying *E. huxleyi* for the duration of the incubation.

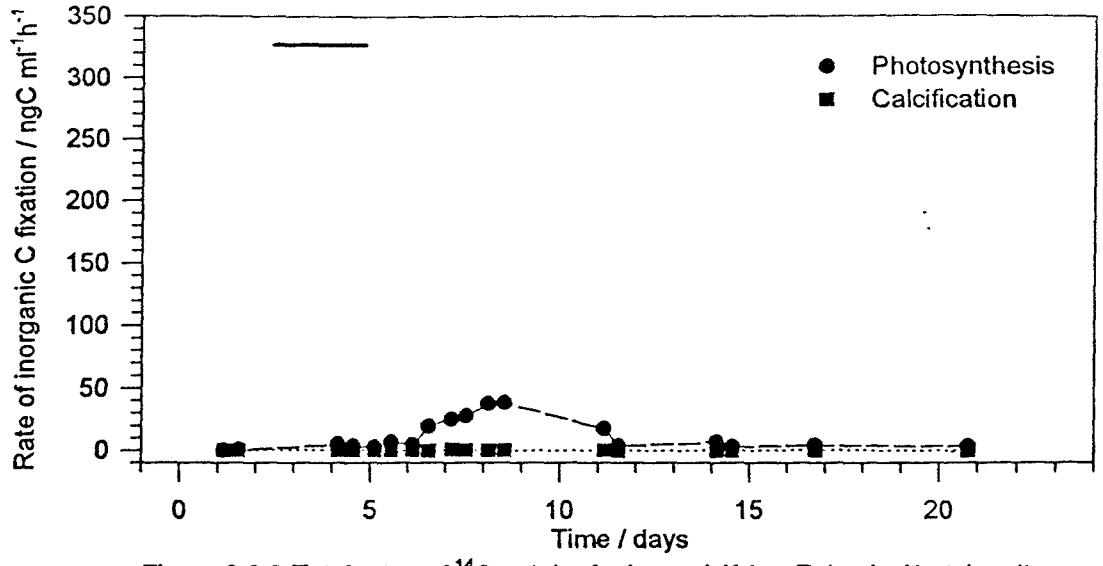

Figure 3.3.9 Total rates of ^{14}C uptake for low-calcifying *E. huxleyi* batch culture (Bar indicates exponential growth phase)

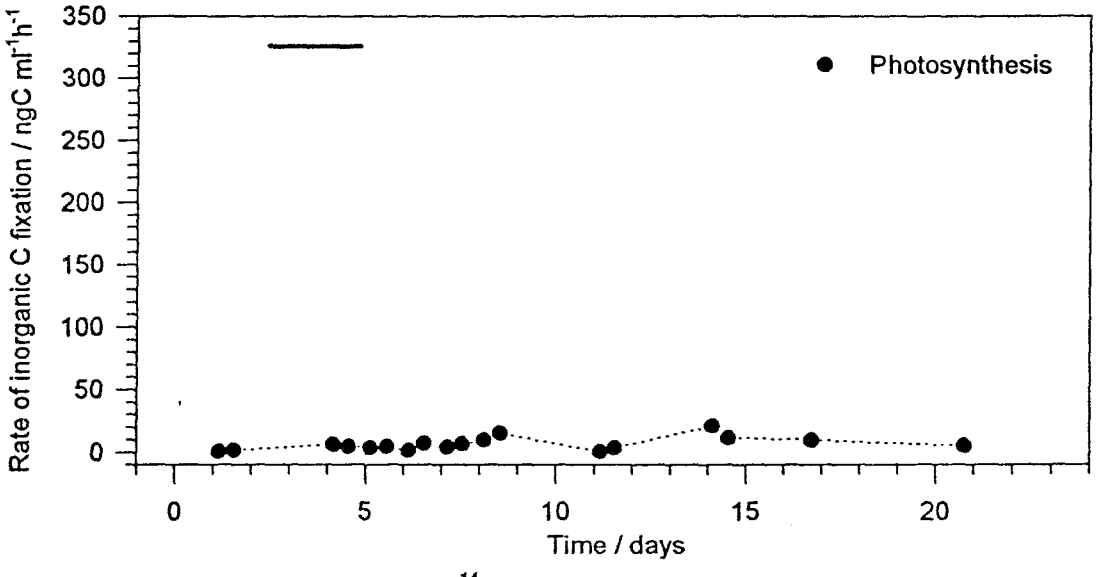

Figure 3.3.10 Total rates of ^{14}C uptake for *I. galbana* batch culture

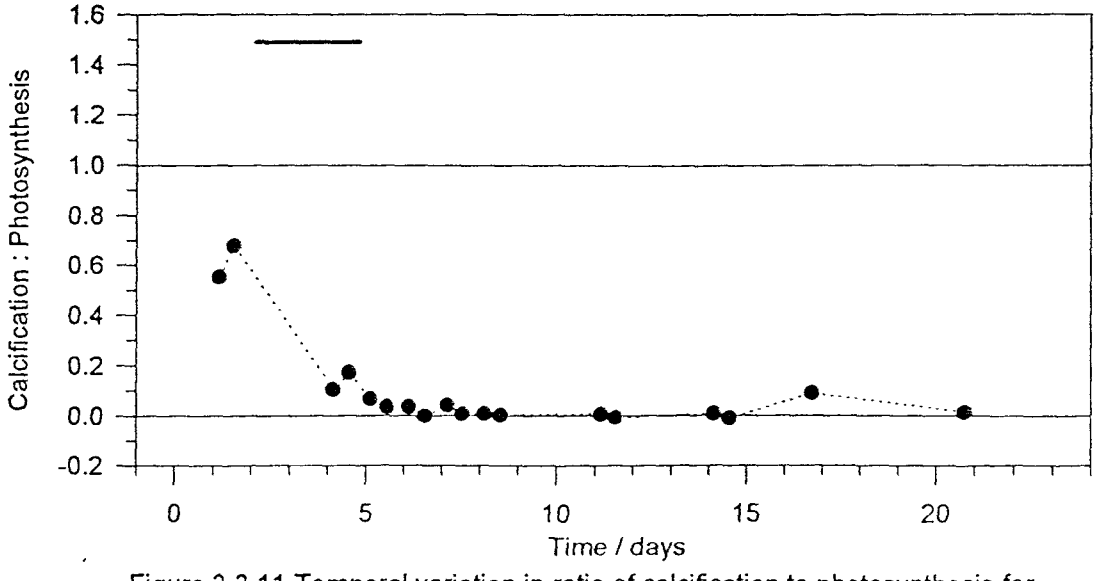

Figure 3.3.11 Temporal variation in ratio of calcification to photosynthesis for low-calcifying *E. huxleyi* batch culture

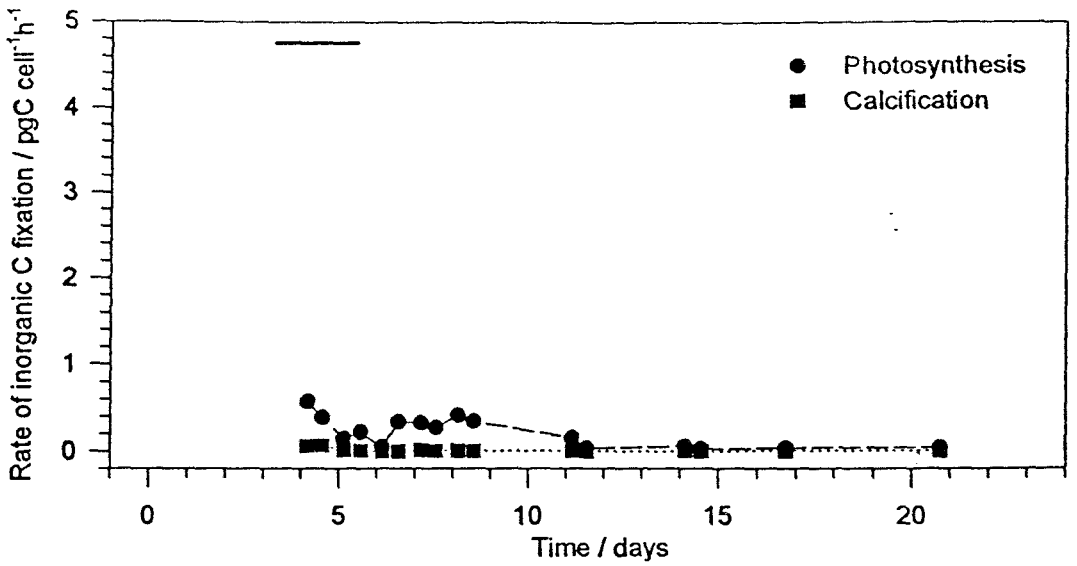

Figure 3.3.12 Rates of ^{14}C uptake per cell for low-calcifying *E. huxleyi* batch culture

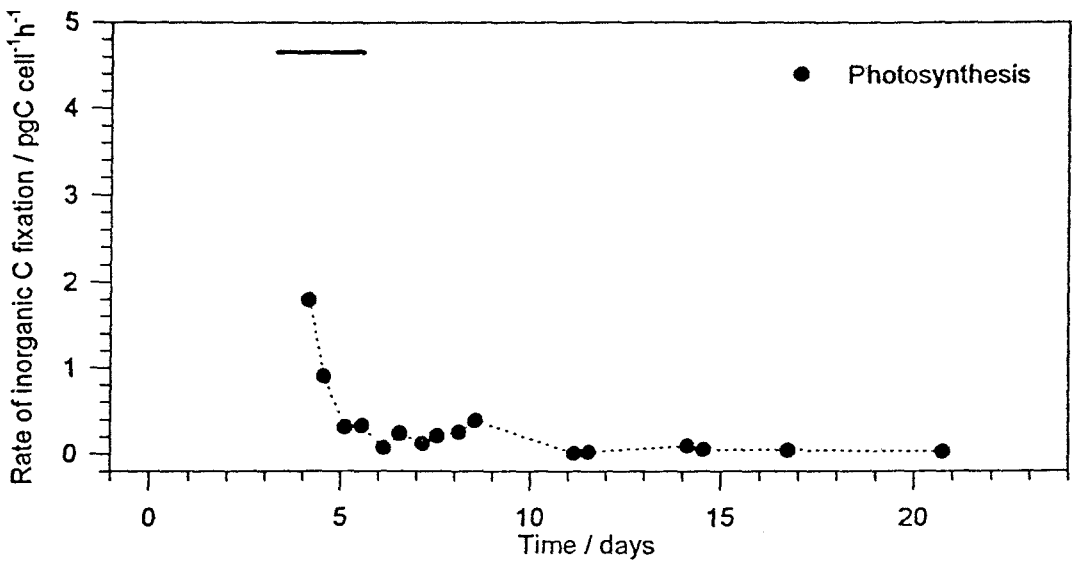

Figure 3.3.13 Rates of ^{14}C uptake per cell for *I. galbana* batch culture

3.3.5 Total dissolved inorganic carbon (C_T) vs total alkalinity (A_T) plots and buffer factor plots

The buffer factor (β) (Figs. 3.3.14-3.3.15) was higher during the initial growth phases than the stationary phase in both cultures, as noted in both previous experiments with high-calcifying *E. huxleyi*, with the initial buffer factor being higher for *I. galbana* (β = 13.50) than low-calcifying *E. huxleyi* (β = 9.46). The stationary phase buffer factors were similar for low-calcifying *E. huxleyi* (β = 7.14) and *I. galbana* (β = 6.92).

The C:P, calculated from C_T vs A_T slope, (Figs. 3.3.16-3.3.17) was lower during the initial growth phases than the stationary phase in both cultures, with *I. galbana* C:P showing no significant calcification in any growth phase as expected for a non-calcifying phytoplankton culture. The C:P for low-calcifying *E. huxleyi* showed a C:P of *ca.* 0.10 throughout the experiment. This was far lower than any of the C:P from the high-calcifying *E. huxleyi* in both previous batch cultures. This again would be expected for a low-calcifying strain of *E. huxleyi*.

3.3.6 Summary of results from batch culture #3

The effect of low-calcifying *E. huxleyi* and *I. galbana* on the dissolved carbonate system was almost identical, if the delay in attaining maximum cell numbers in the *I. galbana* culture was considered. The effect of both cultures on alkalinity was minimal and the net reduction of C_T approximately 30% of that attained by high-calcifying *E. huxleyi* cultures.

For the ^{14}C radiotracing incubations the rates of photosynthesis per cell for both cultures were considerably lower than those found for corresponding high-calcifying *E. huxleyi* cultures (*i.e.* 1.0P), and calcification per cell was negligible for low-calcifying *E. huxleyi* throughout the incubation.

The trends seen in the ^{14}C uptake derived C:P were similar to the C_T vs A_T derived C:P.

Table 3.1.1 shows a summary of these results.

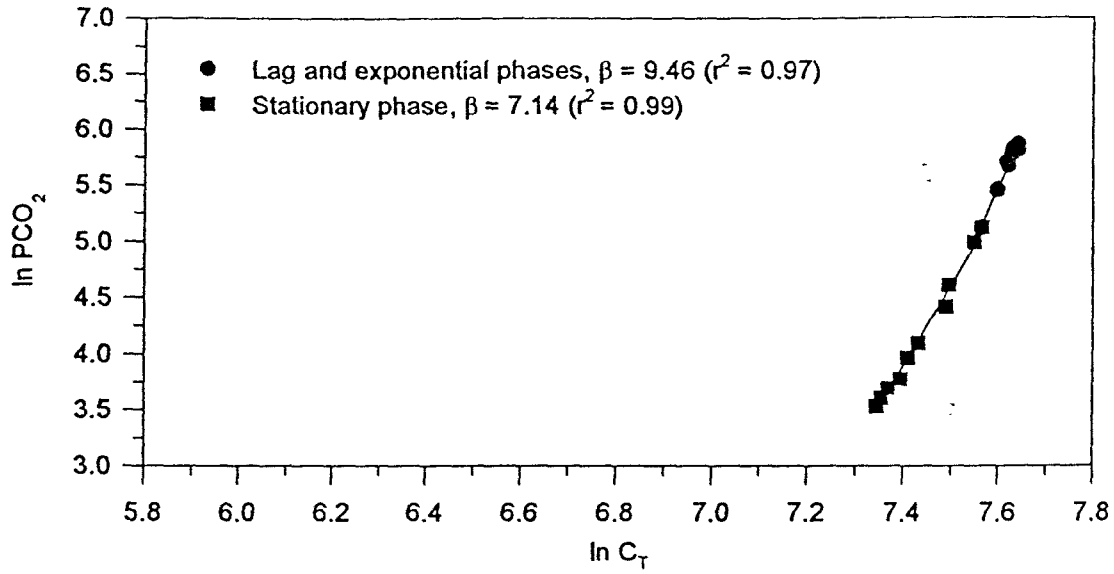

Figure 3.3.14 Plot of lnC_T against $lnPCO_2$ for low-calcifying *E. huxleyi* batch culture (Slope of regression line represents β)

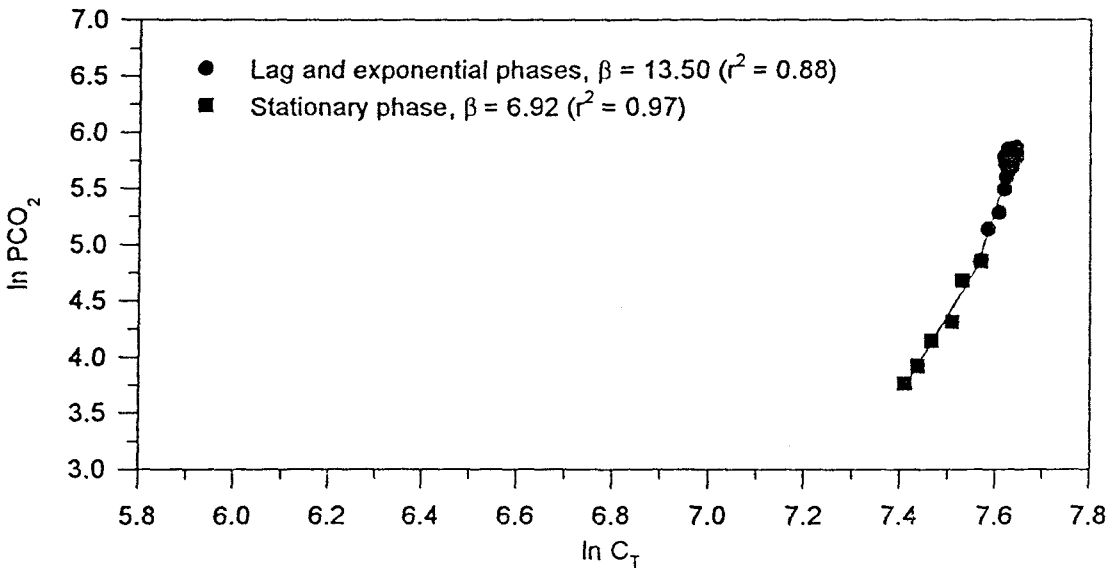

Figure 3.3.15 Plot of lnC_T against $lnPCO_2$ for *I. galbana* batch culture

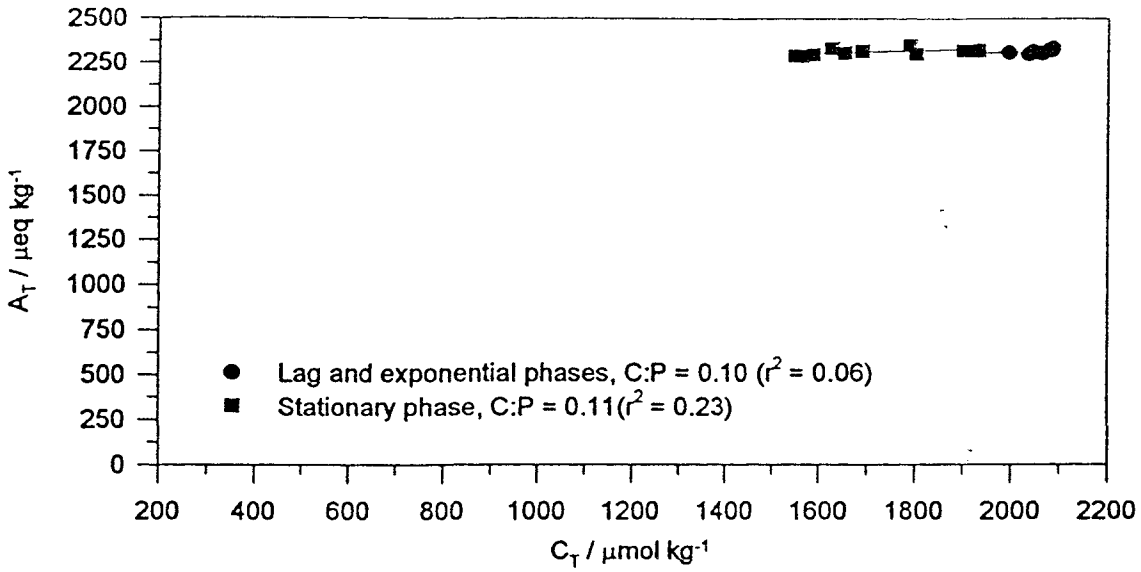

Figure 3.3.16 Plot of C_T against A_T for low-calcifying *E. huxleyi* batch culture (C:P derived from slope of regression)

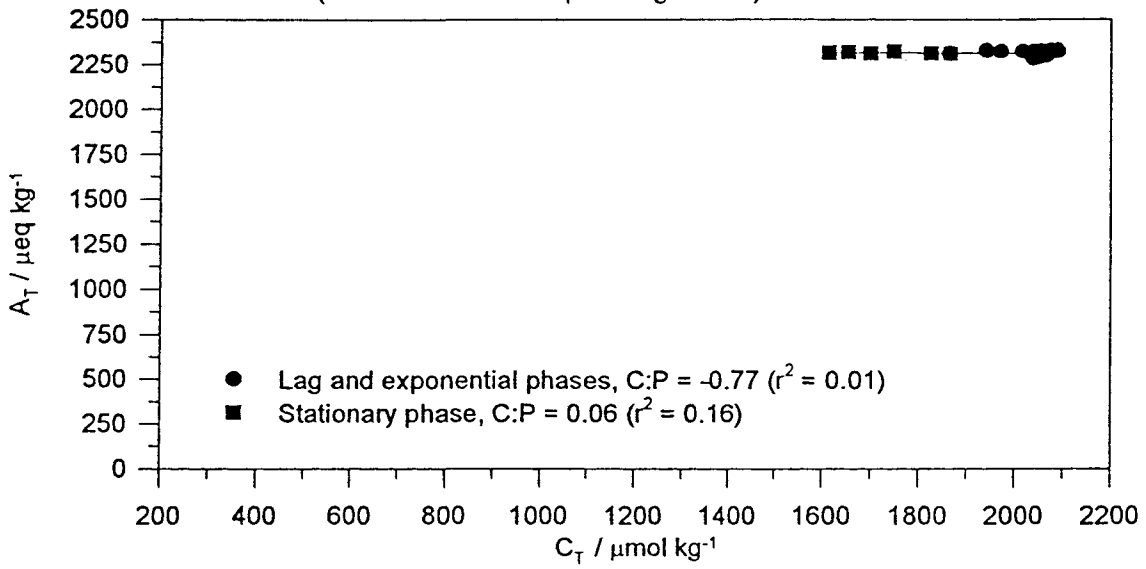

Figure 3.3.17 Plot of C_T against A_T for *I. galbana* batch culture

Expt no & culture	Species & strain	μ_{max} / d^{-1}	Max cell no / x 10^3 ml^{-1}	Max p'synth rate / pgC $cell^{-1}$ h^{-1}	Max calc rate/ pgC $cell^{-1}$ h^{-1}	Max ^{14}C C:P	A_C derived max calc rate / ngC$ml^{-1}h^{-1}$	Initial PCO_2 / µatm	Max PCO_2 / µatm	Min PCO_2 / µatm	Final PCO_2 / µatm	Δ PCO_2 / µatm
#1 / 0.5P	*E. huxleyi* / 92E	1.06	197 (21)	1.10 (4)	0.51 (5)	0.62 (5)	32.12	429	557 (2)	235 (20)	235	322
#1 / 1.0P	*E. huxleyi* / 92E	1.03	455 (21)	0.98 (4)	0.66 (5)	0.82 (10)	66.75	401	487 (2)	104 (20)	104	383
#1 / 2.0P	*E. huxleyi* / 92E	1.17	825 (14)	1.37 (5)	1.20 (5)	0.98 (6)	81.38	395	486 (2)	60 (20)	60	426
#2 / 0.5P	*E. huxleyi* / 92E	0.88	143 (11)	3.39 (2)	3.27 (2)	1.44 (0)	38.38	318	318 (0)	114 (9)	222	204
#2 / 1.0P	*E. huxleyi* / 92E	0.97	278 (15)	3.85 (2)	2.33 (2)	1.33 (0)	55.97	308	313 (1)	56 (9)	63	257
#2 / 2.0P	*E. huxleyi* / 92E	0.86	480 (8)	3.2 (2)	2.58 (2)	1.29 (0)	53.60	304	313 (0)	28 (15)	28	285
#3 / 1.0P	*E. huxleyi* / CCAP 920/2	1.03	113 (10)	0.56 (4)	0.20 (4)	1.8 (4)	-	338	352 (1)	30 (20)	31	322
#3 /1.0P	*I. galbana* / CCAP 927/1	0.88	237 (15)	1.80 (4)	-	-	-	351	351 (0)	33 (22)	34	318

Table 3.1.1 Summary of results for all batch cultures - (Bracketed number corresponds to day number of experiment)

Expt no & culture	Species & strain	Initial A_T / µeq kg^{-1}	Final A_T / µeq kg^{-1}	ΔA_T / µeq kg^{-1}	Initial A_C / µeq kg^{-1}	Final A_C / µeq kg^{-1}	ΔA_C / µeq kg^{-1}	Initial C_T / µmol kg^{-1}	Final C_T / µmol kg^{-1}	ΔC_T / µmol kg^{-1}
#1 / 0.5P	*E. huxleyi* / 92E	2168	923	1245	2141	876	1265	2011	840	1171
#1 / 1.0P	*E. huxleyi* / 92E	2109	636	1473	2088	553	1535	1985	519	1466
#1 / 2.0P	*E. huxleyi* / 92E	2155	529	1626	2081	449	1632	1979	412	1567
#2 / 0.5P	*E. huxleyi* / 92E	2344	1355	989	2264	1288	976	2084	1202	882
#2 / 1.0P	*E. huxleyi* / 92E	2383	1008	1375	2363	890	1473	2117	775	1342
#2 / 2.0P	*E. huxleyi* / 92E	2375	1051	1324	2301	878	1423	2130	706	1424
#3 / 1.0P	*E. huxleyi* / CCAP 920/2	2302	2273	29	2256	2047	209	2085	1536	549
#3 / 1.0P	*I. galbana* / CCAP 927/1	2326	2308	18	2253	2056	197	2089	1584	505

Table 3.1.1 Summary of results for all batch cultures (continued) - (Bracketed number corresponds to day number of experiment)

Expt no & culture	Species & strain	Growth phase	Buffer factor / β	C_T vs A_T derived C:P	Av ^{14}C C:P
#1 / 0.5P	*E. huxleyi* / 92E	Lag and exponential	3.97	0.76	0.25
		Stationary	0.17	1.50	0.21
#1 / 1.0P	*E. huxleyi* / 92E	Lag and exponential	3.18	1.16	0.44
		Stationary	0.43	1.57	0.36
#1 / 2.0P	*E. huxleyi* / 92E	Lag and exponential	3.61	0.78	0.56
		Stationary	0.76	1.49	0.37
#2 / 0.5P	*E. huxleyi* / 92E	Lag and exponential	7.12	0.31	0.34
		Stationary	1.56	1.24	0.21
#2 / 1.0P	*E. huxleyi* / 92E	Lag and exponential	4.44	0.65	0.54
		Stationary	2.14	1.05	0.29
#2 / 2.0P	*E. huxleyi* / 92E	Lag and exponential	4.28	0.66	0.43
		Stationary	2.41	0.99	0.17
#3 / 1.0P	*E. huxleyi* / CCAP 920/2	Lag and exponential	9.46	0.10	0.27
		Stationary	7.14	0.11	0.02
#3 / 1.0P	*I. galbana* / CCAP 927/1	Lag and exponential	13.50	-0.77	-
		Stationary	6.92	0.06	-

Table 3.1.1 Summary of results for all batch cultures (continued) - (Bracketed number corresponds to day number of experiment)

CHAPTER FOUR : NORWAY MESOCOSM RESULTS

The phytoplankton communities that developed in both mesocosms were dominated by three diatom species (*Leptocylindricus danicus, Pseudonitzschia* spp. and *Skeletonema costatum*) and the coccolthophorid *Emiliania huxleyi*. Both experimental enclosures (mesocosms) showed a rapid increase in phytoplankton biomass following the initial additions of nutrient supplements which were 15µM nitrate, 1µM phosphate and 10µM silicate for bag 3 and 15µM nitrate and 1µM phosphate for bag 5. In bag 3 an initial mixed bloom of diatoms and *E. huxleyi* developed (Fig. 4.1.7) which reached coincident population maxima on day 6, corresponding to 2 days after the peak in chlorophyll. Both diatoms and *E. huxleyi* numbers and chlorophyll concentration then declined to a minimum between days 12-16. *E. huxleyi* subsequently dominated a second bloom with cell numbers peaking on day 22. During the secondary bloom chlorophyll concentration peaked on day 23 but did not reflect the changes in cell number. In bag 5 an almost monospecific bloom of *E. huxleyi* developed immediately (Fig. 4.1.11) with a peak in chlorophyll on day 5 and maximum cell numbers on day 8. Chlorophyll and cell numbers then declined to reach the minima on day 12. Subsequently a second bloom of *E. huxleyi* developed and attained maximum cell numbers on day 18, as in bag 3 chlorophyll levels did not reflect cell numbers.

After a period of reasonable weather during the first week of the experiment, conditions deteriorated after day 8 and did not improve, apart from day 12, until the third week (day 14 onwards) which was characterised by a period of clear skies and bright sunshine (Fig. 4.1.10/4.1.22). Maximum phytoplankton cell numbers were detected during the periods of higher surface irradiance.

Table 4.1.1 shows a summary of all results.

4.1.1 ^{14}C uptake measurements

^{14}C incubations were carried out on alternate days for the duration of the experimental period. Figure 4.4.1 shows four examples of PvI and CvI curves with two graphs for each mesocosm. The parameters investigated using PvI and CvI incubations were: P_{max}, the light saturated rate of photosynthesis; P_{max}^{B} the light saturated rate of photosynthesis normalised to chlorophyll *a*; α, the initial slope of the light saturated curve (photosynthetic efficiency); α^{B}, the initial slope of the light saturated curve normalised to chlorophyll *a*; C_{max}, the light saturated rate of calcification; and C_{max}^{B} the light saturated rate of calcification normalised to chlorophyll *a*.

The ^{14}C incubation results shown coincided with maximum phytoplankton cell numbers for both mesocosms. Maximal P_{max} values for both mesocosms were recorded during the first bloom (Figs. 4.1.2 and 4.1.14), on day 3 for bag 5 and day 5 for bag 5 when

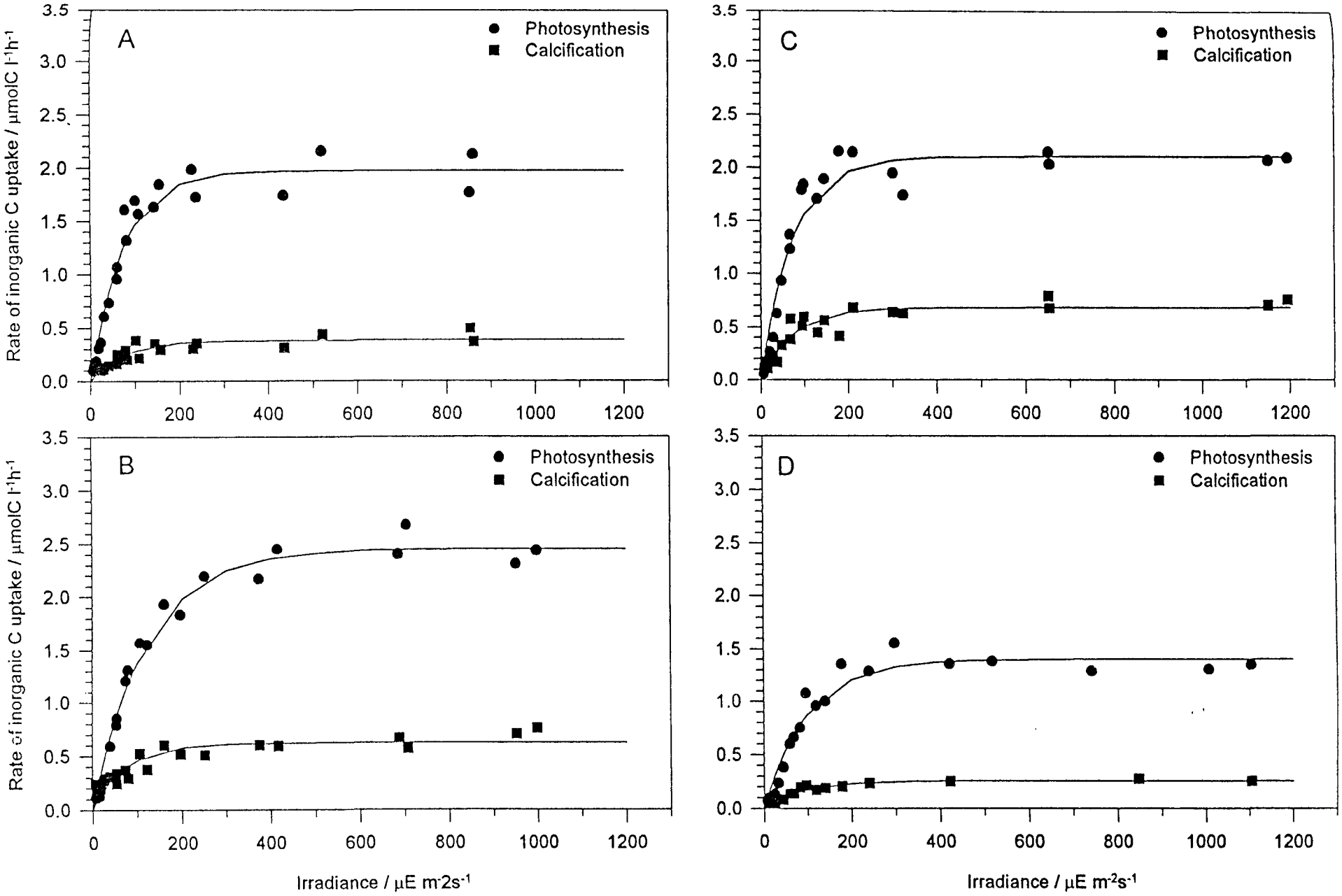

Figure 4.1.1 Comparisons of calcification and photosynthetic rate versus irradiance for: A Bag 3 day 5; B bag 3 day 21; C bag 5 day 7; and D bag 5 day 21

chlorophyll levels were at or near maximal values. P_{max} subsequently declined to minima on day 13 for both mesocosms as chlorophyll levels also reached their minima. In bag 3 a second distinct peak in P_{max} was observed on day 21 as *E. huxleyi* cell numbers peaked again. A less sharply defined increase in P_{max} was noted between days 17 and 21 in bag 5 and again corresponded to the maximum in *E. huxleyi* cell numbers.Maximal C_{max} values (Figs. 4.1.2 and 4.1.14) also showed peaks in activity which generally corresponded to the peak in *E. huxleyi* cell numbers in each enclosure. In bag 3 C_{max} initially peaked at maximal chlorophyll levels, 2 days after maximal P_{max}. The maximal C_{max} peak in bag 5 during the first bloom corresponded to maximal P_{max}. In both mesocosms C_{max} was seen to increase during the secondary monospecific *E. huxleyi* blooms. For bag 5 C_{max} peaked on day 19 at maximum cell numbers, but in bag 3 C_{max} was still increasing at the end of the sampling period on day 25.

The highest values for P_{max}^{B} for both mesocosms were recorded at the start of the experimental period (Figs. 4.1.3 and 4.1.15). A second peak of comparable magnitude to the initial P_{max}^{B} values in bag 3 was observed on day 21 and a secondary broad P_{max}^{B} maximum was observed in bag 5 around day 19. In bag 3 C_{max}^{B} showed a broad maximum during the secondary bloom between days 15 and 25 but no comparable change was seen during the first mixed bloom. C_{max}^{B} in bag 5 showed two broad maxima peaking on days 5 and 19 with a minimum on day 11(Figs. 4.1.3 and 4.1.15). α and α^{B} showed similar temporal variability to P_{max} and P_{max}^{B} respectively in both bags (Figs. 4.1.4 and 4.1.16).

The ratio of calcification to photosynthesis derived (C:P) from ^{14}C results had two broad maxima for both mesocosms (Figs. 4.1.5 and 4.1.17). In bag 3 the first maxima of 0.24 was observed subsequent to maximum cell numbers on day 7 followed by a decline to zero on day 10. The C:P increased to 0.53 on day 17 during the net growth of the second bloom but reached a maximum level on the last day of the experiment with a C:P of 1.2. For bag 5 an initial maximal peak of 0.35 on day 5 was followed by a decline to a minimum on day 11 followed by a broad lesser maximum *ca.* 0.25 from days 13-21 which corresponded to the growth and stationary phase of the secondary *E. huxleyi* dominated bloom. For bag 5 there is no calcification data shown on day 17 due to a very high anomalous value which was not supported by any other data.

Bag 3 initially showed low calcification in the dark (Fig. 4.1.6) followed by an increase to a maximum on day 20, then by a short decline and an increase to a maximum on the last day of the sampling period which coincided with the highest ^{14}C C:P. The dark calcification rate for bag 5 (Fig. 4.1.18) showed a steady low level with a distinct maximum on day 15 during the net growth phase of the second bloom. The dark calcification results are derived from one dark incubated bottle and are therefore subject to unquantifiable error.

4.1.2 Dissolved carbonate system

Total alkalinity (A_T) and total dissolved inorganic carbon (C_T) (Figs. 4.1.8 and 4.1.20) initially showed values of *ca.* 100 μeq kg^{-1} and 100 μmol kg^{-1} higher in bag 3 than bag 5. After 3 days C_T started to decline to a minimum on day 7 and day 8 for bags 3 and 5 respectively. This reduction in C_T was approximately three times greater in bag 3 than bag 5. C_T then increased to a broad peak for both mesocosms between days 14 and 21 and days 12-17 for bags 3 and 5 respectively. C_T then declined again for the remainder of the experimental period. For bag 5 A_T followed the same trends as C_T reaching an initial minimum on day 8, but in bag 3 the magnitude of the initial decline in C_T was not matched by A_T which declined steadily during the whole experimental period.

PCO_2 for bag 3 (Fig. 4.1.9) initially increased reaching a maximum of 295μatm on day 2 followed by a rapid decline to a minimum on day 7 (92μatm), coincident with the rapid increase in phytoplankton biomass. PCO_2 then increased to reach a broad secondary maximum of *ca.* 250μatm for the remainder of the experimental period. PCO_2 for bag 5 (Fig. 4.1.21) also initially increased reaching a maximum of 277μatm on day 2 but was followed by a smaller decline, in comparison to bag 3, to a minimum on day 6 of 213μatm. PCO_2 then increased to a maximum of 302μatm on day 14, again followed by a secondary decline to a value of 237μatm on day 19.

4.1.3 Oxygen consumption rate

The O_2 consumption (or respiration) rates for both mesocosms started at approximately the same level (Figs. 4.1.9 and 4.1.21) and increased to reach maxima on days 4 and 8 for bag 3 and 5 respectively. Bag 3 showed the higher rate which is consistent with the higher chlorophyll levels in this mesocosm. The respiration rate in both mesocosms declined to minima on day 14 with bag 5 showing the lower rate. The respiration rate for bag 3 then continued to increase during the remainder of the experimental period, and bag 5 showed a broad secondary maximum rate between days 16 and 20.

4.1.4 Total dissolved inorganic carbon (C_T) versus total alkalinity (A_T) plots and buffer factor plots

In each bag four growth periods were defined (as a-d) relating to growth and decline phases of the blooms to allow the comparison of the carbonate system derived parameters (Figs 4.1.11 and 4.1.23). Variation in the buffer factor (β) and C:P, derived from the slope of

A_T vs C_T plots, are shown in figures 4.1.12 and 4.1.13 for bag 3 and figures 4.1.24 and 4.1.25 for bag 5.

In both mesocosms first bloom β was lowest during the growth of the first blooms (a), with the higher β attained in bag 3 decline (Figs. 4.1.12 and 4.1.24), with the equivalent values of β in bag 5 at approximately 50% of those seen in bag 3. In the second *E. huxleyi* dominated blooms β was initially higher during the growth in both bags and then declined to a minimum of -0.27 in bag 3.

For both blooms in bag 3 the A_T vs C_T derived C:P (Fig. 4.1.13) were highest during the growth of the blooms and reached maxima for the growth and decline phases during the second bloom reaching a maximum of C:P of 1.79. In bag 5 (Fig. 4.1.25) during the initial *E. huxleyi* and diatom mixed bloom the C:P was constantly low (*ca.* 0.25). The C:P then increased as the mesocosm showed growth of the second *E. huxleyi* dominated bloom and as this declined C:P reached a maximum for both mesocosms of 2.89.

4.1.5 Alkalinity difference derived calcite standing stock

The A_C derived standing stock (Fig. 4.1.26) showed similar trends to that noted for the cell numbers with maxima for bag 5 on day 8 and day 19, with an intermediate minimum on day 14. The increases and declines in A_C were due to net calcification and net dissolution of calcite respectively. The data for bag 3 was very scattered and this was suspected to be due to methodological errors and not changes occurring in the mesocosm. If the general trends of the curve are considered the maxima are coincident *E. huxleyi* cell numbers, with maxima on day 6 and day 24 with an intermediate minimum on day 12.

These trends are also seen in the calcite data (Fig 4.1.27) which was determined using flame atomic absorption spectrometry. Figure 4.1.28 directly compares the spectrometry and alkalinity difference data sets. The data lie around the 1:2 line as expected, although as in figure 4.1.26 again the data was very scattered, although this was not solely due to bag 3 alkalinity derived calcite.

The total net calcification rate (Figure 4.1.29) from the alkalinity derived total net calcification data for bag 3 was too scattered to show any changes during the course of the experiment. The total net calcification rate for bag 5 shows a maxima on day 6 and a secondary maxima on day 16 at approximately the same time and of the same magnitude as that shown by the ^{14}C radiotracing incubation experiments.

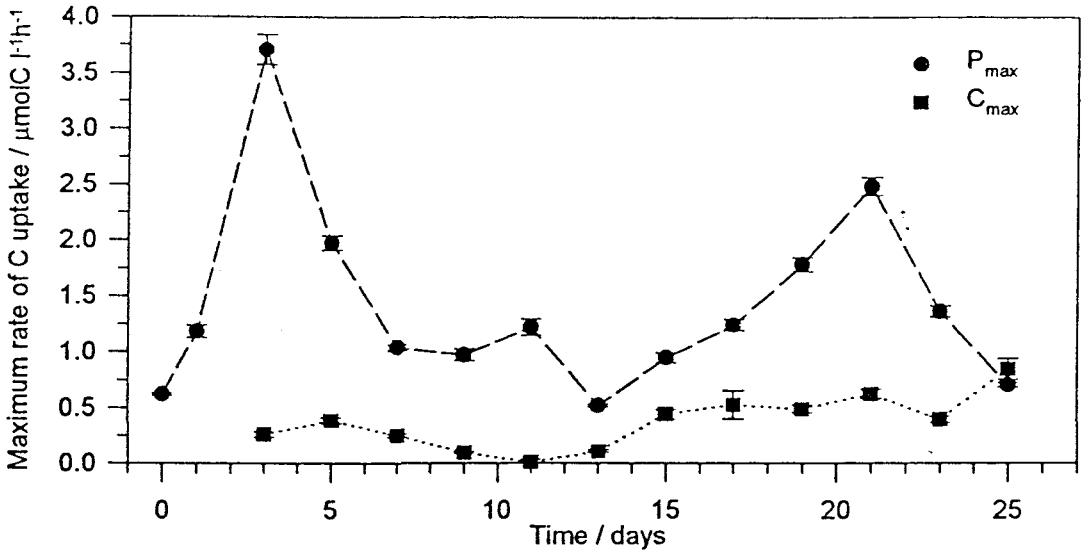

Figure 4.1.2 Temporal variation in P_{max} and C_{max} for bag 3 (Error bars show ± SE)

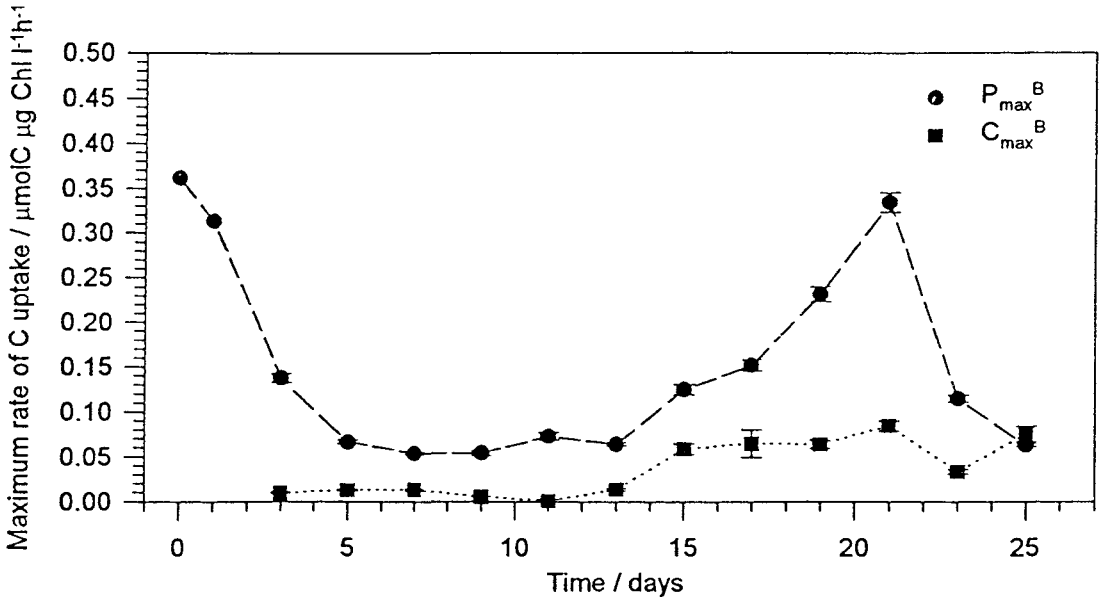

Figure 4.1.3 Temporal variation in P_{max}^B and C_{max}^B for bag 3 (Error bars show ± SE)

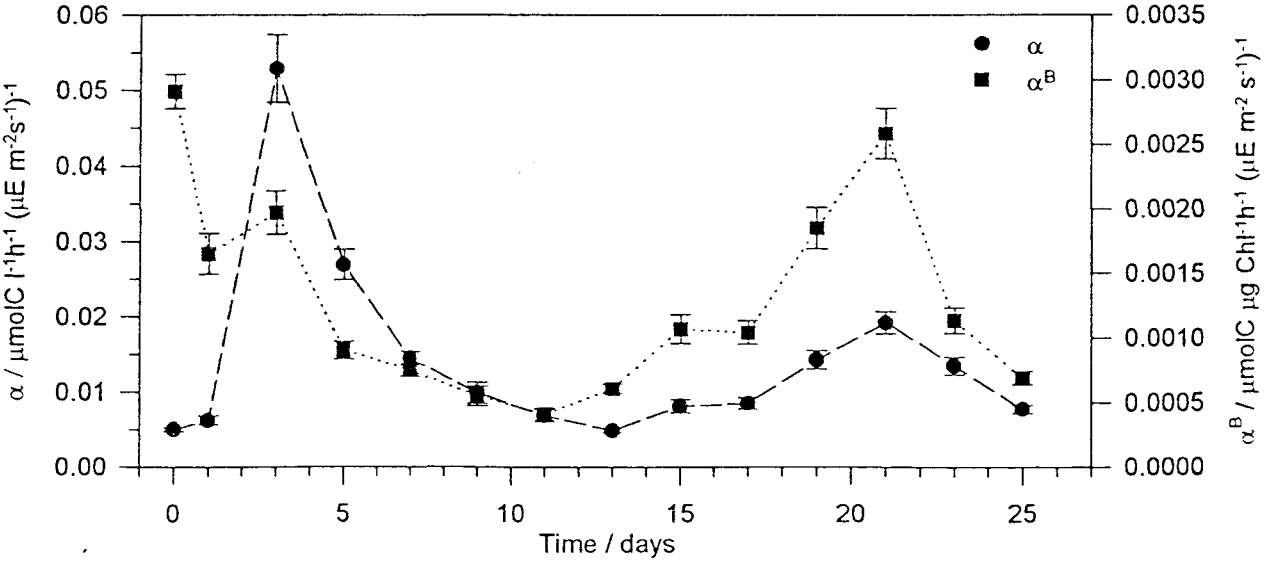

Figure 4.1.4 Temporal variation in α and α^B for bag 3 (Error bars show ± SE)

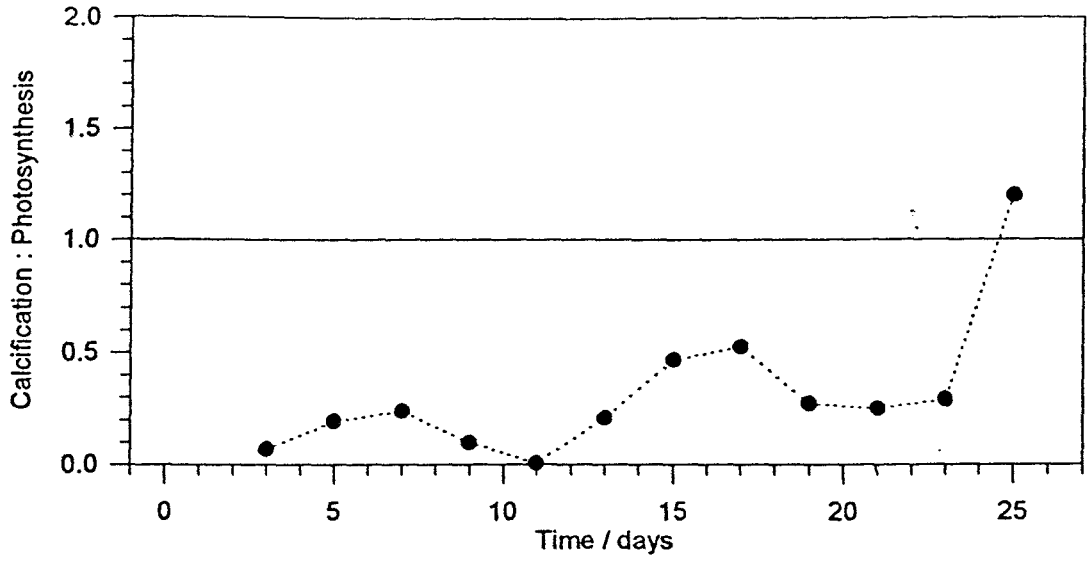

Figure 4.1.5 Temporal variation of ratio of calcification to photosynthesis for bag 3

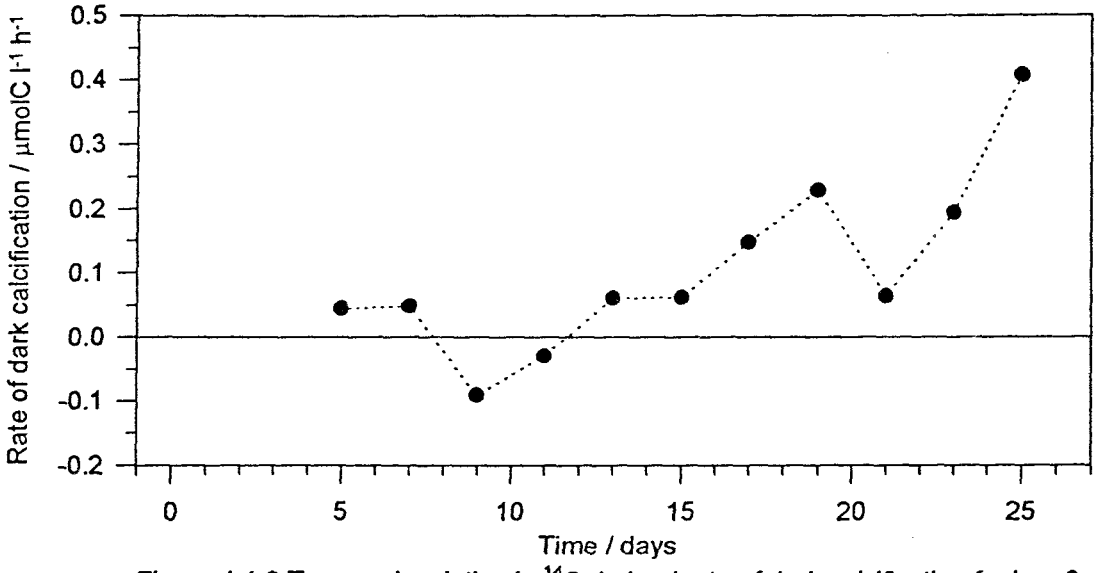

Figure 4.1.6 Temporal variation in ^{14}C derived rate of dark calcification for bag 3

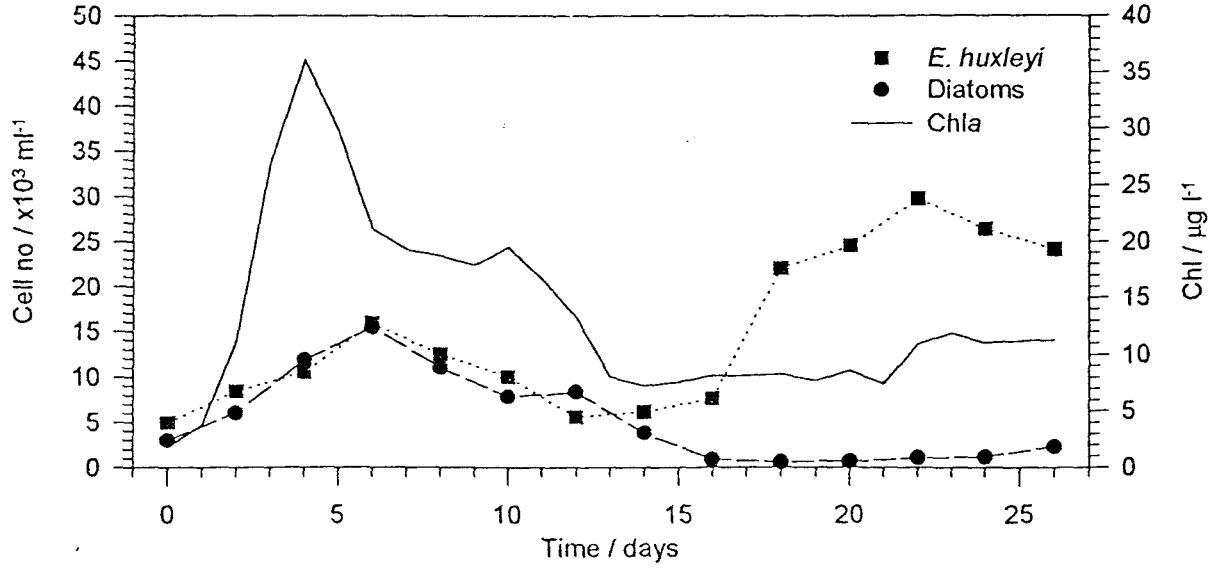

Figure 4.1.7 Cell counts of *E. huxleyi* and diatoms plotted with chlorophyll levels for bag 3

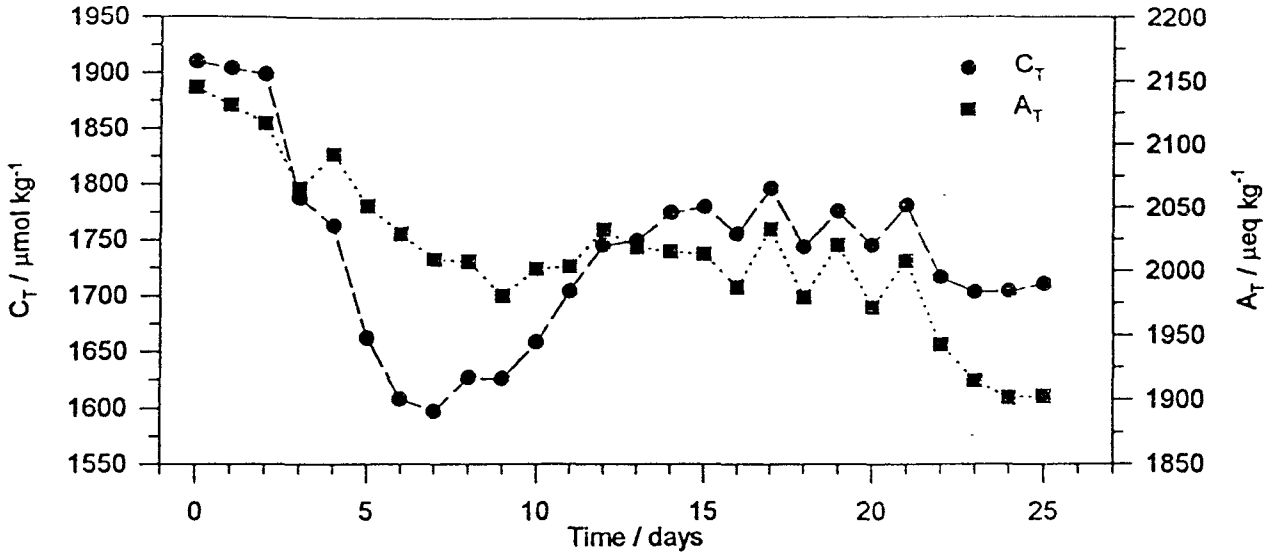

Figure 4.1.8 Daily values for total dissoved inorganic carbon and total alkalinity for bag 3

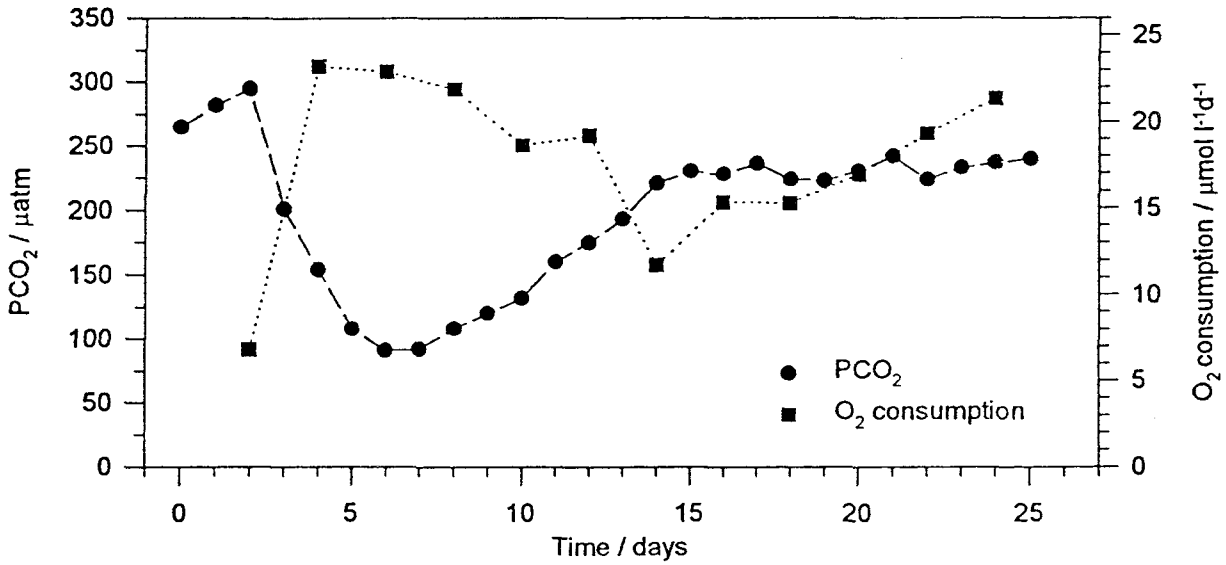

Figure 4.1.9 Daily values of PCO_2 plotted with rates of O_2 consumption for bag 3

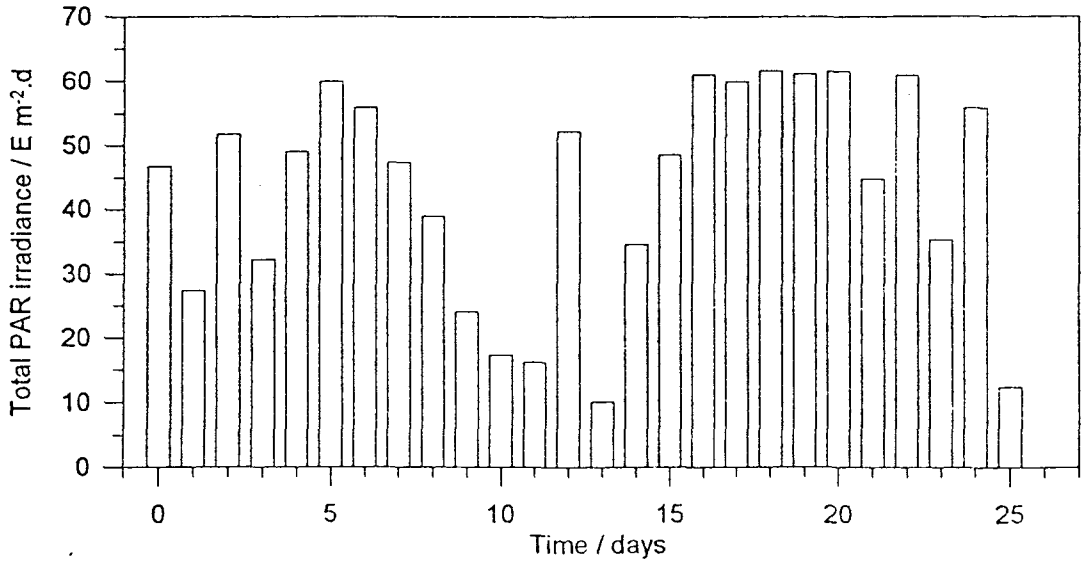

Figure 4.1.10 Daily values of total incident irradiance

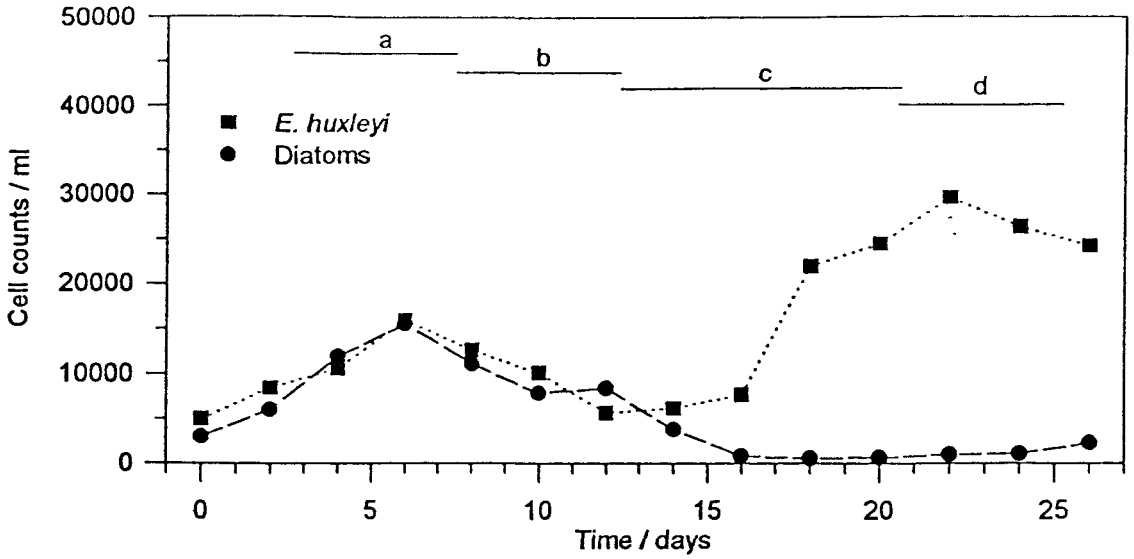

Figure 4.1.11 Cell counts of *E. huxleyi* and diatoms for bag 3
(Bars indicate the periods for which buffer factors and A_T derived C:P were calculated)

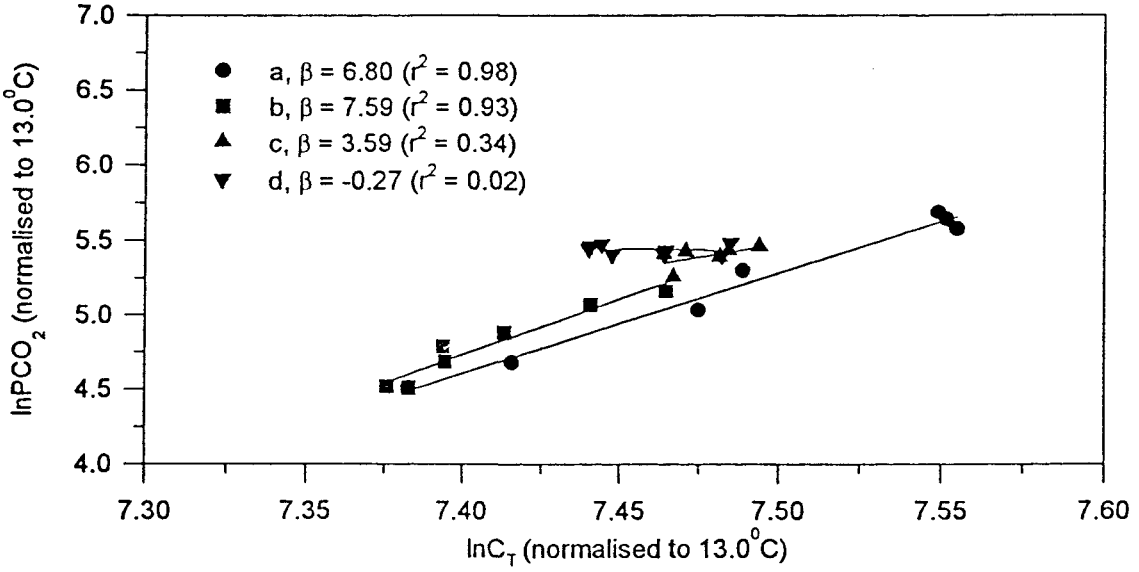

Figure 4.1.12 Plot of lnC_T against $lnPCO_2$ for bag 3 (Slope of regression line represents β)

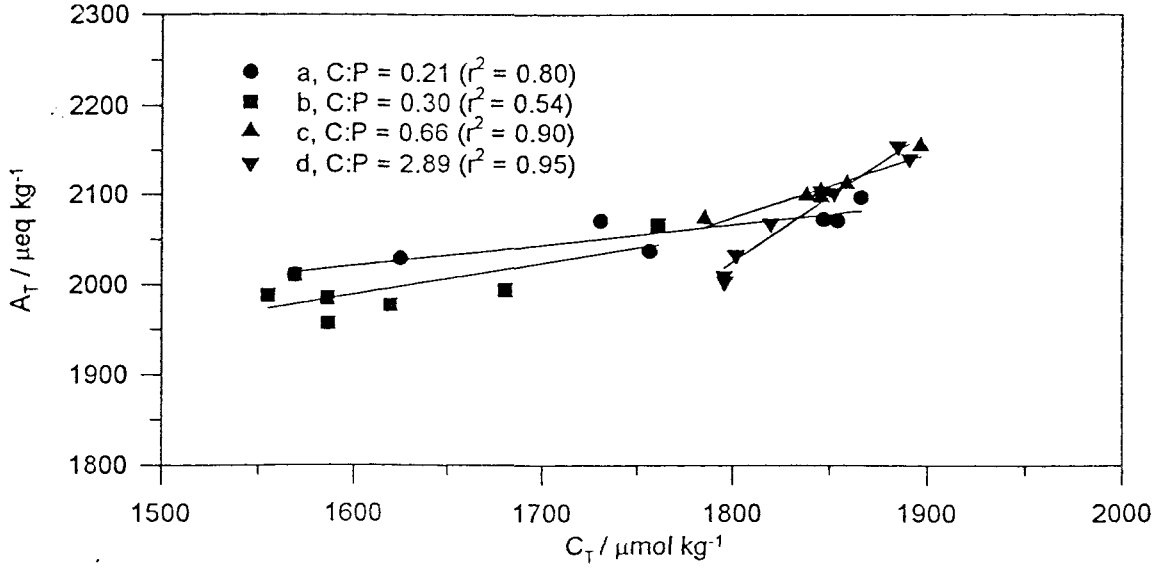

Figure 4.1.13 Plot of C_T against A_T for bag 3 (C:P derived from slope of regression)

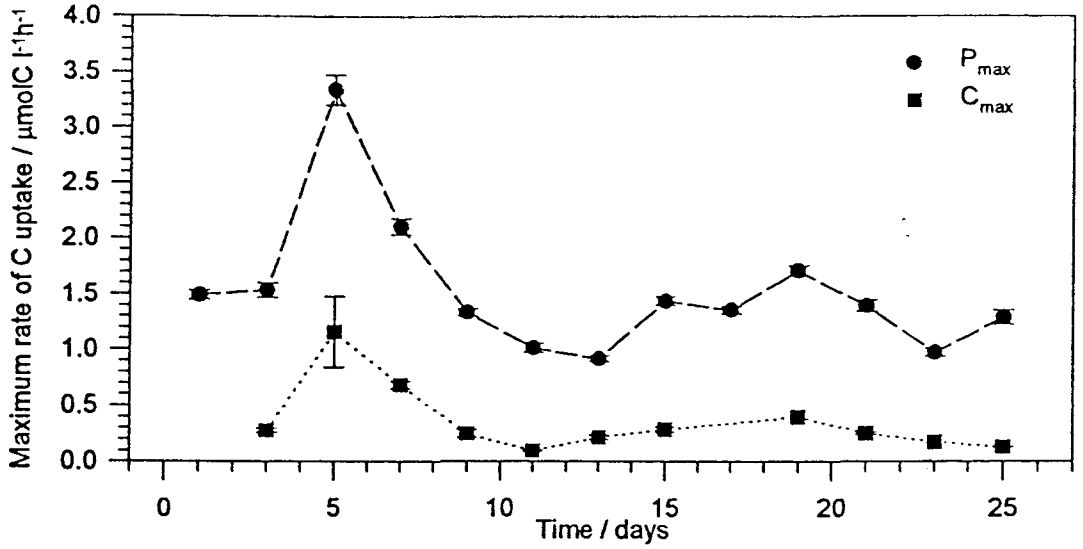

Figure 4.1.14 Temporal variation in P_{max} and C_{max} for bag 5 (Error bars show ± SE)

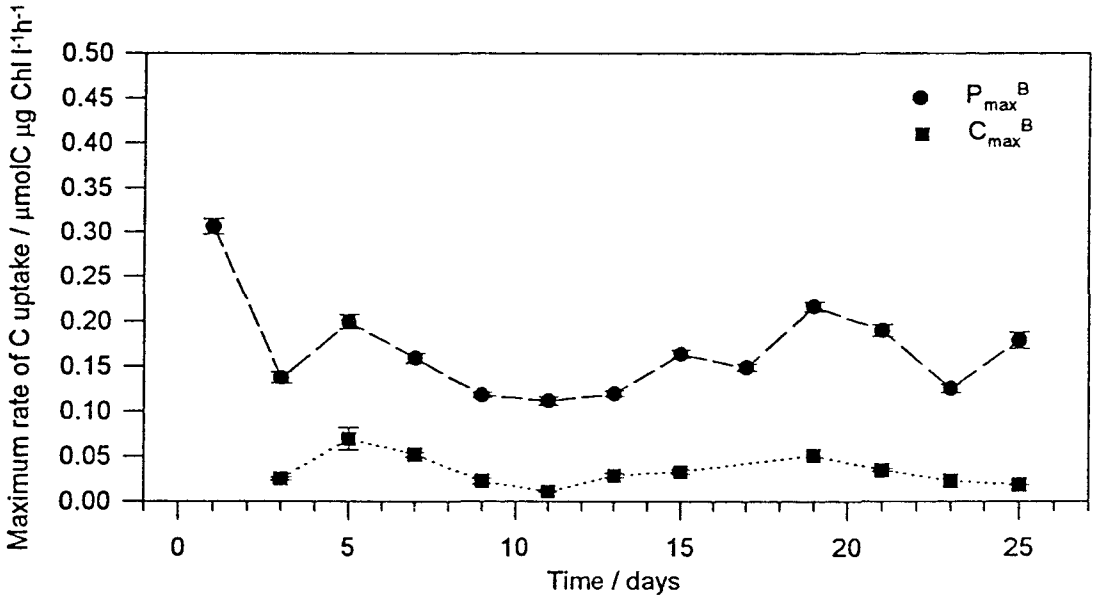

Figure 4.1.15 Temporal variation in P_{max}^{B} and C_{max}^{B} for bag 5 (Error bars show ± SE)

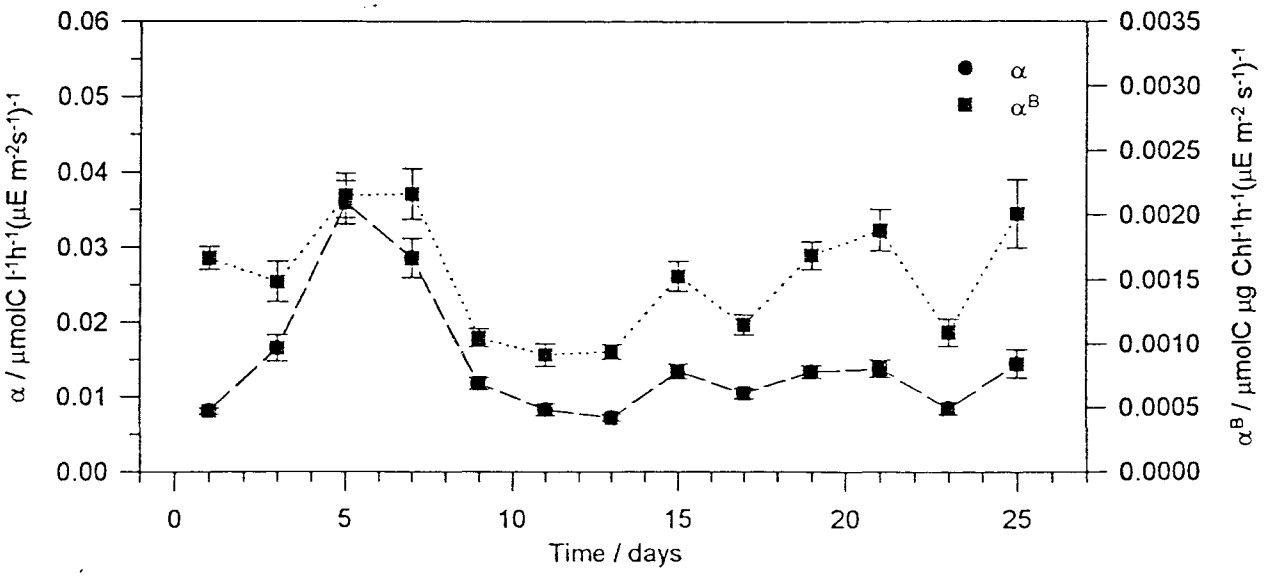

Figure 4.1.16 Temporal variation in α and α^{B} for bag 5 (Error bars show ± SE)

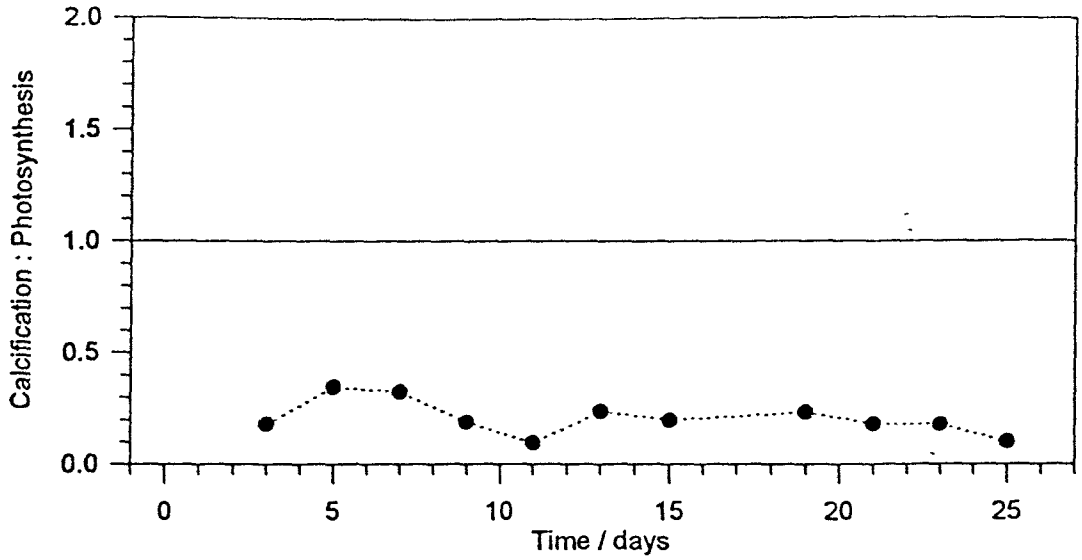

Figure 4.1.17 Temporal variation in ratio of calcification to photosynthesis for bag 5

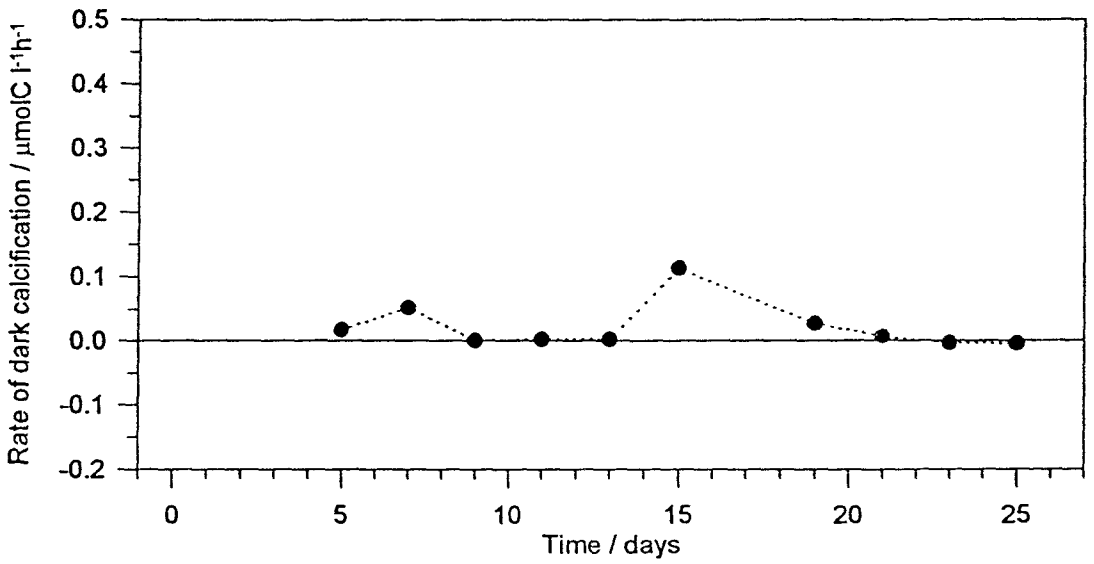

Figure 4.1.18 Temporal variation in rate of ^{14}C derived dark calcification for bag 5

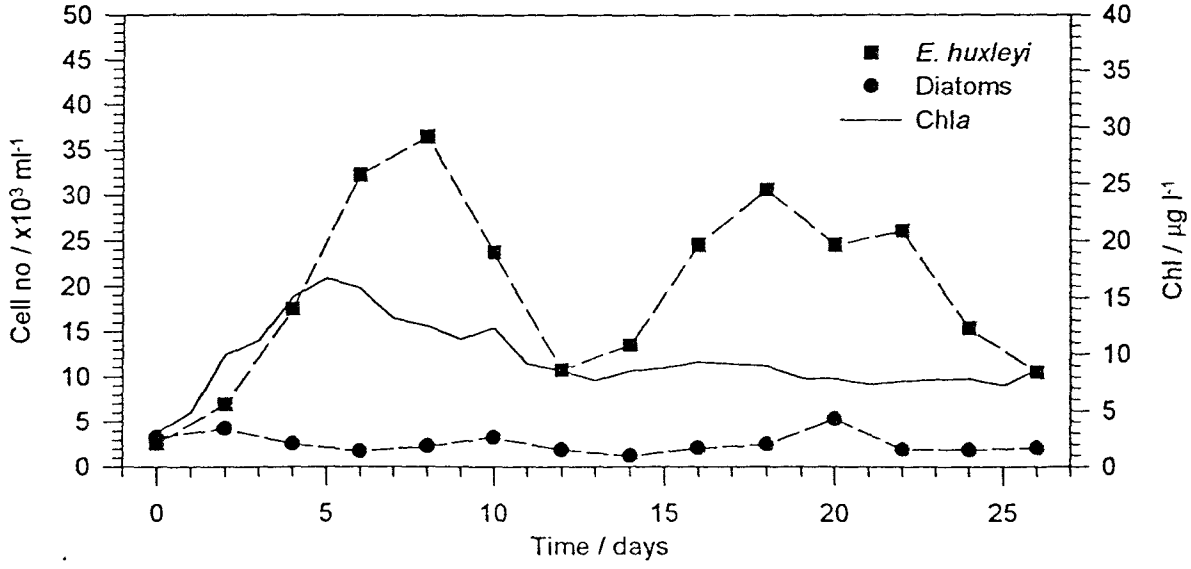

Figure 4.1.19 Cell counts of *E. huxleyi* and diatoms plotted with chlorophyll levels for bag 5

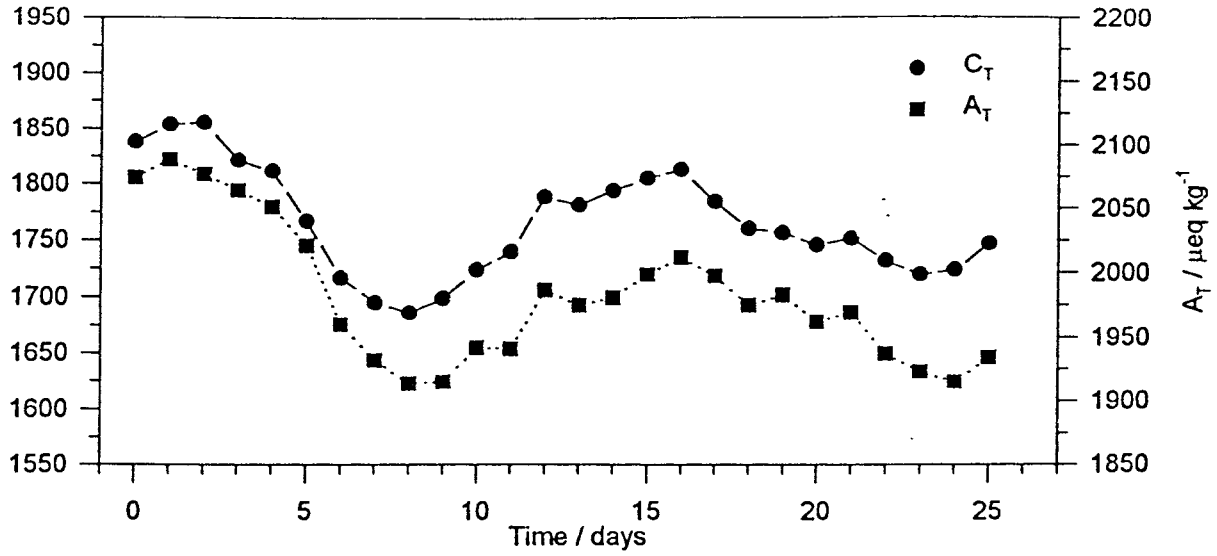

Figure 4.1.20 Daily values of total dissolved inorganic carbon and total alkalinity for bag 5

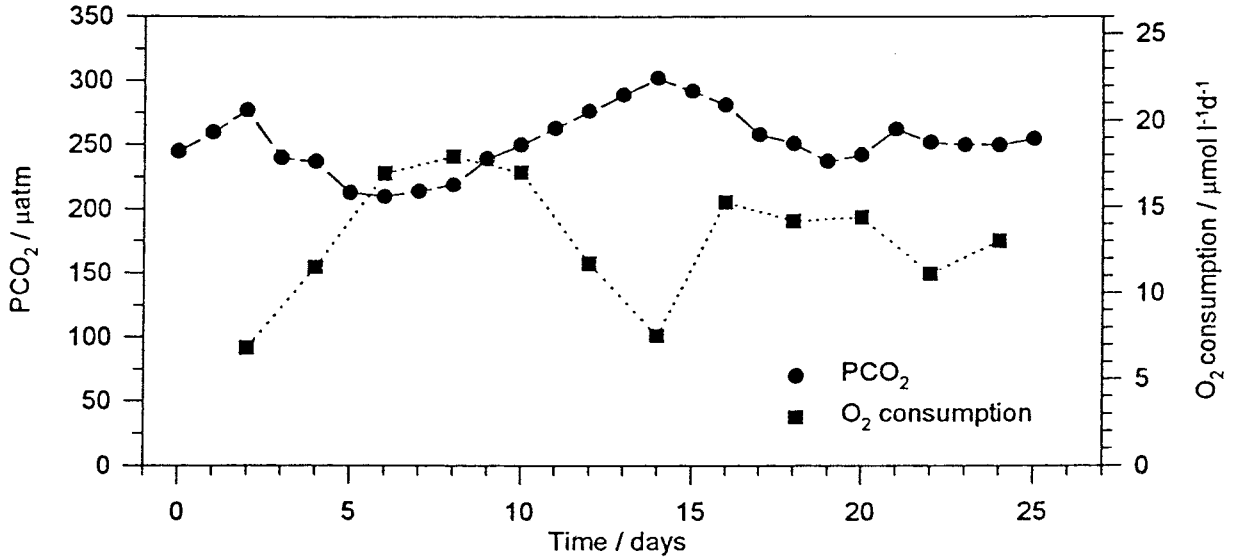

Figure 4.1.21 Daily values of PCO_2 plotted with rates of O_2 consumption for bag 5

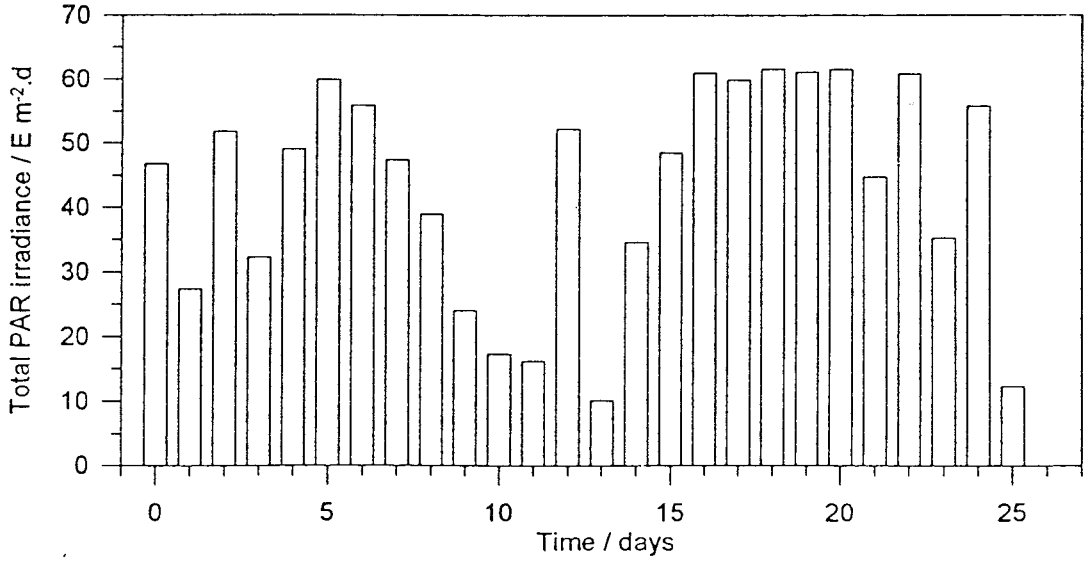

Figure 4.1.22 Daily values of total incident irradiance

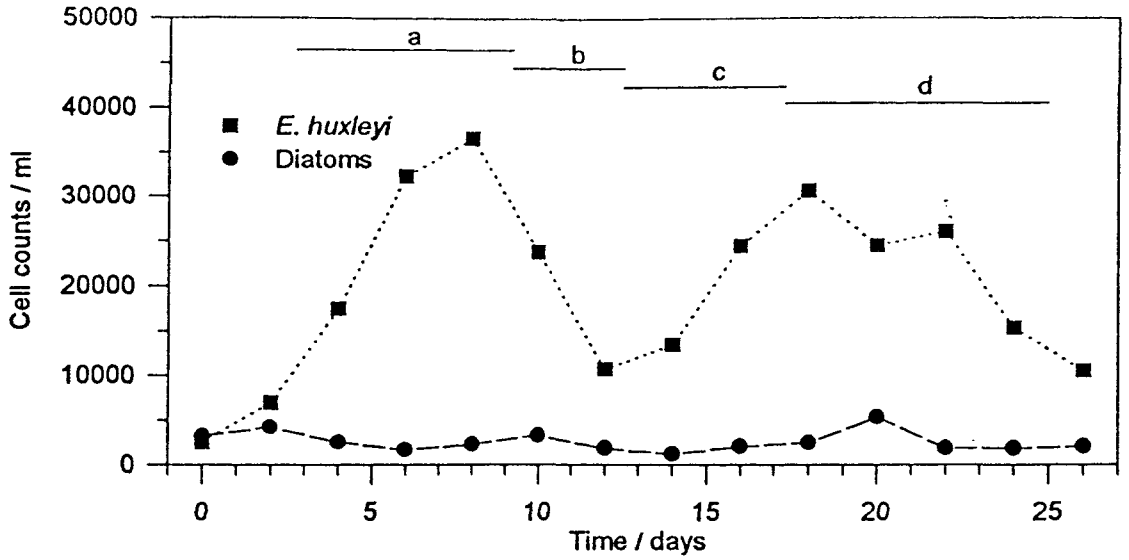

Figure 4.1.23 Cell counts of *E. huxleyi* and diatoms for bag 5
(Bars indicate the periods for which buffer factors and A_T derived C:P were calculated)

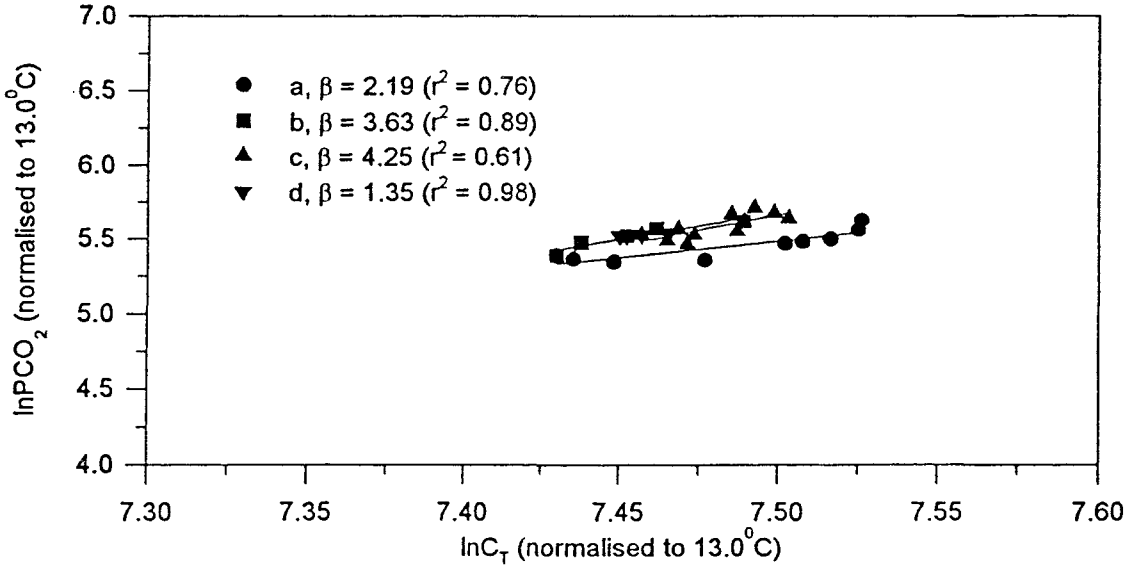

Figure 4.1.24 Plot of $\ln C_T$ against $\ln PCO_2$ for bag 5 (Slope of regression line represents β)

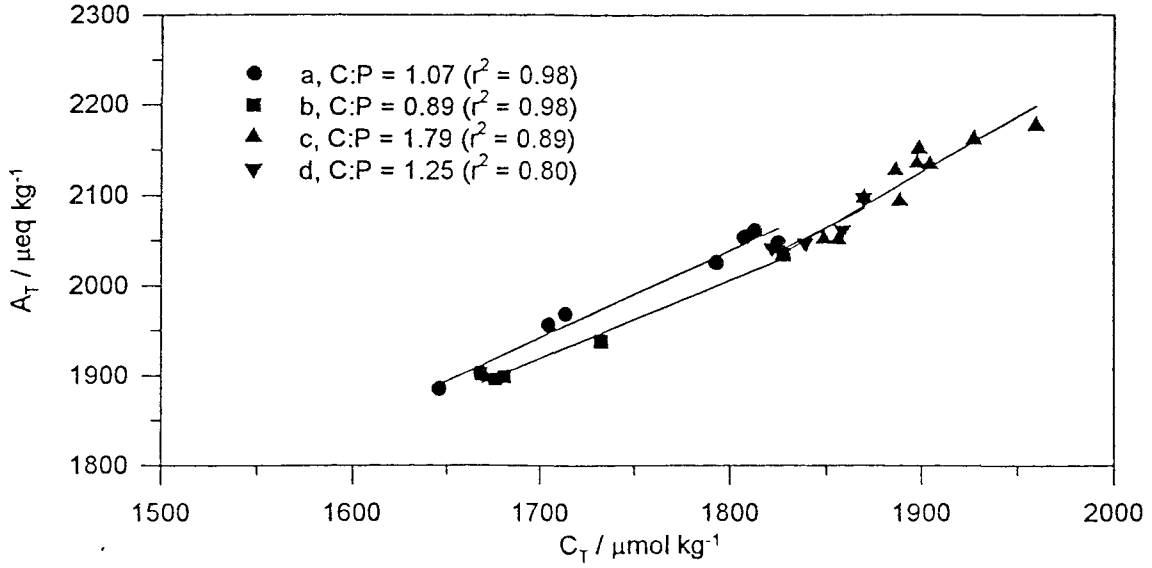

Figure 4.1.25 Plot of C_T against A_T for bag 5 (C:P derived from slope of regression)

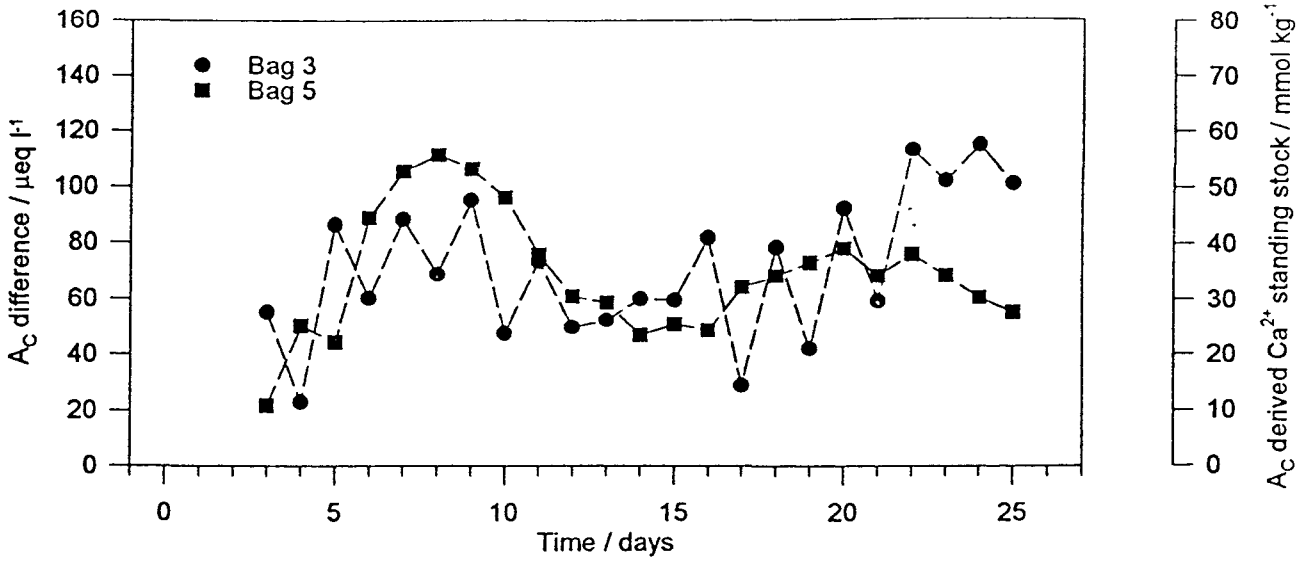

Figure 4.1.26 Carbonate alkalinity derived calcite standing stock

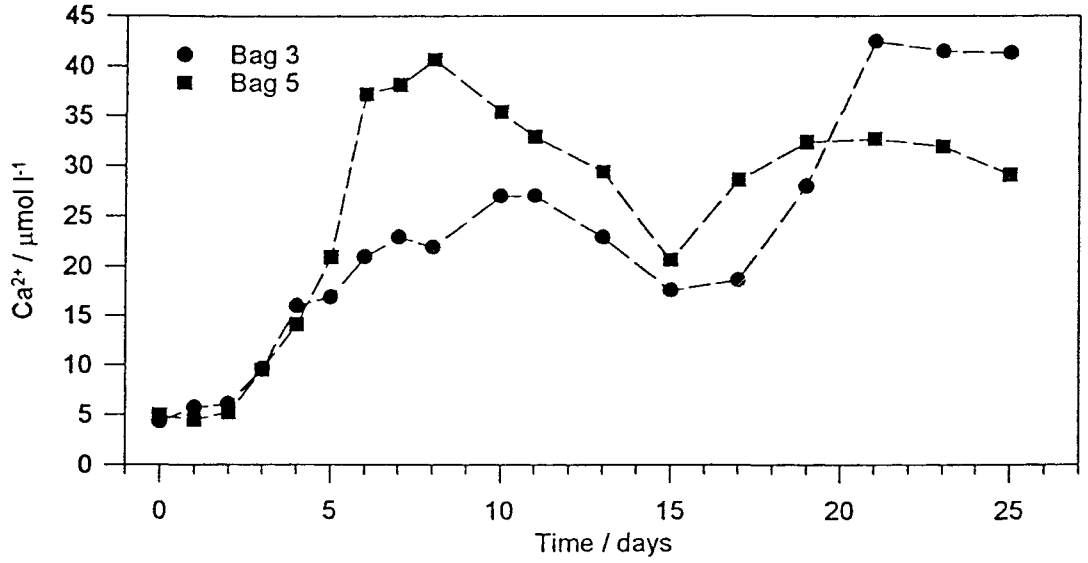

Figure 4.1.27 Flame photometry derived calcite standing stock

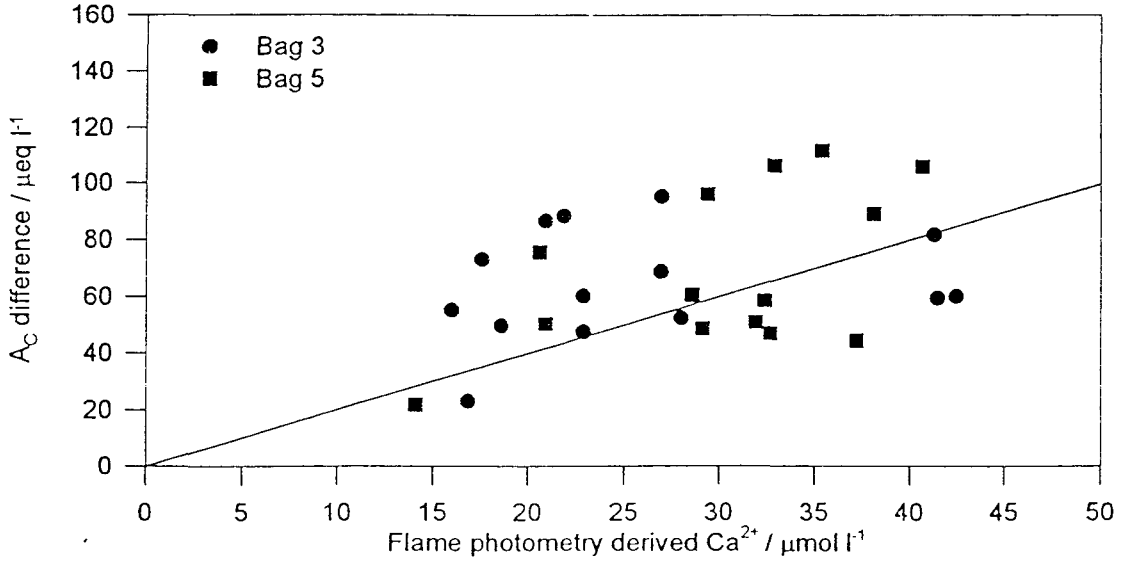

Figure 4.1.28 Plot of flame photometry determined Ca^{2+} against carbonate alkalinity difference (Line shows 1:2 ratio)

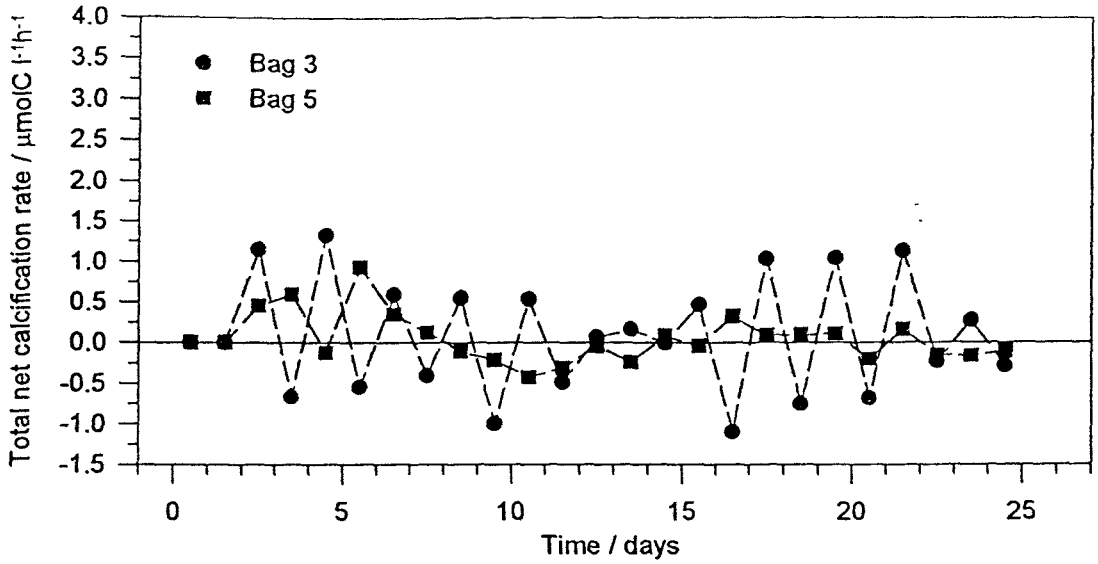

Figure 4.1.29 Carbonate alkalinity derived total net calcification rate

Bag no	Time period / d	Max *E. huxleyi* cell count / ml	Max diatom cell count / ml	Max P_{max} / $\mu molCl^{-1}h^{-1}$	Max C_{max} / $\mu molCl^{-1}h^{-1}$	Max P_{max}^{B} / $\mu molC\ \mu gChl^{-1}h^{-1}$	Max C_{max}^{B} / $\mu molC\ \mu gChl^{-1}h^{-1}$	Max α / $\mu molCl^{-1}h^{-1}\ (\mu E\ m^{-2}s^{-1})^{-1}$	Max α^{B} / $\mu molC\ \mu gChl^{-1}h^{-1}\ (\mu E\ m^{-2}s^{-1})^{-1}$
3	0-12	15470 (6)	15870 (6)	3.71 (3)	0.38 (5)	0.36 (0)	0.013 (13)	0.053 (3)	$2.91x10^{-3}$ (0)
3	12-25	29710 (22)	3790 (14)	2.47 (21)	0.84 (25)	0.33 (21)	0.075 (21)	0.019 (21)	$2.58x10^{-3}$ (21)
5	0-12	36500 (8)	4260 (2)	3.34 (5)	1.16 (5)	0.31 (0)	0.069 (5)	0.036 (5)	$2.89x10^{-3}$ (5)
5	12-25	30630 (18)	5340 (20)	1.71 (19)	0.40 (19)	0.22 (19)	0.051 (19)	0.014 (25)	$1.91x10^{-3}$ (25)

Bag no	Time period / d	Max ^{14}C C:P	Max C_T vs A_T derived C:P	Av ^{14}C C:P	Av C_T vs A_T derived C:P	A_C derived max calc rate / $\mu molC\ l^{-1}h^{-1}$	Max O_2 consumption / $\mu mol\ l^{-1}d^{-1}$	Min O_2 consumption / $\mu mol\ l^{-1}d^{-1}$	$\Delta\ O_2$ consumption / $\mu mol\ l^{-1}d^{-1}$
3	0-12	0.24 (7)	0.30	0.13	0.26	1.33 (4)	23.22 (4)	6.61 (0)	16.61
3	12-25	1.20 (25)	2.89	1.50	1.78	1.13 (21)	21.34 (24)	11.68 (16)	9.66
5	0-12	0.35 (5)	1.07	0.23	0.98	0.93 (5)	17.90 (8)	6.94 (0)	10.96
5	12-25	0.24 (13)	1.79	0.38	1.52	0.32 (16)	15.25 (16)	7.53 (14)	7.72

Bag no	Time period / d	Max A_T / $\mu eq\ kg^{-1}$	Min A_T / $\mu eq\ kg^{-1}$	$\Delta\ A_T$ / $\mu eq\ kg^{-1}$	Max C_T / $\mu mol\ kg^{-1}$	Min C_T / $\mu mol\ kg^{-1}$	$\Delta\ C_T$ / $\mu mol\ kg^{-1}$	Max PCO_2 / μatm	Min PCO_2 / μatm	$\Delta\ PCO_2$ / μatm
3	0-12	2145 (0)	1981 (9)	164	1910 (0)	1597 (7)	313	295 (2)	91 (6)	204
3	12-25	2034 (17)	1902 (24)	132	1797 (17)	1703 (23)	94	242 (21)	175 (12)	67
5	0-12	2088 (1)	1914 (8)	174	1856 (2)	1686 (8)	170	277 (2)	210 (6)	67
5	12-25	2012 (16)	1915 (24)	97	1814 (16)	1720 (23)	94	302 (14)	251 (18)	51

Table 4.1.1 Summary of results for mesocosm experiments (Bracketed number corresponds to day number of experiment)

CHAPTER FIVE : DISCUSSION

5.1 Growth of *Emiliania huxleyi* in batch culture

5.1.1 Effect of culturing conditions on *Emiliania huxleyi*

The results of growth rates found for both strains of *E. huxleyi* and *I. galbana* were in agreement with the range of values in the literature for batch cultures, (see table 5.1.1) and also below the suggested absolute μ_{max} for *E. huxleyi* of 1.27 (Paasche, 1967).

The ratio of nitrate to phosphate (N:P) was altered in the first two batch cultures in order to see the effect of phosphate limitation on a strain of high-calcifying *E. huxleyi.* For all cultures there was depletion of nitrate and phosphate to undetectable levels in the media and it can therefore be assumed that these nutrients were limiting during the stationary phase. Final cell numbers of *E. huxleyi* in both batch culture #1 and #2 reflected the initial phosphate concentration supplied but had little effect on μ_{max}. Maximum cell density between the first two batch cultures, grown under the same conditions, was however approximately halved in the second experiment, although nutrient uptake was apparently similar. This may to be due ageing of the culture which also manifested itself with significant cell motility detected in batch culture #2, and has been documented in other studies, *e.g.* Paasche (1964) and Nielsen (1995). In addition a decrease in the net total organic and inorganic production occurred due to the decrease in maximum cell numbers attained, although the rates of photosynthesis and calcification per cell did not significantly differ between cultures.

Nutrient limitation and its effect on the rate of calcification has been studied by other workers who have found an increased level of calcification relative to photosynthesis under reduced levels of nitrate and,or phosphate. Paasche (1994) showed that cells grown in P-limited chemostats at half μ_{max} produced 60% more calcite relative to organic carbon in comparison with exponentially growing cells in a nutrient replete medium. An increase in the level of nitrate to 1000μM in an *E. huxleyi* culture showed 20% of the calcification rate of a culture grown at 20μM nitrate (Nimer and Merrett, 1993), and van Bleijswijk *et al.* (1994) showed that depriving two clones of *E. huxleyi* in batch culture of phosphate increased the C:P from 0.52 to 2.22 and from 0.77 to 1.39 respectively. Linschooten *et al.* (1991) also showed coccolith production was increased five-fold in cultures which were phosphate and nitrate limited. Maximum ^{14}C derived C:P ratios (see table 5.1.1) in this study have been found to be similar those in the literature for the lag and exponential phases in high-calcifying *E. huxleyi* cultures. Calcification rates then declined rapidly during the mid-exponential phase and stationary phase as culture growth slowed. These lower C:P values are also in agreement with

those values seen in field studies (Fernandez *et al.*, 1993) where blooms are often suspected to have been encountered when in stationary phase or decline.

An explanation for the increase in calcification in nutrient deplete conditions may be to enable coccolithophores to sink to nutrient rich deeper water (Baumann, 1978). Nutrient depletion is often thought to initiate calcification in all cell types of *E. huxleyi*, however results from this study would seem to suggest that the rate of calcification in C-type cells only is enhanced, and not initiated in motile cells. In addition, very low calcification was measured in the low-calcifying strain of *E. huxleyi* grown in this study and its effect on the total alkalinity (A_T) was comparable to *I. galbana*. Paasche and Brubak (1994) however reported results on a non-calcifying strain of *E. huxleyi* in which calcification was induced in phosphate-limited cultures. The theory that low phosphate concentration will induce calcification in non-calcifying *E. huxleyi* cultures may therefore be strain specific.

This increase in calcification at low phosphate concentrations has prompted Paasche and Brubak (1994) to suggested that P-containing cell constituents are involved in the control or complete blocking of calcification, and that this control is released when the intracellular phosphate level drops in response to an inadequate external phosphate supply.

5.1.2 Effect of high-calcifying *E. huxleyi* on the dissolved inorganic carbonate system

It is well established that the effect of a non-calcifying phytoplankton compared to that of a high-calcifying phytoplankton species on the dissolved inorganic carbonate system is drastically different (Crawford and Purdie, 1997). Although growth of both of calcifying and non-calcifying phytoplankton results in a decrease in C_T, PCO_2 and free CO_2, only the high-calcifying *E. huxleyi* acts to reduce the alkalinity due to calcification which removes HCO_3^- from solution. The removal of CO_2 alone will have no effect upon the total alkalinity of the medium. In both the low-calcifying strain of *E. huxleyi* and in *I. galbana* no decrease in total alkalinity is measured and therefore both can be assumed to utilise solely free CO_2. If phytoplankton are only able to utilise free CO_2 for photosynthesis the maximum amount of the total dissolved inorganic carbon (C_T) which they can use is approximately half that of the original level, ignoring the action of minor bases (see figure 3.3.8), since the uptake of free CO_2 will act to drive the carbonate equilibrium towards the carbonate ion and increase the pH, as seen by the higher pH reached in the low-calcifying *E. huxleyi* and *I. galbana* cultures (Nimer, Dixon, and Merrett, 1992; Nimer and Merrett, 1992).

^{14}C C:P	^{14}C POC / ^{45}Ca PIC	^{14}C Ps /pgC/cell/ h	^{14}C Calc /pgC/cell/ h	µmax / d	β	A_T vs C_T C:P	Notes[(a)]	Growth phase of culture	Light:Dark period / h	Batch / continuous culture	I / $\mu Em^{-2} s^{-1}$	Ref
1.04-1.62	-	*ca.* 0.30	*ca.* 0.30	-	-	-	-	Exponential	Constant light	Batch	180	Paasche (1964)
-	-	-	-	1.27	-	-	Absolute growth rate	-	Constant light	Semi-continuous	100	Paasche (1967)
-	-	-	-	1.73	-	-	-	-	14:10	Batch	60	Brand and Guillard (1981)
-	-	-	-	1.04	-	-	-	-	14:10	Batch	60	Brand (1982)
-	-	-	-	1.09	-	-	-	-	14:10	Batch	60	Brand (1982)
-	-	-	-	1.19	-	-	-	-	14:10	Batch	60	Brand (1982)
--	-	-	-	1.07	-	-	-	-	14:10	Batch	60	Brand (1982)
-	-	-	-	1.1	-	-	-	-	Constant light	Batch	150	Falkowski *et al.* (1985)

Table 5.1.1 Radiotracing ^{14}C derived parameters and dissolved carbonate system parameters in culture from the literature
[(a)] All strains are high-calcifying unless noted; where different nutrient concentrations have been used nutrient concentration of the culture is noted in table.

^{14}C C:P	^{14}C POC / ^{45}Ca PIC	^{14}C Ps /pgC/cell/ h	^{14}C Calc /pgC/cell/ h	μmax / d	β	A_T vs C_T C:P	Notes [(a)]	Growth phase of culture	Light:Dark period / h	Batch / continuous culture	I / $\mu Em^{-2} s^{-1}$	Reference
ca. 2	-	*ca.* 0.30	*ca.* 0.30	-	-	-	-	Early exponential	-	Batch	?	Balch *et al.* (1992)
ca. 1	-	*ca.* 0.25	*ca.* 0.25	-	-	-	-	Late exponential	-	Batch	?	Balch *et al.* (1992)
ca. 1	-	*ca.* 0.25	*ca.* 0.25	-	-	-	-	Exponential	-	Batch	50	Nimer and Merrett (1992)
-	-	-	*ca.* 0.02	-	-	-	Low-calcifying	Exponential	-	Batch	50	Nimer and Merrett (1992)
ca. 1	-	*ca.* 0.25	*ca.* 0.25	-	-	-	20μM N	Exponential	-	Batch	50	Nimer and Merrett (1993)
0.88	-	0.27	0.24	-	-	-	20μM N	Exponential	-	Batch	50	Nimer, Guan, and Merrett (1994)
0.82	-	*ca.* 0.30	*ca.* 0.25	1.26	-	-	-	Exponential	Constant light	Batch	220	Paasche and Brubak (1994)
0.88	-	*ca.* 0.20	*ca.* 0.20	0.31	-	-	-	-	Constant light	Continuous	220	Paasche and Brubak (1994)
0.97	-	*ca.* 0.30	*ca.* 0.30	0.67	-	-	-	-	Constant light	Continuous	220	Paasche and Brubak (1994)

Table 5.1.1 (continued) Radiotracing ^{14}C derived parameters and dissolved carbonate system parameters in culture from the literature

[(a)] All strains are high-calcifying unless noted; where different nutrient concentrations have been used nutrient concentration of the culture is noted in table.

^{14}C C:P	^{14}C POC / ^{45}Ca PIC	^{14}C Ps /pgC/cell/ h	^{14}C Calc /pgC/cell/ h	µmax / d	β	A_T vs C_T C:P	Notes[(a)]	Growth phase of culture	Light:Dark period / h	Batch / continuous culture	I / $\mu Em^{-2} s^{-1}$	Reference
-	0.52	-	-	-	-	-	35µM N, 0.3µM P	-	16:8	Batch	70	van Bleijswijk *et al.* (1994)
-	2.22	-	-	-	-	-	10µM N, 0.1µM P	-	16:8	Batch	70	van Bleijswijk *et al.* (1994)
-	0.77	-	-	-	-	-	35µM N, 0.3µM P	-	16:8	Batch	70	van Bleijswijk *et al.* (1994)
-	1.39	-	-	-	-	-	10µM N, 0.1µM P	-	16:8	Batch	70	van Bleijswijk *et al.* (1994)
0.2-0.7	-	0.16-0.54	0.6-0.36	0.24-0.75	-	-	-	-	-	Continuous	75	Balch *et al.* (1996)
ca. 1	-	*ca* 0.2	*ca* 0.2	0.28	-	-	-	Exponential	-	-	?	Nimer *et al.* (1996)

Table 5.1.1 (continued) Radiotracing ^{14}C derived parameters and dissolved carbonate system parameters in culture from the literature

[(a)] All strains are high-calcifying unless noted; where different nutrient concentrations have been used nutrient concentration of the culture is noted in table.

Max 1.44	-	Max 3.39	Max 3.27	1.06	0.17-7.2	0.33-1.5	16µM N, 0.5µM P	All	16:8	Batch	100	This study *E. huxleyi* 92E
Max 1.33	-	Max 3.85	Max 2.33	1.03	0.43-4.44	0.31-1.57	16µM N, 1.0µM P	All	16:8	Batch	100	This study *E. huxleyi* 92E
Max 1.29	-	Max 3.2	Max 2.58	1.17	0.76-4.28	0.66-1.49	16µM N, 2.0µM P	All	16:8	Batch	100	This study *E. huxleyi* 92E
Max 0.69	-	Max 0.56	Max 0.2	1.03	7.14-9.46	0.10-0.11	16µM N, 1.0µM P	All	16:8	Batch	100	This study *E. huxleyi* CCAP 920/2
-	-	Max 1.80	-	0.88	6.92-13.50	-0.77-0.06	16µM N, 1.0µM P	All	16:8	Batch	100	This study *I. galbana* CCAP 927/1

Table 5.1.1 (continued) Radiotracing ^{14}C derived parameters and dissolved carbonate system parameters in culture from the literature

If therefore artificial buffers are added to the culture media, as is often standard practice, this "50%" C_T limitation will not be noted since buffers will maintain the pH of the medium and therefore the availability of free CO_2, resulting in much higher cell numbers (D.W. Crawford, pers. comm.). From the change in the level of C_T in the low-calcifying *E. huxleyi* and *I. galbana* cultures, which show a reduction of approximately 25%, growth was not limited by the availability of free CO_2 (see fig. 3.3.8).

The C_T level in the high-calcifying *E. huxleyi* cultures is reduced by greater than 50% in almost all of the cultures studied due to the utilisation of HCO_3^- in calcification, which will have a lesser effect on the pH of the media and hence the availability of free CO_2 (see figs. 3.1.8-3.1.10). A culture of high-calcifying *E. huxleyi* is able to reduce C_T to close to zero, since it is able to utilise both free CO_2 and HCO_3^-, with the latter being the major carbon species in the marine environment, if not limited by another factor *e.g.* inorganic nutrients (Merrett, Dong, and Nimer, 1993). This supports the suggestion that inorganic nutrients were limiting in all high-calcifying *E. huxleyi* cultures since C_T was never depleted below a value of 400μmol kg^{-1}. At high pH and there will be almost no free CO_2 available and *E. huxleyi* will be able to out compete those non-calcifying phytoplankton which do not posses carbonic anhydrase in this situation.

For *I.galbana* and low-calcifying *E. huxleyi* there is little detectable change in the A_T which would be expected to increase by 16μeq due to the uptake of nitrate during growth (see fig. 3.3.5) (Goldman and Brewer, 1980). The A_C declines during the removal of CO_2 due the presence of boric acid and other minor bases which can provide protons, although to a lesser degree than bicarbonate, for the dehydration of HCO_3^- (see fig. 3.3.6). A_T is therefore conserved as A_C declines (Smith and Key, 1975). Since alkalinity remained constant and there is reduction in C_T this decrease must be due to the removal of free CO_2, as has also been shown by Nimer, Dixon and Merrett, (1992)and Dong *et al.* (1993) for a different low-calcifying *E. huxleyi* strain

For all high-calcifying cultures of *E. huxleyi* expected changes occurred to the carbonate system, *i.e.* reduction in the A_T by uptake of HCO_3^- due to calcification and a decrease in the C_T below the level which can be achieved by non-calcifying phytoplankton (see figs. 3.1.5-3.1.6 and 3.2.7-3.2.8)(Crawford and Purdie,1997). PCO_2 was also reduced indicating that the CO_2 being produced by calcification was not the only source for photosynthesis.

There were similar net changes in the levels of PCO_2 in all cultures, with the initial increase in PCO_2 thought to be due to bacterial respiration, as had been noted in previuos experiments (pers. observation). It is, however, the change of PCO_2 relative to C_T which is significant in air-sea exchange as this drives the uptake of CO_2 from the atmosphere into the culture or vice versa. This can demonstrated using the homogenous buffer factors, the value of which reflects the ability of seawater to equilibrate with atmospheric CO_2, due to the effect of changes in C_T on the buffering ability of seawater (Stumm and Morgan, 1985). The use of buffer factors in relation to the effect of phytoplankton in the natural environment on the

dissolved carbonate system has only recently been applied by marine biologists, *e.g.* Robertson *et al.* (1994) and Purdie and Finch (1994). This is the first study to apply the use of derived buffer factors from changes in the dissolved carbonate system to phytoplankton cultures.

The limited use of this approach in estimating the effect of phytoplankton on the marine carbonate system is in part due to the fall from favour of pH based measurements. Hansson stated that "The pH value of the seawater sample obtained by this procedure is not a measurement of the concentration of H^+ or the activity of H^+ ..... it is just a value read on the pH meter." (Hansson, 1973).The complexity of the marine carbonate system and the nature of the marine chemistry literature also do not aid its understanding and application by marine biologists (Crawford and Harrison, 1997). Advances since Hansson's statement in both analytical and theoretical aspects of CO_2 chemistry have considerably improved the precision and accuracy of measured and calculated carbonate parameters, *i.e.* use of potentiometric and spectrophotometric methods standardised with seawater buffers. These techniques are however expensive, require technical expertise and use large volumes of culture. Due to the latter two reasons, and possibly the former, marine biologists conducting small scale culture experiments generally adopt the one point alkalinity titration method, which would probably be deemed inadequate by marine chemists. However, improvements of the methodology as used in this study and adapted from Anderson and Robinson (1946) and calculations to derive the C_T when using non-seawater scale buffers (Crawford and Harrison, 1997), *i.e.* NBS scale buffers, justify its use especially in culture based studies.

The understanding of the relevance of buffer factors in calcifying and non-calcifying phytoplanktonic communities has been improved due to the model reported by Crawford and Purdie (1997). Previous development of the use of buffer factors has mainly been advanced in coral reef communities by Frankignoulle (1994) and resulting in a proposed relationship of simultaneous organic and inorganic carbon metabolism based on the estimate of β. This relationship is relevant only for standard conditions of PCO_2, A_T, temperature and salinity and cannot be applied to the varying conditions during blooms in the open ocean, or to batch cultures where large changes of the carbonate system parameters occur. Robertson *et al.* (1994) however achieved an estimate of C:P by comparing changes in A_T relative to C_T, and since the buffer factor was derived from the same pH and alkalinity titration results as the slope of the C_T vs A_T plots, they allow different interpretations of the same data.

Buffer factors were lower in batch culture #1 relative to batch culture #2 for the same initial nutrient concentrations in comparable growth phases, due to the higher rate of calcification relative to photosynthesis, *i.e.* a lower net change in PCO_2 for the same decline in C_T (see figs. 3.1.20-3.1.22 and 3.2.22-3.2.24). In batch culture #1 the range of β was 3.18-3.97 and 0.17-0.76 in lag and exponential growth phases and stationary phase respectively. The lower the value of β the higher the A_T vs C_T derived C:P value. The C:P is therefore higher in the stationary phase than in the lag and exponential phases ranging from 1.19-1.57 and 0.76-1.16 respectively (see figs. 3.1.23-3.1.25). In batch culture #2 β ranged from 4.28-

7.12 and 1.56-2.14 in the lag and exponential phases and stationary phase respectively. These higher values of β corresponded to lower C:P values than seen in batch culture #1 ranging from 0.31-0.66 and 0.99-1.24 in the lag and exponential phases and stationary phase respectively (see figs. 3.2.25-3.2.27). These C_T vs A_T derived C:P ratios are however slightly overestimating the C:P because the C_T change is underestimated by uptake of free CO_2 from the atmosphere. This uptake cannot be calculated in these experiments.

Comparison of β and C_T vs A_T plots from high-calcifying cultures with those of the low-calcifying cultures shows that for similar growth phases the value of β is greater in low-calcifying *E. huxleyi* and *I. galbana* as would be expected (Crawford and Purdie, 1997). This is also shown by the very low or negative A_T vs C_T derived C:P, although for these calculations the alkalinity titration technique is at the limit of its resolution. There is evidence of some calcification for the low-calcifying *E. huxleyi* although again this may not be real since these measurements were made at the limit of detection for the technique used. The higher calcifying cultures therefore act to decrease the PCO_2 atmosphere-culture gradient, due to CO_2 production by calcification, relative to non-calcifying phytoplankton, as is shown by changes in β.

Measurements of β have been made in field and mesocosm studies (Robertson *et al.* (1994) and Purdie and Finch (1994) respectively) and culture derived values are in agreement with the range found for *E. huxleyi* and diatom dominated natural blooms, although a negative value of β, in an *E. huxleyi* dominated bloom, was seen in mesocosm experiments from this study. β is negative due to a net increase in PCO_2 at the same time as a corresponding net decrease in C_T. This situation was also observed in the culture studies but a negative β was not derived due to the net decrease in both PCO_2 and C_T over the period for which β was derived.

As previously mentioned, in the 0.5P culture for both high-calcifying *E. huxleyi* batch culture experiments, an increase in PCO_2 was measured, while both A_T and C_T were decreasing. This increase in PCO_2 is generally thought to occur due to the C:P ratio being greater than 1, since the CO_2 produced during calcification would be in excess of that utilised by photosynthetic inorganic carbon fixation. Due to the effects of organic and inorganic carbon production on the marine carbonate system, Crawford and Purdie (1997) calculated that if diurnal $C_{net}:P_{net}$ is greater than 1.5 PCO_2 will increase during the growth of a culture. However the C:P is 1.5 and 1.24 for 0.5P cultures #1 and #2 respectively, so PCO_2 would not be expected to increase as was noted. However, the model developed by Crawford and Purdie (1997) showed that nocturnal respiration (R) may be a key factor in understanding PCO_2 changes. Assuming a $C_{net}:P_{net}$ of 1 over a diel period when $R:(P+C)_{net} > 0.15$ *E. huxleyi* could achieve a net increase in PCO_2 at the same time as net decreases in C_T and A_T. It is therefore suspected that this nocturnal respiration is the cause of the increase in PCO_2 which may be higher in the 0.5P culture and may explain this phenomenon although it was not directly

measured in these batch culture experiments. Dark calcification may also be important with respect to the PCO_2 increase since it will increase the C:P over the diel period.

Calcite standing stocks for the high calcifying *E. huxleyi* cultures were also calculated from the A_C difference between filtered and unfiltered samples, and this agreed with the range of rates measured in ^{14}C derived total calcification.

5.1.3 ^{14}C derived production rates

^{14}C radiotracing and oxygen measurements are the standard methods in physiological studies both *in situ* and *in vitro* for calculating rates of productivity and a review of rates from the literature is shown in table 5.1.1. The rates of calcification and photosynthetic inorganic ^{14}C uptake shown in this study are generally higher, but are of the same order of magnitude, as that noted by other workers, especially during the early exponential growth phase. This may be due to the low levels of nutrients used in these experiments or may be strain specific. The significance of these uptake rates is shown when the C:P ratio is calculated since as discussed previously this may aid the understanding of the impact of the phytoplankton on the air-sea gradient of PCO_2.

The rates of photosynthesis and calcification were seen to show a periodicity in batch culture #2 (Only one measurement per light period was made in batch culture #1), as has been previously demonstrated (Eppley *et al.*, 1971) with a general pattern of higher rates of ^{14}C uptake during the start of the diurnal period, emphasising the assertion that short term incubations show only what happens during the period of incubation (see figs. 3.2.14-3.2.16). Comparison of rates per cell between experiments is therefore slightly compromised since the incubations were carried over different periods of the light cycle. This is not true for the C_T vs A_T plot derived of C:P rates since these reflect longer term changes. There was also a change in the methodology for which direct comparisons have not been made (see table 2.1.2).

Average C:P ratios were similar between experiment #1 and #2 with no overall discernible trends in their differences with different treatments. In batch culture #1 in the 1.0P and 2.0P cultures the C:P was *ca.* 1 in the stationary phase and the mid-exponential phase, but in the second batch culture experiment the C:P was greater than 1 in the lag phase for all cultures and also in the stationary phase for 1.0P (see figs. 3.1.15-3.1.17 and 3.2.17-3.2.19). At these times the rate of release of CO_2 during calcification was greater than that utilised in photosynthetic carbon fixation. This should therefore result in a reduced uptake of PCO_2 relative to C_T, as was seen in the carbonate system, thus reducing the culture-atmosphere gradient of PCO_2 relative to a similar biomass of non-calcifying phytoplankton photosynthesising at the same rate.

When the rates of calcification and photosynthesis are contrasted with those determined for the low-calcifying strain of *E. huxleyi* and the rate of photosynthesis of *I. galbana* the rates of photosynthesis were similar for both cultures, but significantly lower than those seen for high-calcifying *E. huxleyi* (see table 5.1.1). The calcification rate for low-

calcifying *E. huxleyi* was minimal throughout the experiment, although again at low cell numbers a high rate of C:P was seen, but the total amount of calcification was too low to significantly affect the carbonate system and therefore had no impact on the levels of PCO_2.

5.1.4 Comparison of carbonate system changes with ^{14}C derived production rates

Robertson *et al.* (1994) stated that "^{14}C uptake measurements are limited due to the conflicting time scales over which biological events affecting the carbonate system occur, *i.e.* radiotracer measurements are a precise estimate of the rate of carbon fixation in a particular sample over a specific incubation period, whereas ambient chemical measurements reflect past biological activity over certain time and space scales." In order to compare these two approaches batch cultures of calcifying and non-calcifying algae were grown enabling short term changes in productivity to be related to longer term changes in the marine carbonate system. Prior to this study comparisons had only be made in field investigations where a limited number of ^{14}C incubations, often as the bloom was in decline, were measured in conjunction with the long term changes in the dissolved carbonate system (see table 5.1.1). Mesocosms have provided more useful comparisons of the relation between the short term radiotracer incubations with longer term derived buffer factors, although no comparisons between radiotracing derived C:P values and A_T vs C_T derived C:P have previously been made. The varied species composition of the blooms makes it impossible to separate the effects of the different species.

The results seen for the low-calcifying *E. huxleyi* and *I. galbana* were as expected, with the high buffer factors indicating minimal or no calcification in either cultures. This was also shown by the ^{14}C uptake incubations, and would result in a flux of CO_2 into the culture from the atmosphere. In the high-calcifying *E. huxleyi* cultures there were highly significant differences between the ^{14}C derived C:P and the A_T vs C_T derived C:P, which reflect changes in the dissolved carbonate system. For the ^{14}C derived C:P ratios the C:P for all cultures was seen to be highest during the lag and exponential growth phase whereas the opposite was seen for the C_T vs A_T derived C:P. The average C:P ratio for experiment #2 in the lag and stationary phases showed good agreement with the average seen in the A_T vs C_T derived C:P ratios. This was however not seen in the first batch culture experiment. It is therefore expected that the ^{14}C derived calcification rate in the first experiment an underestimate. This should be expected since the number of ^{14}C uptake incubations in the second was greatly increased, and an improved ^{14}C technique was also used.

5.2 Studies of *Emiliania huxleyi* growth in mesocosms

5.2.1 Effect of nutrient enrichment on bloom composition

The experimental enclosures (mesocosms) sampled for this study were; a mesocosm to which additions of 15μM nitrate, 1μM phosphate and 10μM silicate; and a mesocosm to which additions of 15μM nitrate and 1μM phosphate were initially added. These were denoted as bag 3 and bag 5 respectively. This was the numbering scheme used to differentiate between the total of 8 bags which were available for study and has therefore been retained for this discussion.

The differences in the initial blooms were as anticipated, with bag 3, which received silicate enrichment, initially promoting a diatom bloom, although unexpectedly a concurrent bloom of *E. huxleyi* also developed. In bag 5, where there was no additional silicate added, the first bloom was almost entirely composed of *E. huxleyi*, as expected since *E. huxleyi* is known to be a good competitor at low phosphate levels (Riegman, Noordeloos and Cadee, 1992). After the decline of these initial blooms essentially monospecific blooms of *E. huxleyi* developed in both mesocosms. This pattern of blooms followed the pattern shown by the total irradiance; after the initial good weather during the first week of the experiment conditions did not generally improve until day 14 coinciding with the initiation of both second blooms. These secondary blooms will not have been nutrient limited due to the daily addition to the mesocosms of 10% of the initial nutrient supplement concentration, to allow for the 10% dilution by external fjord water each day. The changes in chlorophyll during both secondary blooms did not seem to increase with cell numbers as occurred in the first blooms in both bags, possibly due to lower chlorophyll content per cell and also the relatively lower chlorophyll content of *E. huxleyi* cells relative to diatoms.

The bloom composition in these mesocosms has been altered due to the addition of nutrient supplements in similar experiments at the University of Bergen field station in previous years *e.g.* Egge and Heimdal (1994) and Egge and Jacobsen (1997)

5.2.2 Effect of bloom composition on Pvl and Cvl derived parameters

The values of P_{max}^{B} and α^{B}, during the first blooms, were highest at the initiation of growth on day 0, showing the maximal rates of photosynthesis and assimilation respectively were highest at this point, declining as the blooms reached maximum cell density and then were seen to increase to a secondary maximum as the secondary *E. huxleyi* blooms reached maximum cell numbers, even though the production of chlorophyll was low (see figs. 4.1.3 and 4.1.15). These values were consistent with values for *E. huxleyi* measured both in field

and laboratory based studies (see table 5.2.1). For α^B and $P_{max}{}^B$ in both mesocosms, particularly in bag 3, there was close temporal covariation in both photosynthetic parameters. Although changes in the light-limited slope (α) and maximum photosynthetic capacity (P_{max}) are thought to represent distinct photoadaptive processes, similar co-variation in α and P_{max} has been noted previously in both short term (Prezelin, Putt and Glover, 1986) and long term observations of natural phytoplankton populations (Cote and Platt, 1983). Under certain circumstances there appears to be a degree of co-ordination in the adaptation of marine phytoplankton to temporal changes in environmental conditions.

The values of $C_{max}{}^B$ were lower than $P_{max}{}^B$ in both mesocosms, with the exception of the last sampling day in bag 3, therefore the rate of calcification was generally lower than photosynthesis (see figs. 4.1.3 and 4.1.15). In bag 5 initial $C_{max}{}^B$ was not measured so no comparisons can be made at the start of the experiment but for the remainder both were measured and $C_{max}{}^B$ followed the same trends as seen in $P_{max}{}^B$. In both bags the maximum in $C_{max}{}^B$ was concurrent with $P_{max}{}^B$ during the second *E. huxleyi* dominated bloom and this may imply that the cellular regulation of calcification acts to synchronise with maximal rates of photosynthesis. This would have the consequence of calcification producing the highest level of free CO_2 for intracellular recycling when photosynthetic rate is also rate at its maximum. The $C_{max}{}^B$ in bag 3 during the initial bloom was far lower than $P_{max}{}^B$ as expected in a mixed bloom of diatoms and *E. huxleyi*.

Direct comparisons of the ratio of $C_{max}{}^B$ to $P_{max}{}^B$ will give the ratio of C:P. This ratio is important in relation to air-sea exchange of CO_2, since the lower the C:P the greater the PCO_2 gradient between the bloom and the atmosphere. Theoretically if the diurnal C:P is 1.5 the calcifying phytoplankton will act as a source of CO_2 to the atmosphere during this period (Crawford and Purdie, 1997). This ratio reached a maximum of *ca.* 0.3 for both initial blooms, despite their compositional differences, because $P_{max}{}^B$ declined to a lower level in bag 3 than in the *E. huxleyi* dominated bloom in bag 5 (see figs. 4.1.5 and 4.1.17).

The trends in C:P were different in the second blooms in both mesocosms despite similar phytoplankton composition. Bag 5 maintained a steady low plateau but after a maximum of 0.5 the calcification rate exceeded that of photosynthesis with a C:P of 1.20 which would therefore make this bloom a potential source of CO_2, and consequently the gradient of PCO_2 between the mesocosm and the atmosphere would be reduced with respect to all other sampling days. The previous maximum ^{14}C derived C:P recorded in mesocosm blooms of 0.45 by Egge and Jacobsen (1997) was similar to the average value found at the peak of cell numbers in this study. C:P derived from ^{14}C POC:^{45}Ca PIC showed a maximum C:P of 0.67 but this is still lower than the maximum C:P noted in this study (see table 5.2.2). The maximum measured C:P of 1.20 and its feasibility is discussed in section 5.2.4.

E. huxleyi clone in culture / Bloom composition in field	P_{max}^{B} / µmolC µg Chl^{-1} h^{-1}	C_{max}^{B} / µmolC µg Chl^{-1} h^{-1}	α^{B} / µmolC µmol Chl^{-1} h^{-1} (µE m^{-2} s^{-1})$^{-1}$	Reference
BT6	0.17	-	0.0031	Schofield, Bidigare, and Prezelin (1990)
88E +2µM N	*ca.* 0.03	*ca.* 0.06	-	Balch, Holligan, and Kilpatrick (1992)[a]
5/90/25j High-calcifying	*ca.* 1.2[a]	-	-	Nanninga and Tyrrell (1995)[a]
B92/371 High-calcifying	0.12	-	0.0013	Nielsen (1995)[b]
B92/371 Low-calcifying	0.20	-	0.0018	Nielsen (1995)[b]
B92/317	0.39	-	0.0031	Nielsen (1997)[b]
E. huxleyi dominated bloom	0.43	-	0.0039	Fernandez *et al.* (1993)
Mixed diatom and *E. huxleyi* (#3)	Max 0.36	Max 0.013	Max 0.0029	This study
E. huxleyi dominated (#3)	Max 0.33	Max 0.075	Max 0.0026	This study
First *E. huxleyi* dominated (#5)	Max 0.31	Max 0.069	Max 0.0029	This study
Second *E. huxleyi* dominated (#5)	Max 0.22	Max 0.051	Max 0.0019	This study

Table 5.2.1 PvI and CvI derived parameters for *E. huxleyi* from the literature

[a] Assume 0.6pg chl $cell^{-1}$

[b] Assume PQ = 1.2

The rate of dark calcification was also measured, albeit on only one filter, which may have important effects on the long term C:P of *E. huxleyi*. If a cell is calcifying in the dark period the ratio of C:P during this period will be infinity, and therefore it is the rate of diel calcification to diurnal photosynthesis which could be measured to elucidate long term trends, in relation to the effect on PCO_2 air-sea gradient.

Dark calcification is undetectable for bag 5 and may be thought to have no influence on the C:P. In bag 3 in the second bloom the dark calcification reaches levels which were similar to the corresponding C_{max}, especially on the last sampling day (see figs. 4.1.6 and 4.1.18). It has also been argued by Linschooten *et al.* (1991) that the presence of dark calcification in these incubations may be spurious since the coccolith producing compartment is lost during mitosis which occurs during the dark period of cells acclimatised to this regime, and no dark calcification was recorded during these incubations. Other workers have however recorded low levels of dark calcification (Balch, Holligan and Kilpatrick, 1992; Fernandez *et al.*, 1993; Paasche and Brubak, 1994).

5.2.3 Effect of bloom composition on the dissolved carbonate system

The effect of the different bloom compositions has profound effects on the marine carbonate system, as would be expected when comparing the relative effects of calcifying with non-calcifying phytoplankton. In the initial mixed diatom and *E. huxleyi* bloom in bag 3 C_T reaches its lowest level and the relative level of drawdown of A_T is far lower resulting in the largest decrease in PCO_2, thus relative to the atmosphere this bloom will have caused an uptake of CO_2 from the atmosphere. As the bloom declined C_T increased due to the exchange of mesocosm water for external fjord water. This continued until day 14 when the second *E. huxleyi* dominated bloom occurred. In contrast to the first mixed bloom, during this second bloom C_T initially remained stable showing a slight decline at the end of the bloom, with A_T continuing to decrease, although curiously A_T showed no increase between blooms. The level of PCO_2 remained unaltered during this bloom and the bloom of *E. huxleyi* was therefore showing little net exchange of CO_2 with the atmosphere (see figs 4.1.8 and 4.1.9).

In bag 5 during the first *E. huxleyi* dominated bloom both C_T and A_T were again drawn down and the reduction of A_T was a similar amount to that of C_T . This was approximately half that for the mixed bloom in bag 3. The effect of this highly productive bloom on PCO_2 was significantly less than that of the mixed bloom, reducing the PCO_2 by approximately 50µatm making it a smaller sink with respect to the atmosphere. As seen in bag 3 as the bloom declined the levels of C_T and PCO_2 recovered, as well as A_T. During the second *E. huxleyi* dominated bloom PCO_2 declined until day 19 as the bloom reached maximum cell numbers and then during the latter stages a slight increase in PCO_2 was seen. The C_T and A_T again showed a similar decline to that which occurred during the first bloom. The *E. huxleyi* bloom may or may not have caused this increase in the PCO_2 since temperature and dilution effects

were not taken into account. The important point is that all *E. huxleyi* blooms had a lesser net impact on the PCO_2 gradient and hence the air-sea exchange of CO_2, in comparison to the effect of the mixed *E. huxleyi* and diatom bloom (see figs. 4.1.20 and 4.1.21).

In order to show long term changes in the marine carbonate system and its ability to buffer changes in PCO_2 in relation to the different bloom compositions the use of buffer factors (β) has recently been applied . The buffer factor is derived from relative changes in C_T and PCO_2. In addition to this C_T vs A_T plots were used to calculate the long term changes in the rate of calcification to photosynthesis, *i.e.* C:P. A fuller background to the use of buffer factors is given in the discussion of the batch culture results (see section 5.1.2). In essence the lower the buffer factor for a removal of a fixed removal of C_T the greater the PCO_2 air-sea gradient, and a negative β implies PCO_2 is increasing with decreasing C_T.

The highest value of β was noted in the mixed *E. huxleyi* and diatom bloom giving an average value of 7.2. This is in close agreement to that measured in an enclosure of a diatom dominated bloom where $\beta = 7.5$ (Purdie and Finch, 1994) and a diatom dominated bloom in the northeast Atlantic Ocean (Finch, 1994; Robertson *et al.,* 1994) which gave a value of β = 8.0-8.4 *in situ* and $\beta = 10.28$ for an incubated sample. The average β for all *E. huxleyi* dominated blooms was far lower with an average β of 2.46, which is also in agreement with β for an *E. huxleyi* dominated bloom in mesocosm (Purdie and Finch, 1994) which gave a value of 2.6 (see table 5.2.2).

For this study each bloom was divided into two periods (growth and decline phase) since different "growth" phases of the blooms had variable effects on the carbonate system. The changes in β in relation to growth phase was as expected. In the first blooms, β was higher for the mixed diatom bloom than the *E. huxleyi* dominated bloom but both showed an increase as the blooms declined. The air-sea gradient was therefore highest during the growth phases and was greater at all times in the diatom mixed bloom. In the second *E. huxleyi* blooms the converse is seen. The values of β for bag 5 remained similar to those in the first bloom implying the effect on air-sea PCO_2 gradient was similar. In the *E. huxleyi* dominated bloom decline in bag 3 the lowest and only negative value of β (-0.27) was recorded. This indicated that the bloom was a net source to the atmosphere of CO_2, while C_T decreased. An increase in directly measured PCO_2 has been noted by Purdie and Finch (1994) in a bloom of similar composition in these mesocosms (see figs. 4.1.12 and 4.1.24).

In order to calculate these buffer factors the C_T and PCO_2 were normalised to 13.0^0C in order to remove the effect of temperature, since increased temperature will act to increase PCO_2 due to the increased dissociation from HCO_3^- . Adjustments for the effect of dilution on C_T and PCO_2 were however not included.

It is also possible to calculate the C:P using the slope of a C_T vs A_T plot as has been discussed previously, and essentially a low β will give a high C:P since both are derived from the same pH and alkalinity data (see section 5.1.2). The A_T vs C_T plots have been corrected for dilution to show the true effect of inorganic and organic production on the carbonate

system. These C_T vs A_T derived C:P ratios are however slightly overestimating the C:P because the C_T change is underestimated by uptake of free CO_2 from the atmosphere.

In bag 3 the C:P ratio was higher during the growth phase than in the decline of the blooms, but the opposite was found for bag 5 where C:P was greater during the decline of the bloom, showing the expected trend in β. An A_T vs C_T derived C:P of 0.17 was found for a diatom dominated bloom in the northeast Atlantic Ocean (Robertson *et al.*, 1994) which is comparable to the higher value for the bag 3 mixed bloom. The *E. huxleyi* dominated blooms in bag 5 showed a C:P greater than 1 during the growth of the first bloom and for both periods of the second bloom. This reflects the very small changes in the PCO_2 levels seen in this mesocosm. During the decline of the second bloom in bag 3 the C:P was greater than 1 only during the decline of the second bloom giving a very high value of 2.89 and this would almost certainly imply that the algae were a net source of CO_2 to the atmosphere (see figs. 4.1.13 and 4.1.25). This is the highest C:P ever noted, although van Bleijswijk *et al.* (1994) recorded a C:P of 2.22 in phosphate limited batch cultures using ^{14}C POC:^{45}Ca PIC (see table 5.2.2).

The difference between the filtered and unfiltered A_C was measured to derive the calcite standing stock, which should theoretically account for this alkalinity difference. Although the data show similar trends to that independently derived from an atomic absorption flame photometer there was a large scatter when the data sets were directly compared (see figs. 4.1.26-4.1.28). The large fluctuations between A_C samples may be due to insufficient equilibration time of the pH probe for the samples in bag 3, and this problem has been highlighted by Crawford and Harrison (1997). This does not however account for the overall differences between the two techniques. These may be due to the chemical composition of the coccolith or the presence of the coccolith associated polysaccharide which covers the coccolith (Westbroek, Young, and Linschooten 1989).

The total rates of calcification calculated from alkalinity difference for bag 3 are too variable to show any practical trends, but the bag 5 data is in agreement with the rates measured using the ^{14}C derived calcification method but is less accurate than the ^{14}C uptake method (see fig. 4.1.29). The A_C difference may therefore be a useful diagnostic tool in the future, especially with respect to its simplicity and time taken for analysis, but the methodology needs further development before accurate results can be obtained.

5.2.4 Comparison of ^{14}C derived and A_T vs C_T derived C:P values

The general trends for the average of both derived values of C:P are the same when considered for each bloom, *i.e.* increasing with the decline of the bloom, but the values for the ^{14}C derived C:P are lower than A_T vs C_T derived C:P for all blooms. As has been previously mentioned it is accepted that the ^{14}C incubations measure the rate of inorganic carbon uptake

Bloom composition	^{14}C C:P	^{14}C POC / ^{45}Ca PIC	^{14}CPs/pg C/cell/h	^{14}CCalc pgC/cell/h	^{45}Ca Calc pgC/cell/h	β (*In situ*)	A_T vs C_T C:P	Reference
E. huxleyi dominated	-	0.05-0.67 Av 0.34	-	-	0.14-0.34 Av 0.29	2.6	-	Purdie and Finch (1994)
Mixed diatom and *E. huxleyi*	-	0.05-0.53 Av 0.22	-	-	0.06-0.32 Av 0.32	5.9	-	Purdie and Finch (1994)
Diatom dominated	-	0.05-0.20 Av 0.10	-	-	0.14-0.33 Av 0.27	7.5	-	Purdie and Finch (1994)
E. huxleyi dominated	Max 0.45	-	-	0.1-0.4	-	-	-	Egge and Heimdal (1994)
Mixed diatom and *E. huxleyi* (#3)	Max 0.24	-	-	-	-	6.80-7.59	0.21-0.30	This study
E. huxleyi dominated (#3)	Max 1.20	-	-	-	-	-0.27-3.59	0.66-2.89	This study
First *E. huxleyi* dominated (#5)	Max 0.35	-	-	-	-	2.19-3.63	0.89-1.07	This study
Second *E. huxleyi* dominated (#5)	Max 0.24	-	-	-	-	1.35-4.25	1.25-1.79	This study

Table 5.2.2 showing radiotracing derived C:P and dissolved carbonate system parameters in mesocosms from literature

Bloom composition	^{14}C C:P	^{14}C POC/ ^{45}Ca PIC	^{14}CPs/pg C/cell/h	^{14}CCalc pgC/cell/ h	β *(in situ)*	β (Incubated sample)	A_T vs C_T C:P	Notes	Reference
Not known - *E. huxleyi* present	-	-	*ca.* 0.90	*ca.* 0.30	-	-	-	-	Balch, Holligan, and Kilpatrick (1992)
Diatom dominated	-	-	-	-	8.0-8.4	10.28	0.17	Northeast Atlantic 1989+90	Robertson *et al.* (1994)
E. huxleyi dominated	Max 0.25	-	-	Max 0.13	1.92	1.65	*ca.* 1.0	Northeast Atlantic 1991	Fernandez *et al.* (1993)
E. huxleyi dominated	-	0.18	-	-	-	-	-	Stationary / decline phase	van der Wal *et al.* (1995)
E. huxleyi dominated	-	0.03	-	-	-	-	-	Stationary / decline phase	van der Wal (1995)
Coral reef	-	-	-	-	6.56	-	-	(C:P = 0.37)	Frankignoulle *et al.* (1996)
Coral reef	-	-	-	-	8.15	-	-	(C:P = 0.25)	Frankignoulle *et al.* (1996)

Table 5.2.3 showing radiotracing derived C:P and dissolved carbonate system parameters in field from literature

for the period of the incubation, and that the A_T vs C_T plots show the long term changes, but such a discrepancy is extremely important when considering the relevance of ^{14}C studies to changes in the air-sea exchange of PCO_2, which is, in this study at least, their raison d'être. These discrepancies are thought to be due to the fact that the diurnal C:P is not the only factor influencing the long-term diel C:P which is calculated by measuring changes in the carbonate system. The ^{14}C studies do not take into account dark calcification which was not measured in the nocturnal period or respiration whichhas shown to be potentially a great influence on air-sea PCO_2 gradient (see section 5.1.2) Crawford and Purdie (1997). The lower the rate of maximum respiration (indicated by dark oxygen consumption) the smaller the difference between ^{14}C derived C:P and C_T vs A_T derived C:P, further reinforcing Crawford's assertion on the impact of respiration on the buffer factor.

Finally to address the "reality" of C_T vs A_T derived C:P value of 2.89 on the last sampling day in bag 3. At the end of this bloom it is suspected that the C:P increased greatly, although r^2 for the regression on the C_T vs A_T is very low (due to changes in the C:P and a limited data set). The ^{14}C results support this finding since the highest value (C:P = 1.20) was also recorded at this time. There was also a very high rate of calcification in the dark which would increase the long term C:P but would not be taken into account if only the changes in the short term in the diurnal period were considered, *i.e.* ^{14}C derived C:P. A caveat is necessary in that this value was determined from only one filter. Although these results do not convincingly stand alone, when considered together seem to imply that a high diurnal C:P (*i.e.*^{14}C) with a high dark calcification and high dark respiration rate resulted in the increase in PCO_2 observed at the end of the second bloom in bag 3, and agrees with the theoretical model of Crawford and Purdie (1997). If these results are "real" , together they have very important implications on the predicted effect of *E. huxleyi* blooms on the air -sea exchange of CO_2 *i.e.* they may be a net source of CO_2 as seen by Purdie and Finch (1994).

5.3 Comparison of laboratory-based culture studies with mesocosm studies

The effect of non-calcifying phytoplankton in relation to calcifying phytoplankton on the carbonate system was similar in culture and mesocosm studies, with comparable buffer factors for *E. huxleyi* dominated blooms and high-calcifying *E. huxleyi* cultures, and also diatom dominated blooms and *I. galbana* and low-calcifying *E. huxleyi* cultures. In these situations *E. huxleyi* therefore will act to decrease the PCO_2 gradient relative to non-calcifying phytoplankton, and was seen to cause a net increase in PCO_2 in culture and possibly in the mesocosms. There was however a great discrepancy in both studies between the ^{14}C derived C:P values and those derived from changes in carbonate system parameters. It is expected to be due to ^{14}C derived C:P being only one of the factors influencing β. In order to fully understand the influence of *E. huxleyi* on β both dark calcification and diel respiration need to be quantified, in addition to photosynthesis and calcification rates.

5.4 Concluding remarks

In contrast to the experiments presented in this thesis, other recent laboratory studies on the effect of nutrients on *E. huxleyi* have reduced the concentration of either nitrate or phosphate. These previous studies have shown significant changes in the ratio of calcification to photosynthesis between treatments due to changes in nutrient concentrations of the media. These changes were caused by differences in nutrient concentration of orders of magnitude, *e.g.* Nimer and Merrett (1994) and van Bleijswijk *et al.* (1994). Results from this study have not shown similar significant variations in rates of calcification and photosynthesis per cell in high-calcifying *E. huxleyi* at limiting phosphate levels, with concurrently low nitrate concentrations. The different initial phosphate concentrations used in this study, and hence N:P ratios, were however shown to have profound effects on PCO_2 levels in cultures, with high-calcifying *E. huxleyi* cultures grown at the lowest initial phosphate concentration possibly acting as a net source of CO_2 to the atmosphere.

This ability of *E. huxleyi* to synthesise CO_2 internally due to calcification has lead to the hypothesis that coccolithophores may be able to outcompete other non-calcifying phytoplankton at limiting free CO_2 levels. However a coincident bloom of both *E. huxleyi* and diatoms, during the mesocosm study, showed that other hypotheses should be examined in conjunction with or instead of limiting free CO_2, as suggested by Tyrell and Taylor (1995), who also discounted this hypothesis as the sole factor in explaining the distribution of *E. huxleyi* in the NE Atlantic.

The application of buffer factors were used to study the effect of differing phytoplankton, *i.e.* calcifying and non-calcifying, on the carbonate system by relating their effect on the relationship of PCO_2 to C_T. The use of buffer factors as an indicator of calcification is a recent development for marine biologists and their application to culture studies has not previously been reported. It is proposed that estimating buffer factors for different bloom densities and compositions will aid the budgeting of the global carbon cycle. To this end Frankignolle (1994) has recently developed a complete set of buffer factors for the seawater acid-base CO_2 system allowing the calculation of changes in PCO_2 for any input-output of dissolved CO_2, carbonate or bicarbonate ions. Using the proposed equations of Frankignoulle (1994), calculated for coral reefs, it may be possible to relate the equilibrium dynamics that occur in open systems, demonstrated by buffer factors, to the released CO_2/precipitated carbonate ratio, also known as the rain ratio (Holligan and Robertson, 1996). The rain ratio describes the relative vertical flux of organic and inorganic carbon and their sedimentation, and is therefore of particular importance in determining the final CO_2 budget of ecosystems that are sites of calcification, *i.e.* coccolithophore blooms. As stated in the objectives, a significant difficulty in calculating the CO_2 budget properly is the unknown contribution of changes in the cycling of marine carbon as calcite (Sunquist, 1993). The development of the application of buffer factors will therefore not only have implications in estimating the changes in air-sea flux of CO_2 by calcifying and non-calcifying phytoplankton

blooms, but also in estimating the relative amounts of organic and inorganic carbon reaching the sedimentary archive.

Further work on the impact of respiration, calcification and photosynthesis on buffer factors, and hence the carbon cycle, are all needed to be studied over the whole of the diel cycle. Short term radiocarbon incubations in this study provided rates of calcification and photosynthesis for the diurnal period only. This limitation was emphasised by comparing ^{14}C derived C:P to A_T vs C_T derived C:P; the discrepancy between the studies of C:P for the two methods may in part be due to the unquantified effects of respiration and dark calcification on the dissolved inorganic carbonate system. Further investigation into the relative importance of these processes is necessary for a more accurate evaluation of the role of calcifying phytoplankton in the global carbon cycle.

APPENDIX

Solution I [(a)]	MW	g kg^{-1}
NaCl	58.44	20.758
Na_2SO_4	124.04	3.477
KCl	74.56	0.587
$NaHCO_3$	84.00	0.170
KBr	119.01	0.0845
H_3BO_3	61.83	0.0225
NaF	41.99	0.0027
Solution II [(a)]		
$MgCl_2.H_2O$	203.33	9.395
$CaCl_2.2H_2O$	147.33	1.316
$SrCl_2.6H_2O$	266.64	0.0214

Table 6.1.1 showing composition of artificial seawater:
Salinity = 30.5 psu ; specific gravity = 1.021at 20^{0}C,
from Parsons, Maita and Lalli, 1984
[(a)] Solutions I and II are made up and autoclaved
separately, and combined to give a total volume of 1l.

	Primary stock		Secondary stock			
	Wt. req.	Volume added to	Volume of 1^0 stock added to 2^o stock	Wt. req.	Volume added to	Volume of stock added to 1l seawater
$NaNO_3$ [a]	-	-	-	7.5g	100ml	1ml
Na_2 glycero PO_4 [a]	-	-	-	0.315g	100ml	1ml
Vitamins						
Thiamin HCl	-			0.010g		
Biotin	1.0mg				100ml	1ml
B_{12}	1.0mg	200ml	0.1ml	-		
Tris [a]	-	-	-	12.1g	100ml	1ml
H_2SeO_3	0.013g	100ml	1ml	-	100ml	1ml
NH_4Cl [a]	-	-	-	0.054g	100ml	1ml
Trace metals						
$MnCl_2.4H_2O$	1.8g			-		
$ZnSO_4.7H_2O$	0.23g			-		
$CoSO_4.7H_2O$	0.14g	100ml	1ml	-	100ml	1ml
$NaMo_4.2H_2O$	0.07g			-		
$CuSO_4.7H_2O$	0.025g			-		
FeNaEDTA	-	-	-	0.429g		
$Na_2EDTA.2H_2O$	-	-	-	3.72g		

Table 6.1.2 showing recipes for Kellers media (Keller, 1987)
[a] see table 6.1.3 for adapted Kellers media recipe used in experimental cultures

Full Kellers ingredient	Modified Kellers ingredient	Primary stock		Secondary stock			Reason for alteration
		Wt. req.	Volume added to	Volume of 1^0 stock added to stock	Volume added to	Volume of 2^o stock added to 1l seawater	
$NaNO_3$	-	8.48g	100ml	1ml	100ml	1ml	Gives 16µM NO_3-N Concentration reduced to reflect natural levels
$Na_2glyceroPO_4$	NaH_2PO4	12.00g	1l	1ml	100ml	1ml	Gives 1µM PO_4-P Changed to simpler compound. Concentration reduced to reflect natural levels
Tris	Not used	-	-	-	-	-	Not used, therefore natural buffering can be studied.
NH_4Cl	Not used	-	-	-	-	-	Not used, therefore nitrogen sources simplified.

Table 6.1.3 showing modifications to Kellers media

CO2 Spreadsheet for PRIME mesocosm bags.

BAG 5

Alkalinity determined on filtered samples

	INPUTS
H+ act. coeff.	0.850
Factor f	0.750

			INPUTS			INPUTS					CALCULATED				
	Date	Day	T	S	D	pHnbs	T1	pH	T2	pHtot	At	Ac	PCO2	CO2	Ct
	Jun-07	0	12.2	30.2	1022.83	8.241	13.2	3.644	21.3	8.205	2074	1996	244	10.2	1837
	Jun-08	1	12.5	30.9	1023.31	8.196	15.5	3.662	20.4	8.184	2088	2010	259	10.7	1853
*	Jun-09	2	12.7	30.4	1022.89	8.184	14.7	3.647	20.9	8.160	2077	2003	276	11.4	1856
	Jun-10	3	12.8	30.0	1022.56	8.222	16.0	3.631	21.8	8.212	2064	1984	239	9.9	1821
	Jun-11	4	12.5	29.9	1022.54	8.216	16.4	3.617	22.1	8.213	2051	1972	236	9.9	1812
	Jun-12	5	12.1	30.7	1023.23	8.257	15.1	3.586	21.8	8.245	2021	1935	212	8.9	1766
	Jun-13	6	12.4	29.9	1022.56	8.242	16.4	3.527	21.4	8.241	1960	1878	209	8.7	1716
	Jun-14	7	12.2	30.5	1023.06	8.244	14.8	3.503	22.5	8.227	1932	1850	213	8.9	1694
	Jun-15	8	12.4	29.9	1022.56	8.230	15.3	3.487	21.7	8.216	1914	1835	218	9.1	1685
	Jun-16	9	12.6	30.0	1022.60	8.211	14.4	3.488	20.3	8.185	1915	1839	238	9.9	1698
	Jun-17	10	12.9	30.4	1022.85	8.199	14.7	3.511	21.9	8.173	1942	1866	249	10.2	1723
	Jun-18	11	12.2	29.8	1022.52	8.178	14.4	3.510	20.3	8.156	1941	1871	262	11.0	1739
	Jun-19	12	12.3	29.1	1021.96	8.178	13.9	3.550	21.8	8.149	1987	1919	275	11.6	1788
	Jun-20	13	13.0	28.7	1021.52	8.168	14.0	3.538	20.1	8.132	1975	1909	288	11.9	1782
	Jun-21	14	12.8	28.8	1021.63	8.148	14.2	3.544	20.8	8.116	1981	1918	301	12.5	1795
	Jun-22	15	12.9	28.5	1021.38	8.167	14.2	3.561	21.4	8.134	1999	1935	290	12.0	1806
	Jun-23	16	13.1	27.6	1020.65	8.177	15.3	3.572	22.3	8.154	2012	1947	280	11.6	1813
	Jun-24	17	13.5	27.6	1020.57	8.202	16.0	3.558	22.3	8.182	1998	1929	257	10.5	1785
	Jun-25	18	13.7	27.6	1020.54	8.211	15.9	3.537	22.9	8.188	1975	1905	250	10.2	1760
	Jun-26	19	13.9	27.5	1020.42	8.232	16.3	3.544	21.4	8.211	1983	1910	236	9.5	1756
	Jun-27	20	13.4	27.5	1020.52	8.224	15.5	3.525	22.6	8.200	1962	1892	241	9.9	1746
	Jun-28	21	13.7	27.5	1020.46	8.198	15.7	3.531	24.1	8.172	1969	1901	261	10.6	1762
	Jun-29	22	13.4	27.5	1020.52	8.211	14.9	3.503	22.1	8.180	1937	1869	251	10.3	1731
*	Jun-30	23	12.8	28.0	1021.01	8.215	13.8	3.492	18.7	8.178	1923	1854	249	10.4	1720
	Jul-01	24	11.5	27.8	1021.09	8.198	13.8	3.486	21.2	8.176	1915	1850	249	10.9	1724
	Jul-02	25	11.0	27.9	1021.25	8.187	13.8	3.502	21.1	8.170	1934	1870	255	11.3	1747
*	Jul-03	26								-0.071	####	####	####	####	####

pHtot = pH on 'total' hydrogen ion scale at in situ temperature

At = total alkalinity (umol/kg)

Ac = carbonate alkalinity (umol/kg)

PCO2 = partial pressure of free CO2 (uatm) at in situ temperature

CO2 = concentration of free CO2 (umol/kg)

Ct = concentration of total CO2 (umol/kg)

All concentrations expressed as umol per kg of solution (seawater)

* T & S data missing: values extrapolated

Table 6.1.4 Example of one point alkalinity titration spreadsheet developed by D.W. Crawford

REFERENCES

Anderson, D.H. and R.J. Robinson. 1946. Rapid electrometric determination of alkalinity of seawater using a glass electrode. Industrial and Engineering Chemistry Analytical Edition 18: 767-769.

Andreae, M.O. 1985. Dimethylsulfide in the water column and the sediment pore waters of the Peru upwelling area. Limnology and Oceanography 30: 1208-1218

Andreae, M.O. 1990. Ocean-atmosphere interactions in the global biogeochemical sulfur cycle. Marine Chemistry 30: 1-29.

Anita, J.J., C.D. McAllister, T.R. Parsons, K. Stephen, and J.D.H. Strickland. 1963. Further measurements of primary production using large volume plastic spheres. Limnology and Oceanography 8: 166-183.

Balch, W.M., J. Fritz, and E. Fernandez. 1996. Decoupling of calcification and photosynthesis in the coccolithophore *Emiliania huxleyi* under steady-state light limited growth. Marine Ecology Progress Series 142: 87-97.

Balch, W.M., P.M. Holligan, and K.A Kilpatrick. 1992. Calcification, photosynthesis, and growth of the bloom-forming coccolithophore, *Emiliania huxleyi*. Continental Shelf Research 12: 1353-1374.

Balch, W.M., K. Kilpatrick, P.M. Holligan, and T. Cucci. 1993. Coccolith production and detachment by *Emiliania huxleyi* (Prymnesiophyceae). Journal of Phycology 29: 566-575.

Baumann, F.G. 1978. The inverse relationship between nutrient nitrate concentration and coccolith calcification in cultures of *Hymenomonas* sp. Journal of Protozoology 25: 253-256.

Berge, G. 1962. Discoloration of the sea due to *Coccolithus huxleyi* 'bloom'. Sarsia 6: 27-41

Bradshaw, A.L. and P.G. Brewer. 1988. High precision accuracy measurements of alkalinity and total carbon dioxide in seawater by potentiometric titration. 2. Measurements of standard solutions. Marine Chemistry 24: 155-162.

Brand, L.E. 1982. Genetic variability and spatial patterns of genetic differentiation in the reproductive rates of the marine coccolithophores *Emiliania huxleyi* and *Gephyrocapsa oceanica*. Limnology and Oceanography 27: 236-245.

Brand, L.E. and R.R.L. Guillard. 1981. The effects of continuous light and light intensity on the reproduction rates of twenty-two species of marine phytoplankton. Journal of Experimental Marine Biology and Ecology 50: 119-132.

Brown, C.W. and J.A. Yoder. 1994 (a). Coccolithophorid blooms in the global ocean. Journal of Geophysical Research 99: 7467-7482.

Buitenhuis, E., J. van Bleijsweik, D. Bakker, and M. Veldhuis. 1996. Trends in inorganic and organic carbon in a bloom of *Emiliania huxleyi* in the North Sea. Marine Ecology Progress Series 143: 271-282.

Butler, J.N. 1992. Alkalinity titration in seawater: how accurately can the data be fitted by an equilibrium model? Marine Chemistry 38: 251-282.

Charlson, R.J., J.E. Lovelock, M.O. Andreae, and S.G. Warren. 1987. Oceanic phytoplankton, atmospheric sulphur, cloud albedo and climate. Nature 326: 655-661.

Cote, B. and T. Platt. 1983. Day to day variations in the spring/summer photosynthetic parameters of coastal marine phytoplankton. Limnology and Oceanography 28: 320-344.

Crawford, D.W. and P.J. Harrison. 1997. Direct measurements of PCO_2 in cultures of marine phytoplankton: how good is the estimate from pH_{NBS} and single point titration of alkalinity? In press .

Crawford, D.W. and D.A. Purdie. 1997. PCO_2 increase during blooms of Emiliania huxleyi: Theoretical considerations on the asymmetry between the acquisition of HCO_3^- and respiration of free CO_2. Limnology and Oceanography 42: 365-372

Crawford, D.W. and D.K. Stoeker. 1996. Carbon content, dark respiration and mortality of the mixotrophic ciliate *Strobidium capitatum.* Marine Biology 126: 415-422.

Davies, C.O. 1982. The importance of understanding phytoplankton life strategies in the design of experimental enclosure experiments. In Marine Mesocosms - Biological and chemical research in experimental ecosystems, ed. G.D. Grice and M.R. Reeve. New York: Springer-Verlag.

Dickson, A.G. 1981. An exact definition of total alkalinity and a procedure for the estimation of alkalinity and total inorganic carbon from titration data. Deep-Sea Research 28A: 609-623.

Dickson, A.G. 1984. pH scales and proton transfer reactions in saline media such as seawater. Geochimica et Cosmochimica Acta 48: 2299-2308.

Dickson, A.G. 1993. The measurement of sea water pH. Marine Chemistry 44: 131-142.

Dickson, A.G. and C. Goyet. 1994. Handbook of methods for the analysis of the various methods of the carbon dioxide system in seawater: U.S. Department of Energy.

Dickson, A.G. and M. Whitfield. 1981. An ion-association model for estimating acidity constants (at 25°C and 1atm total pressure) in electrolyte mixtures related to seawater (ionic strength , 1mol kg^{-1} H_2O). Marine Chemistry 10: 315-333.

Dickson, D.M.J. and G.O. Kirst. 1987.Osmotic adjustment in marine eukaryotic algae: the role of inorganic ions, quaternary ammonium, tertiary sulphonium and carbohydrate solutes. II. Prasinophytes and haptophytes. New Phytologist 106: 657-666

Dong, L.F., N.A. Nimer, E. Okus, and M.J. Merrett. 1993. Dissolved inorganic carbon utilisation in *Emiliania huxleyi* (Lohmann) Kamptner. New Phytologist 123: 679-684.

Edmond, J.M. 1970. High precision determination of titration alkalinity and total carbon dioxide content of seawater by potentiometric titration. Deep-Sea Research 17: 737-750.

Egge, J.K. and B.R. Heimdal. 1994. Blooms of phytoplankton including *Emiliania huxleyi* (Haptophyta). Effect of nutrient supply in different N:P ratios. Sarsia 79: 333-348.

Egge, J.K. and A. Jacobsen. 1997. Influence of silicate on particulate carbon production in phytoplankton. Marine Ecology Progress Series 147: 219-230.

Eppley, R.W, Holmes, R.W. and J.D.H. Strickland. 1967. Sinking rates of marine phytoplankton measured with a flourometer. Journal of Experimental Marine Biology and Ecology 1: 191-208

Eppley, R.W., J.N. Rogers, J.J. McCarthy, and A. Sournia. 1971. Light/dark periodicity in nitrogen assimilation of the marine phytoplankters *Skeletonema costatum* and *Coccolithus huxleyi* in N-limited chemostat culture. Journal of Phycology 7: 150-154.

Falkowski, P.G., Z. Dubinsky, and K. Wyman. 1985. Growth-irradiance relationships in phytoplankton. Limnology and Oceanography 30: 311-321.

Fell, N. and P. Liss. 1993. Can algae cool the planet? New Scientist 21 August: 34-38.

Fernandez, E., P. Boyd, P.M. Holligan, and D. Harbour. 1993. Production of organic and inorganic carbon within a large coccolithophore bloom in the N.E. Atlantic. Marine Ecology Progress Series 97: 271-285.

Finch, M.S. 1994. The contrasting effects of organic phytoplankton production and calcification on surface ocean carbon dioxide and oxygen concentrations. Ph.D., University of Southampton.

Fisher, N.S. and S. Honjo. 1989. Intraspecific differences in temperature and salinity responses in the coccolithophore *Emiliania huxleyi*. Biological Oceanography 6: 355-361.

Frankignoulle, M. 1994. A complete set of buffer factors for acid/base CO_2 system in seawater. Journal of Marine Systems 5: 111-118.

Frankignoulle, M., J.-P. Gattuso, R. Biondo, I. Bourge, G. Copin-Montegut, and M. Pichon. 1996. Carbon fluxes in coral reefs. II. Eulerian study of inorganic carbon dynamics and measurement of air-sea CO_2 exchanges. Marine Ecology Progress Series 145: 123-132.

Gartner, S. and D. Bukry. 1969. Tertiary holococcoliths. Journal of Paleaontology. 43: 1213-1221.

Goldman, J.C. and P.G. Brewer. 1980. Effect of nitrogen source and growth rate on phytoplankton-mediated changes in alkalinity. Limnology and Oceanography 25: 352-357.

Green, J.C. 1994. Life cycles of haptophyte algae. In The Haptophyte Algae, ed. J.C. Green and B.S.C. Leadbeater:173-186. Oxford: Clarendon Press.

Green, J.C. and R.W. Jordan. 1994. Systematic history and taxonomy. In The Haptophyte Algae, ed. J.C. Green and B.S.C. Leadbeater. Oxford: Clarendon Press.

Guillard, R.R.L and J.H. Ryther. 1962. Studies on marine planktonic diatoms. 1. *Cyclotella nana* Hustedt and *Detonula confervacea* (Cleve) Gran. Canadian Journal of Microbiology 8: 220-239.

Hansson, I. 1973. A new set of pH-scales and standard buffers for seawater. Deep-Sea Research 20: 479-491.

Harris, R.P. 1996. Coccolithophorid dynamics: The European *Emiliania huxleyi* programme, EHUX. Journal of Marine Systems 9: 1-12.

Harrison, P.J., R.E. Waters, and F.J.R. Taylor. 1980. A broad spectrum artificial seawater medium for coastal and open ocean phytoplankton. Journal of Phycology 16: 28-35.

Heimdal, B.R., J.K. Egge, M.J.W. Veldhuis, and P. Westbroek. 1994. The 1992 Norwegian *Emiliania huxleyi* experiment. An overview. Sarsia 79: 285-290.

Holligan, P.M, E. Fernandez, J. Aiken, W.M. Balch, P. Boyd, P.H. Burkill, M. Finch, S.B. Groom, G. Malin, K. Muller, D.A. Purdie, C. Robinson, C.C. Trees, S.M. Turner, and P. van der Wal. 1993. A biogeochemical study of the coccolithophore, *Emiliania huxleyi*, in the North Atlantic. Global Biogeochemical Cycles 7: 879-900.

Holligan, P.M. and J.E. Robertson. 1996. Significance of ocean carbon budgets for the global carbon cycle. Global Change Biology 2: 85-95

Iverson, R.L., H.F. Bittaker, and V.B. Myers. 1976. Loss of radiocarbon in direct use of Aquasol for liquid scintillation counting of solutions containing ^{14}C-$NaHCO_3$. Limnology and Oceanography 21: 756-758.

Keeling, C.D. 1991. In Trends '91, A compendium of data on global change :24-27: Oak Ridge National Laboratory.

Keller, M.D., R.C. Selvin, W. Claus, and R.R.L. Guillard. 1987. Media for the culture of oceanic ultraphytoplankton. Journal of Phycology 23: 633-638.

Keller, M.D. 1989. Dimethyl sulfide production and marine phytoplankton: The importance of species composition and cell size. Biological Oceanography 6: 375-382

King, D.W. and D.R. Kester. 1989. Determination of seawater pH from 1.5 to 8.5 using colorimetric indicators. Marine Chemistry 26: 5-20.

Kirk, J.T.O. 1988. Solar heating of water bodies as influenced by their inherent optical properties. Journal of Geophysical Research 93: 10987-10908.

Klaveness, D. 1972 (a). *Coccolithus huxleyi* (Lohmann) Kamptner I - Morphological investigations on the vegetative cell and the process of coccolith formation. Protistologica 8: 335-346.

Klaveness, D. 1972 (b). *Coccolithus huxleyi* (Lohm) Kamptn II. The flagellate cell, aberrant cell types, vegetative propagation and life cycles. British Phycological Journal 7: 309-318.

Kuiper, J. 1977. Development of North Sea coastal plankton in separate bags under identical conditions. Marine Biology 44: 97-107.

Leadbeater, B.S.C.Cell coverings. In The Haptophyte Algae, ed. J.C. Green and B.S.C. Leadbeater. Oxford: Clarendon Press.

Lecourt, M., D.L. Muggli, and P.J. Harrison. 1996. Comparison of growth and sinking rates of non-coccolith- and coccolith-forming strains of Emiliania huxleyi (Prymnesiophyceae) grown under different irradiances and nitrogen sources. Journal of Phycology 32: 17-21.

Linschooten, C., J.D.L. van Bleijsweik, P.R. van Emburg, J.P.M. de Vrind , E.S. Kempers, P. Westbroek, and E.W. de Vrind-de Jong. 1991. Role of light-dark cycle and medium composition on the production of coccoliths by *Emiliania huxleyi*. Journal of Phycology 27: 82-86.

Malin, G., Liss, P.S. and S.M. Turner. 1994 Dimethyl sulfide:production and atmospheric consequences. In The Haptophyte Algae ed J.C. Green and B.S.C. Leadbeater 303-320 Clarendon Press.

McAlice, B.J. 1971. Phytoplankton sampling with the Sedgewick-Rafter cell. Limnology and Oceanography 16: 19-28.

McAllister, C.D., K.S. Parsons, and J.D.H. Strickland. 1961. Measurements of primary production in coastal seawaters using a large plastic sphere. Limnology and Oceanography 6: 237-258.

McIntyre, A. and A. Be. 1967. Modern coccolithophoridae in the Atlantic Ocean. I. Placoliths and cryoliths. Deep-Sea Research 14: 561-597.

Merrett, M.J., L.F. Dong, and N.A. Nimer. 1993a. Nitrate availability and calcite production in *Emiliania huxleyi* Lohmann. European Journal of Phycology 28: 243-246.

Merrett, M.J., L.F. Dong, and N.A. Nimer. 1993b. Nitrate availability and calcite production in *Emiliania huxleyi* Lohmann. European Journal of Phycocolgy 28: 243-246.

Millero, F.J., S.R. Schrager, and L.D. Hansen. 1974. Thermometric titration analysis of seawater for chlorinity, sulfate and alkalinity. Limnology and Oceanography 19: 711-715.

Nanninga, H.J. and T. Tyrrell. 1995. Importance of light for the formation of algal blooms by *Emiliania huxleyi*. Marine Ecology Progress Series 136: 195-203.

Nielsen, M.V. 1995. Photosynthetic characteristics of the coccolithophorid *Emiliania huxleyi* (Prymnesiophyceae) exposed to elevated concentrations of dissolved inorganic carbon. Journal of Phycology 31: 715-719.

Nielsen, M.V. 1997. Growth, dark respiration and photosynthetic parameters of the coccolithophorid *Emiliania huxleyi* (Prymnesiophyceae) acclimated to different daylength-irradiance combinations. Journal of Phycology In press.

Niiler, P.P. 1993. The ocean circulation. In The Climate System, ed. R.E. Trenburth:117-148: Cambridge University Press.

Nimer, N.A., G.K. Dixon, and M.J. Merrett. 1992. Utilization of inorganic carbon by the coccolithophorid *Emiliania huxleyi* (Lohmann) Kamptner. New Phytologist 120: 153-158.

Nimer, N.A., Q. Guan, and M.J. Merrett. 1994. Extra- and intra-cellular carbonic anhydrase in relation to culture age in a high-calcifying strain of *Emiliania huxleyi* Lohmann. New Phytologist 126: 601-607.

Nimer, N.A. and M.J. Merrett. 1992. Calcification and utilization of inorganic carbon by the coccolithophorid *Emiliania huxleyi* Lohmann. New Phytologist 121: 173-177.

Nimer, N.A. and M.J. Merrett. 1993. Calcification rate in *Emiliania huxleyi* Lohmann in response to light, nitrate and availability of inorganic carbon. New Phytologist 123: 673-677.

Nimer, N.A., M.J. Merrett, and C. Brownlee. 1996. Inorganic carbon transport in relation to culture age and inorganic carbon concentration in a high calcifying strain of *Emiliania huxleyi* (Prymnesiophyceae). Journal of Phycology 32: 813-818.

Paasche, E. 1962. Coccolith formation. Nature 193: 1094-1095.

Paasche, E. 1964. A tracer study of inorganic carbon uptake during coccolith formation and photosynthesis in the coccolithophorid *Coccolithus huxleyi*. Physiologia Plantarum Supplementum III: 1-82.

Paasche, E. 1967. Marine plankton algae grown with light-dark cycles. I. *Coccolithus huxleyi*. Physiologia Plantarum 20: 946-956.

Paasche, E. and S. Brubak. 1994. Enhanced calcification in the cocclithophorid *Emiliania huxleyi* (Haptophyceae) under phosphorus limitation. Phycologia 33: 324-330.

Parsons, T.R., Y. Maita, and C.M. Lalli. 1984. A Manual of Chemical and Biological Methods for Seawater Analysis: Pergamon Press.

Perez, F.F. and F. Fraga. 1987. A precise and rapid analytical procedure for alkalinity determination. Marine Chemistry 21: 169-182.

Peterson, B.J. 1980. Aquatic primary productivity and the ^{14}C-CO_2 method: A history of the productivity problem. Annual Review of Ecology Systematics 11: 359-385.

Porter, K.G. and Y.S. Feng. 1980. The use of DAPI for identifying and counting aquatic microflora. Limnology and Oceanography 25: 943

Prezelin, B.B., M. Putt, and H.E. Glover. 1986. Diurnal patterns in photosynthetic capacity and depth-dependent photosynthesis-irradiance relationships in *Synecoccus* spp. and larger phytoplankton in three water masses in the Northwest Atlantic Ocean. Marine Biology 91: 205-217.

Purdie, D.A. and M.S. Finch. 1994. Impact of a coccolithophore bloom on the partial pressure of carbon dioxide in seawater enclosures in a Norwegian fjord. Sarsia 79: 379-388.

Raven, J.A. and A.M. Johnston. 1991. Mechanisms of inorganic-carbon acquisition in marine phytoplankton and their implications for other resources. Limnology and Oceanography 36: 1701-1714.

Riegman, R., A.M. Noordeloos, and G.C. Cadee. 1992. *Phaeocystis* blooms and eutrophication of the continental coastal zones of the North Sea. Marine Biology 112: 479-484.

Robertson, J.E., C. Robinson, D.R. Turner, P. Holligan, A.J. Watson, P. Boyd, E. Fernandez, and M. Finch. 1994. The impact of a coccolithophore bloom on oceanic carbon uptake in the northeast Atlantic during summer 1991. Deep-Sea Research 41: 297-314.

Riebsell, B., Wolf-Gladrow, D.A. and V. Smetacek. 1993 Carbon dioxide limitation of marine phytoplankton growth rates Nature 361: 249-251

Schofield, O., R.R. Bidigare, and B.B. Prezelin. 1990. Spectral photosynthesis, quantum yield and blue-green light enhancement of productivity rates in the diatom *Chaetoceros gracile* and the prymnesiophyte *Emiliania huxleyi.* Marine Ecology Progress Series 64: 175-186.

Siegenthaler, U. and J.L. Sarmiento. 1993. Atmospheric carbon dioxide and the ocean. Nature 365: 119-121

Sikes, C.S. and K.M. Wilbur. 1982. Functions of coccolith formation. Limnology and Oceanography 27: 18-26

Skirrow, G. 1975. The dissolved gases - carbon dioxide. In Chemical Oceanography, ed. J.P. and Skirrow Riley, G., 2:1-92: Academic.

Smith, S.V. and G.S. Key. 1975. Carbon dioxide and metabolism in marine environments. Limnology and Oceanography 20: 493-495.

Steedmann, H.F. 1976. General and applied data on formaldehyde fixation and preservation if marine zooplankton. In Zooplankton Fixation and Preservation, ed. H.F. Steedman:103-154. Paris: UNESCO.

Strickland, J.D.H. and T.R. Parsons. 1972. A practical handbook of seawater analysis (Bulletin 167): Fisheries Research Bulletin of Canada.

Stumm, W. and J.J. Morgan. 1985. Aquatic chemistry: an introduction emphasizing chemical equilibria in natural waters: Wiley and sons.

Sundquist, E.T., L.N. Plummer, and T.M.L. Wigley. 1979. Carbon dioxide in the ocean surface: The homogenous buffer factor. Science 204: 1203-1205.

Takahashi, M., W.H. Thomas, D.L.R. Siebert, J. Beers, P. Koeller, and T.R. Parsons. 1975. The replication of biological events in enclosed water columns. Archive Hydrobiologia 76: 5-23.

Throndsen, J. 1978. Preservation and storage. UNESCO Phytoplankton Manual, 69-74.

Tyrell, T. and A.H. Taylor 1995. Latitudinal and seasonal variations in carbon dioxide and oxygen in the northeast Atlantic and the effects on *Emiliania huxleyi* and other phytoplankton. Global Biogeochemical Cycles 9: 585-604

van Bleijswijk, J.D.L., R. Kempers, M.J. Veldhuis, and P. Westbroek. 1994. Cell and growth characteristics of types A and B of *Emiliania huxleyi* (Prymnesiophyceae) as determined by flow cytometry and chemical analyses. Journal of Phycology 30: 230-241.

van der Wal, P., R.S. Kempers, and M.J.W. Veldhuis. 1995. Production and downward flux of organic matter and calcite in a North Sea bloom of the coccolithophore *Emiliania huxleyi*. Marine Ecology Progress Series 126: 247-265.

Watabe, W. and K.M. Wilbur. 1966. Effects of temperature on growth, calcification, and coccolith formation in *Coccolithus huxleyi* (Coccolithineae). Limnology and Oceanography 11: 567-575.

Webb, W.L., M. Newton, and D. Star. 1974. Carbon dioxide exchange of *Almus rubra*. A mathematical model. Oecologica 17: 281-291.

Westbroek, P., C.W. Brown, J. van Bleijswijk, C. Brownlee, G.J. Brummer, M. Conte, J. Egge, E. Fernandez, R. Jordan, M. Knappertsbusch, J. Stefels, M. Veldhuis, P. van der Wal, and J. Young. 1993. A model system approach to biological climate forcing. The example of *Emiliania huxleyi*. Global and Planetary Change 8: 27-46.

Westbroek, P., E.W. de Jong, P. van der Wal, A.H. Borman, J.P.M. de Vrind, D. Kok, W.C. de Bruijn, and S.B. Parker. 1984. Mechanism of calcification in the marine alga *Emiliania huxleyi*. Philosophical Transactions of the Royal Society of London B 304: 435-444.

Westbroek, P., J.R. Young, and K. Linschooten. 1989. Coccolith production (Biomineralization) in the marine alga *Emiliania huxleyi*. Journal of Protozoology 36: 368-373.

Williams, P.J.leB. and N.W. Jenkinson. 1982. A transportable microprocessor controlled precise Winkler titration suitable for field station and shipboard use. Limnology and Oceanography 27: 576-584.

Winter, A., R.W. Jordan, and P.H. Roth. 1994. Biogeography of living coccolithophores in ocean waters. In Coccolithophores, ed. A. Winter and W.G. Siesser:161-178. Cambridge: Cambridge University Press.

Young, J.R., Didymus, J.M., Brown, P.R., Prins, B. and S. Mann. 1992. Crystal assembly and phylogenetic evolution in heterococcoliths. Nature 356: 256-258.

Young, J.R. 1994. Functions of coccoliths. In Coccolithophores, ed. A. Winter and W.G. Siesser: 102-145. Cambridge: Cambridge University Press.